universität wien

MASTERARBEIT / MASTER'S THESIS

Titel der Masterarbeit / Title of the Master's Thesis

„Targeted metabolomics of biofluids and extracellular vesicles of ovarian cancer patients“

verfasst von / submitted by

Ines Muzaferovic, BSc

angestrebter akademischer Grad / in partial fulfilment of the requirements for the degree of

Magistra pharmaciae (Mag.pharm.)

Wien, 2022 / Vienna, 2022

Studienkennzahl lt. Studienblatt / degree program code as it appears on the student record sheet:	UA 066 605
Studienrichtung lt. Studienblatt / degree program as it appears on the student record sheet:	Masterstudium Pharmazie
Betreut von / Supervisor:	a.o. Univ.- Prof. Mag. Dr. Franz Gabor

Acknowledgements

I would like to express my gratitude to Prof. Paula Alves for giving me the chance to work at ITQB/iBET as an interface between Biosystem and Data Science and Uni MS, where I was warmly welcomed by both departments. I would also like to express my gratitude to Univ.-Prof. Franz Gabor. Without him, as a contact person and supervisor at the University of Vienna all this would not have been possible. Thank you for your trust!

In addition, a big thank you goes to Dr. Ines Isidro and Dr. Rita Mendes, both my supervisors. You helped me with your assistance, encouragement and understanding in guiding me through the master thesis. Besides, I want to thank the team from Uni MS, especially Dr. Sandra Diniz Silva and Dr. Ana C. L. Guerreiro as well as Ana Barbara Pereira, MSc for helping me with the data processing. Without their expertise, my thesis would not have been completed so successfully. Last but not least, Goncalo Trindade, MSc deserves to be mentioned, who helped me with all my questions during as well as after the internship.

For the samples, which were essential for my work, I would like to thank the Instituto Português de Oncologia de Lisboa Francisco Gentil (IPOLFG). This work was funded by Fundação para a Ciência e Tecnologia/Ministério da Ciência, Tecnologia e Ensino Superior (FCT/MCTES, Portugal) through national funds to iNOVA4Health (UIDB/04462/2020 and UIDP/04462/2020) and the Associate Laboratory LS4FUTURE (LA/P/0087/2020).

A big thank you also goes to Nikolaus, who stood by me from day one and not only helped me enormously with work-related issues but also outside of work, whether it was finding accommodation, recommendations of restaurants around Lisbon or hints and tricks in Portugal. You were always the first person to talk to when I was in despair and you always knew the perfect words to cheer me up again. Through my work I have gained a very valuable new friend, which makes me a very lucky person.

Thanks to my friends and colleagues, my time as a student were not only characterized by studying but I will always remember the countless celebrations after exams, the many enjoyable moments in the labs and the exchanges between students. My friends outside of pharmacy helped me to balance my studies. You showed me that life is not only about studying, and you were the ones who encouraged me the most to decide to do my thesis abroad. Since this was the best decision, I will be forever grateful!

However, the biggest thanks deserve my parents Sulta and Ismet who raised me with unconditional love and a lot of support to become the person I am today. Not only did you support me financially during my professional career and make my semester abroad possible, but you were always there to help me and even when I was desperate, I knew you would always be there for me. So much love that you gave me, no one can put it into words! Thank you so much!

Abstract

Ovarian cancer is the eighth most common female cancer worldwide and compared to other gynecologic malignancies, ovarian cancer has the highest mortality rate. The accumulation of ascitic fluids in the peritoneal cavity is associated with a worse prognosis and a more aggressive course. In addition, extracellular vesicles (EVs) circulating within the ascitic fluids, participate in the intercellular crosstalk in the tumour microenvironment. Since metabolic alteration is one of the hallmarks of cancer, and so far, studies of EVs have mostly focused on proteomics and transcriptomics, it is essential to study the metabolome of EVs.

This work aimed to detect and analyse the metabolomic profile of biofluids, namely ascitic fluids and peritoneal washes, of ovarian cancer patients and of the corresponding isolated EVs. For this, a method with the use of the AbsoluteIDQ® p180 metabolomic kit (Biocrates), coupled with an LC-MS system and FIA analysis was implemented in the lab.

After the successful implementation of the method, 155 metabolites were identified in the ascitic fluids and peritoneal washes. A smaller number of 69 metabolites could be detected in the EVs from ascitic fluids and 43 metabolites in EVs from the peritoneal washes. Multivariate data analysis such as principal component analysis and hierarchical clustering analysis shows that no significant differences between the two biofluids or between their EVs could be found. Nevertheless, the metabolic yield of the biofluids differed significantly from the EVs concerning 1) the metabolite classes and 2) the quantifications of metabolites. Only in the biofluids amino acids, biogenic amines and acylcarnitines were quantified, whereas the EVs were enriched in lipids such as sphingomyelins and phosphatidylcholines.

A follow-up analysis could include patient information such as age, treatment, and relapse, to find biomarkers for diagnosis, prognosis, and support more targeted treatment.

Abstrakt

Eierstockkrebs ist die achthäufigste Krebserkrankung bei Frauen weltweit und im Vergleich zu anderen gynäkologischen Malignomen hat Eierstockkrebs die höchste Sterblichkeitsrate. Die Entwicklung von Aszites in der Peritonealhöhle ist mit einer schlechteren Prognose und einem aggressiveren Verlauf verbunden. Extrazelluläre Vesikel (EVs), die in den Aszitesflüssigkeiten produziert und sezerniert werden, werden für den interzellulären Crosstalk in der Mikroumgebung des Tumors (TME) verwendet. Da metabolische Veränderungen eines der „hallmarks of cancer" darstellt und der Fokus bezüglich des Inhaltes der EVs nur auf Proteomik und Transkriptomik lag, ist es wichtig, das Metabolom von EVs zu untersuchen.

Ziel dieser Arbeit war es, das metabolomische Profil von Bioflüssigkeiten wie Aszites und Peritonealspülungen von Eierstockkrebspatientinnen und den entsprechenden isolierten EVs zu erkennen und zu analysieren. Zu diesem Zweck wurde im Labor eine Methode unter Verwendung des AbsoluteIDQ® p180 Metabolomic Kits (Biocrates), gekoppelt mit einem LC/MS-System und FIA-Analyse, implementiert.

Nach erfolgreicher Implementierung der Methode wurden 155 Metaboliten in den Aszitesflüssigkeiten und Peritonealspülungen identifiziert. Im Vergleich zu den Bioflüssigkeiten konnte eine geringere Anzahl von 69 Metaboliten aus den isolierten EVs der Aszitesflüssigkeit und 43 Metaboliten aus den isolierten EVs der Peritonealspülungen nachgewiesen werden. Multivariate Datenanalysen wie Principal Component Analysis und Hierarchical Clustering Analysis zeigen, dass keine signifikanten Unterschiede zwischen den Bioflüssigkeiten oder zwischen den EV-Gruppen gefunden werden konnte. Dennoch unterschied sich die metabolische Ausbeute der Bioflüssigkeiten signifikant von der der EVs hinsichtlich 1) der Metabolitenklassen und 2) der Quantität der Metaboliten. Nur in den Bioflüssigkeiten wurden Aminosäuren, biogene Amine und Acylcarnitine quantifiziert, während die EVs mit Lipiden wie Sphingomyelinen und Phosphatidylcholinen angereichert waren.

Eine detailliertere Analyse könnte Patienteninformationen wie Alter, Behandlung und Rückfall einbeziehen, um Biomarker für die Diagnose, Prognose und eine zielgerichtetere Behandlung zu finden.

Table of content

Abbreviations

ADC	Adenocarcinoma
AF(s)	Ascitic fluid(s)
AF-EV(s)	EVs, isolated from AFs
ApoA-I	Apolipoprotein-I
BRAF	Serine/threonine kinase
BRCA1/2	Breast cancer 1/2 gene
CA125	Cancer antigen 125
CAA(s)	Cancer-associated adipocytes
CAF(s)	Cancer-associated fibroblast(s)
Cal1-7	Calibration standards 1-7
CE-MS	Capillary electrophoresis mass spectrometry
CT	Computer tomography
DC	Disease carrier
DD	Diseased from disease
DF	Disease-free
DNA	Desoxyribonucleic acid
EC	Endometrium carcinoma
ECM	Extracellular matrix
EOC	Epithelial ovarian cancer
ERK	Extracellular signal-related kinase
ESI	Electro spray ionisation
EV(s)	Extracellular vesicle(s)
FDA	Food and drug administration
GC	Gas chromatography
HCA	Hierarchical clustering analysis
HE4	Human epididymis protein 4
HGSC	High-grade serous (adeno)carcinoma
HPLC	High performance liquid chromatography
IL	Interleukin
ISEV	International Society of Extracellular Vesicles
KRAS	Kirsten rat sarcoma viral oncogene homolog
LC	Liquid chromatography
LGSC	Low-grade serous (adeno)carcinoma
LLOQ	Lower limit of quantification
LOD	Limit of detection
lyso-PC	Lysophosphatidylcholine
m/z	Mass-to-charge ratio
MAP	Mitogen-activated protein
MRI	Magnet resonance imaging
MRM	Multi reaction monitoring
MS	Mass spectrometry
MSEA	Metabolite set enrichment analysis
N.A.	Not available
NACT	Neoadjuvant chemotherapy
NG-ADC	Non-gynecological adenocarcinoma
NMR	Nuclear-magnet resonance
NTA	Nanoparticle tracking analysis
OC	Ovarian cancer
OXPHOS	Oxidative phosphorylation
PARP	Poly ADP-ribose polymerase
PBS	Phosphate-buffered saline
PC	Phosphatidylcholine
PCA	Principal component analysis
PET	Positron emission tomography
PIK3CA	Phosphatidylinositol-4,5-biphosphate 3 kinase catalytic subunit A
PITC	Phenylisothiocyanate
PLS	Partial least squares
PTEN	Phosphatase and tensin homolog
PW(s)	Peritoneal wash(es)
PW-EV(s)	EVs, isolated from PWs
QC1-3	Quality controls 1-3
RB	Retinoblastoma protein
RNA	Ribonucleic acid
SM	Sphingomyelin
SM(OH)	Hydroxysphingomyelin
SST	System suitability test
TAM(s)	Tumour-associated macrophage(s)
TASC(s)	Tumour-associated stromal cell(s)
TCA	Tricarboxylic acid
TEM	Transmission electron microscopy
TME	Tumour microenvironment
TSG101	Tumour susceptibility gene 101
UHPLC	Ultra-high performance liquid chromatography

1. Introduction

1.1 Ovarian Cancer

1.1.1 Epidemiology

Ovarian cancer is the eighth most common cancer in women worldwide in 2020 behind breast, colorectal, lung cervical, cervix uteri, thyroid, corpus uteri and stomach cancer and compared to other gynecological malignancies, has the highest mortality rates [1]–[3]. 1 out of 78 women will get ovarian cancer during their lifetime, while 1 out of 108 dies of the disease [4]. Ovarian cancer is considered a silent killer as 70% of all cases are diagnosed in advanced stages [1]. While the 5-year survival rate of patients in early stages (I-IIA) is more than 80%, it decreases to less than 40% in advanced stages (IIB-IV) [5].

1.1.2 Pathophysiology

Ovarian cancer has a heterogeneous morphology and histology. The classification of ovarian cancer is determined by histology (epithelial or non-epithelial), time of diagnosis (early or late diagnosis relates to early or advanced stages), and the grade of malignancy (low or high-grade) [6]. Ovarian cancer can arise from three areas: the germ cells, the stroma, and the surface epithelium. Epithelial ovarian cancer (EOC) is the most common type, accounting for 90% of all ovarian cancer cases [7].

In turn, EOC can be divided into two subtypes: Type 1 and Type 2. Type 1 often develops from benign lesions of the ovary and has mutations in genes like phosphatidylinositol-4,5-biphosphate 3 kinase catalytic subunit A (PIK3CA), phosphatase and tensin homolog (PTEN), Kirsten rat sarcoma viral oncogene homolog (KRAS), serine/threonine kinase b-raf (BRAF), mitogen-activated protein (MAP), and extracellular signal-related kinase (ERK). Type 2 is associated mainly with malignant ascites, is more aggressive and has higher genomic instability associated with genes such as p53 tumour suppressor, breast cancer gene (BRCA1/2), and retinoblastoma protein (RB) [8]. Genetic disposition due to mutations in BRCA1 and BRCA2 genes account for 10-15% of hereditary ovarian cancer cases [7]. Nevertheless, only a small percentage of 10% of all ovarian cancer cases are hereditary [9]. Type 1 includes low-grade endometrioid ovarian cancer, clear cell carcinomas, low-grade serous carcinoma (LGSC), seromucous carcinoma and malignant Brenner tumours while Type 2 tumours include carcinosarcomas, undifferentiated carcinoma and high-grade serous carcinoma (HGSC) [8].

In addition to the previous classification, focusing on the genes and malignancy, EOC can also be differentiated into at least five different histological types: serous, endometrial, mucinous, clear cell and squamous cell carcinoma [10]. Accounting for 75% of all cases, HGSC is the most common among type of EOC,

affects mainly women in advanced ages and is responsible for more than 70-80% of ovarian cancer-related deaths [8], [11]. Other histological classification types namely endometrial carcinoma, mucinous carcinoma and clear cell carcinoma occur primarily at a younger age [7], [10].

In advanced stages (III-IV), the tumour starts to spread. There are three routes for ovarian cancer forming metastases: lymphatic (spread through the lymph system), hematogenous (spread through the blood), and transcoleomic (spread of malignancy into the body cavities such as peritoneal cavity via penetration of the surface and arrives, building up metastasis). In around 70% of ovarian cancer cases, the transcoleomic route can be observed due to the proximity of the ovarian to the peritoneal cavity and contributes to increased mortality and morbidity because the metastases can affect the surrounding organs such as those from the gastrointestinal tract [8], [12]. The transcoleomic metastases are highly associated with the production and accumulation of biofluid in the peritoneal cavity, known as ascites [8].

1.1.3 Ascites

Under physiological conditions, the capillary membrane of the peritoneal cavity constantly produces fluid to keep the serosa surface smooth and to maintain an exchange of small molecules between the peritoneum and adjoining organs. Under ovarian cancer-associated pathophysiological conditions, fluid production increases due to the leakage of tumour microvasculature and lymphatic obstruction. Initially, lymph obstruction was thought to be the only cause of ascites formation; however, biofluid accumulation can occur even without lymph obstruction. Thus, it is inevitable that ascites formation is multifactorial, probably due to an interplay of lymph obstruction, increased capillary vascular permeability, and increased production of biofluid caused by resident tumours, stromal and immune cells [8], [13].

In advanced stages (III-IV), about 40% of ovarian cancer patients present malignant ascites, associated with a poorer prognosis because it contributes to a microenvironment promoting cancer development [12]. Ascites is also associated with disease relapse. The fact that stage IA, in which the tumour is restricted in the ovary, has fewer relapses (29%) than stage IC (59%), where peritoneal washes tested positive on tumour cells, confirms this hypothesis [13].

In the past few decades, components of malignant ascites have been gaining significancy for cancer progression. Ascitic of fluid comprises cellular and acellular components. Acellular features include cytokines such as interleukin-6 (IL-6) and interleukin-8 (IL-8), proteins, and several metabolic products. Cellular components include tumour cells formed by spheroids or individual cells, as well as stromal cells, including fibroblasts, endothelial cells, and inflammatory cells. The presence of these cell populations is a strong indication of the existence of malignant tumours in the peritoneal cavity [8]. In addition to a poor prognosis,

ascites is associated with symptoms such as abdominal pain, nausea or vomiting, fatigue and early satiety, leading to a deterioration in the quality of life [8], [13].

1.1.4 Diagnosis

Cancer antigen 125 (CA125) is a glycoprotein that can be detected on the cell surface of ovarian cancer cells. For over 30 years, CA125 was the gold standard in the diagnosis of ovarian cancer and in detecting recurrence of the disease. Unfortunately, there are limitations such as low sensitivity, as CA125 remains undetected in 50% of early-stage cases and 10% of advanced stages [10]. In addition, CA125 is expressed under physiological conditions such as pregnancy, menstruation, or other pathological processes like endometriosis and pelvic inflammatory disease, which leads to low specificity [1], [6]. Due to these limitations, additional biomarkers are necessary for diagnosing ovarian cancer. One possible candidate is the human epididymis protein 4 (HE4). HE4 is slightly expressed in respiratory epithelium tissue and reproductive organs but overexpressed in ovarian tumours. Even though HE4 has a similar sensibility and specificity as CA125, recent studies show a higher sensitivity to diagnosis of EOC in early stages (HE4: 64%, CA125: 45,9%) [10]. It can be said that the combination of HE4 with CA125 provides a more reliable diagnosis than CA125 alone [6].

Other diagnostic examinations to detect ovarian cancer include transvaginal ultrasound, abdominal ultrasonography, computer tomography (CT), magnet resonance imaging (MRI) and positron emission tomography (PET) alone or in combination. Transvaginal ultrasound is well suited to determine more about the tumour mass, such as size, complexity, and localisation. Still, there is no way to determine if the tumour is benign or malign through transvaginal ultrasound. Combining all these methods, along with biomarkers such as CA125 and HE4, may be a good indication, but only a biopsy of the tissue will confirm the diagnosis of ovarian cancer [11].

Since early diagnosis poses difficulties due to asymptomatic progression and up to now, there is no substantial possibility of diagnosis without invasive surgery, the search for a non-invasive biomarker at an early stage is necessary [6], [11].

1.1.5 Treatment and relapse

First-line therapy of ovarian cancer includes cytoreduction surgery for tumour bulking and adjuvant chemotherapy or neoadjuvant chemotherapy (NACT), which is the administration of chemotherapy before surgery, followed by cytoreduction surgery and adjuvant chemotherapy. A combination of platinum-based chemotherapeutics such as cisplatin or carboplatin with a taxane agent like paclitaxel or docetaxel is the current mean of choice [8], [11].

Although more than 70% of ovarian cancer patients respond well to initial treatment, 80% relapse in the first 8-12 months, mainly due to platinum resistance [10], [14]. Since second-line therapy is not yet successfully addressed, the overall survival for patients with platinum resistance is one year [15]. The resistance usually comes from increased drug efflux, reduced drug accumulation, drug inactivation, or activating cancer survival mechanisms such as increased DNA repair regulations and upregulation of anti-apoptotic cells [16].

In recent years, much work has been done on molecular targeting. For example, poly ADP-ribose polymerase (PARP) inhibitors and inhibitors of angiogenesis are already FDA approved, and PARP-inhibitor Niraparib is used in advanced ovarian cancer after relapse [6], [15].

1.2 Altered metabolism and tumour microenvironment in ovarian cancer

1.2.1 Cancer metabolism

In general, the most well-known hallmark of cancer is the Warburg effect: While cells under physiological conditions absorb nutrients, which are broken down in a series of metabolic reactions through cytosolic glycolysis, followed by mitochondrial tricarboxylic acid (TCA) cycle and oxidative phosphorylation (OXPHOS), tumour cells reprogram their metabolic machinery to meet enhanced energy production for cell division and biosynthesis of macromolecules through a less efficient but 100 times faster process known as 'anaerobic glycolysis' even though enough oxygen is available. During the process, a high amount of glucose is broken down by glycolysis, followed by lactate acid fermentation in the cytosol [17]–[19].

Besides glucose, glutamine metabolism and consumption play a significant role in cancer growth and proliferation and are gaining importance in the characteristics of cancer cells [18], [20]. Glutamine is not only used for the biosynthesis of essential compounds such as amino acids and nucleic acids but also for glutaminolysis, a process in which glutamine is converted into TCA cycle intermediates and lactate, used as an additional source of energy for the cancer [20]. In fibroblasts, among other substrates, glutamine is required to synthesise proline to produce collagen, making it vital in this case [18]. Furthermore, there is evidence that glutamine metabolism is significantly higher in cancer-associated fibroblast (CAFs) than in tumour cells of pancreatic cancer. The background could be that the quiescent fibroblasts focus more on pyruvate carboxylase to produce the intermediates for TCA cycle, with CAFs focusing on glutaminase expression to drive glutamine metabolism for growth and proliferation [18]. Nevertheless, further investigations around glutamine metabolism are needed.

1.2.2 Role of tumour microenvironment in cancer

The tumour microenvironment (TME) is the tissue surrounding the tumour. It consists of stromal cells called tumour-associated stromal cells (TASCs). These include CAFs, tumour-associated macrophages (TAMs), cancer-associated adipocytes (CAAs) and cancer-associated immune cells. All together are responsible for the maintenance and structure of the extracellular matrix, progression, proliferation, angiogenesis of the tumour and drug resistance by producing various second messengers such as cytokines like interleukin IL-6 and IL-8, growth factors, chemokines, and extracellular vesicles (EVs) [11], [19], [21], [22].

The most representative stroma cells within the tumour are CAFs. Usually, fibroblasts play a major role in synthesising extracellular matrix (ECM) proteins under physiological conditions, which gives the tissue

structure and stability. Those fibroblasts can be permanently activated during the tumorigenesis and become cancer-associated fibroblasts (CAFs) [18]. In tumour progression, CAFs promote tumour growth, proliferation, invasion, and metastasis and are a mediator in drug resistance [18], [23]. Moreover, CAFs positively affect the aerobic glycolysis of the tumour, which is called the reverse Warburg effect [18]. It promotes glycogen metabolism and glycolysis in cancer cells through the production of cytokines, which in turn release growth factors to the CAFs. This signalling loop between the cancer cells and CAFs results in proliferation, invasion, and metastasis of the tumour [23]. During tumorigenesis, progression, and metastasis, TME ensures that pro-tumour immune cells such as M2 macrophages and regulatory T cells are activated. At the same time, anti-tumour immune cells such as CD8+ T cells and M1 macrophages are eliminated [19].

Glutamine from the CAFs of prostate and breast cancer carcinoma may also be secreted into the TME, serving other stromal and cancer cells as an energy source for the TCA cycle [24]. Furthermore, a metabolic coupling has been found for lactate, which is secreted by CAFs and used for the metabolism of breast cancer cells. In addition to that, CAAs release fatty acids used as an energy source in metastatic ovarian cancer cells [18], [25]. Moreover, there is evidence that glutamine metabolism, besides glucose metabolism, also contributes to the metabolic crosstalk between endothelial cells and other cells in the TME [18].

1.2.3 Extracellular vesicles in cell communication and cancer progression

Extracellular vesicles (EVs) are a heterogeneous group of membrane-bound vesicles produced and secreted by all cell types during physiological and pathological processes including tumours. Depending on the biogenesis, they are called exosomes (generated via the endolysosomal pathway), ectosomes (also called microvesicles and formed by protrusion and pinching off the cell membrane) or apoptotic bodies (formed during controlled cell death by membrane) [26]. Further classifications are made by size, density, function, morphology, and biochemical compositions [27], [28]. For a long time, it was assumed that crosstalk between cells only occurred via the release of soluble factors such as chemokines, cytokines, hormones, and growth factors and through direct cell-cell communication. EVs have previously been associated only with waste disposal systems allowing cells to secrete undesired cellular components into the extracellular space [29]. In recent years, attention has been drawn to the essential role of EVs in cell communication, through reaching the recipient cells in the local environment (paracrine mode) or through transportation to distant tissue via the circulation system (endocrine mode) [27], [28]. EVs contain proteins, nucleic acids, RNAs and metabolites, that can be exchanged or released as part of cell-cell communication [30]. Some proteins and lipids are expressed on the surface of the EVs, and others are found in the cargo. EVs, especially exosomes, are of great interest because their formation and secretion pathway allow the study of intracellular regulators and provide a fingerprint of their cell of origin [30], [31]. Stress, inflammation, or cell cycle

are among the many influences that can alter the cargo of EVs and thereby provide insight into general processes during physiological or pathological conditions [29].

There is evidence that cancer cells release more EVs than normal cells, which makes the analysis of the cargo of cancer EVs attractive [32]. Indeed, EVs can influence the behaviour of stromal cells, namely CAFs, CAAs and immune cells, by releasing nucleic acids, signalling molecules, oncogenic proteins and several second messengers, leading to tumour growth, invasion, and metastasis [19]. A study by Alharbi et al. [33] observed that low oxygen tension led to increased expression of hypoxia-related proteins and induced tumour-derived EV secretion. Moreover, those hypoxia-related proteins were involved in metabolic reprogramming, specifically related to the glycolytic pathway. In addition, normal cells, which were exposed to EVs secreted by hypoxic cells, show a significant increase in platinum resistance. Those results suggest that EVs containing hypoxia-related proteins can transmit chemoresistance to other tumour cells, which leads to further progression of the disease [33]. Since EVs are well protected from proteases and nucleases by their bi-layer structure of lipids, they can be isolated in many biofluids such as urine, blood, saliva, plasma and ascitic fluid. Therefore, EVs have great potential as a sensitive and non-invasive target to detect biomarkers for early diagnosis, follow-up and monitoring in cancer research [28], [32], [34], [35].

1.3 Metabolomics

1.3.1 Importance of metabolomics nowadays

Many studies regarding cancer research have focused on the expression of RNA and proteins, and some EV-derived cancer biomarkers have been transferred to clinical use. Small molecules such as metabolites have been somehow neglected, although they have the potential to rapidly reveal dynamic changes in metabolism downstream of proteins expression and genetic regulations [32].

Metabolomics, which is the newest member of the "omics" family, was first described in the scientific literature in the late 1990s and early 2000s. After the study of genomes (genomics), RNA transcripts (transcriptomics) and proteins (proteomics), metabolomics is the last element in the "omic" cascade and describes the study of small/low-weight molecules and yields the closest to the phenotype profile of an organism [36], [37]. Thus, metabolites represent the downstream, resulting in a relative amplification of changes in the genome, transcriptome, or proteome [38], [39].

The study of the metabolome has several advantages over the transcriptome and genome. First, an enzymatic reaction always depends on the availability of substrate and product as well as on the gene expression. Even if changes in expression level in proteins would have slight changes in fluxes, these can significantly affect the concentrations of metabolites. As a result, the metabolome is more sensitive to interfering factors than the transcriptome or proteome. In addition, metabolomic profiling is less expensive with higher throughput [39]. Metabolic response to changes in the environment varies rapidly (within seconds), whereas modifications in protein or mRNA take hours, days or even weeks. This rapid shift can be an advantage in the detection and progression of aggressive cancers [29]. Another advantage is the rapid separation and detection of metabolites by different substances such as proteins, nucleic acids and lipids with different chemical structures [1]. Moreover, while proteins and genomes are highly species-dependent, metabolites are mostly the same among species through the highly conserved metabolic pathways [29]. Since cancer is considered a metabolic disease, it is, therefore, useful to study the metabolome of cancer patients with the hope of finding metabolites as biomarkers for earlier diagnosis, progression, and treatment [1], [38], [40].

Although its many advantages, there are some limitations to metabolomics: In general, dynamic studies such as metabolomics, are very susceptible to physiological variations of the sample caused by genetic and environmental influences [41]. Inter- and intra-individualities such as gender, age, and genetic predisposition as much as lifestyle and diet have a great impact on the metabolome and should be considered when interpreting and analysing the generated data [36]. Increasing sample size can reduce those biological variations, however generating another limitation, namely the large amount of data generated, making the

interpretation and data analysis challenging [36], [41]. Unfortunately, metabolic profiling is a non-complete coverage technique in contrast to transcriptomics, as it is not possible to measure the whole metabolome of an organism due to technical restrictions resulting from the diverse chemical nature of metabolites and broad concentration range in which metabolites are present. Moreover, metabolic profiling of a sample is always a snapshot in time [39], [42]. This limitation can be minimised by sequential sampling and/or time series [41]. To get as close as possible to the complete metabolome, various technical applications can be combined to facilitate the extraction, detection, identification, and quantification of the metabolites [36]. The study design should be standardised in terms of sample collection, preparation, and analysis to ensure reproducibility. In addition, the influence of gender, age, diet, and samples such as saliva, plasma, and urine should be accurately documented, as all have a potential impact on the metabolome [36]. To reach the most complete coverage of the metabolome, a combination of analytical techniques such as high-performance liquid chromatography (HPLC), nuclear magnet resonance (NMR), enzymatic metabolite quantification and capillary electrophoresis coupled to mass spectrometry (CE-MS) should be applied [39], [42]. In addition, a combination of different sample preparation methods should be combined. For example, the solvent choice gives a high bias towards specific metabolic classes, that is why a combination of more than two extraction solvents covers a bigger metabolome [43].

1.3.2 Subdivisions of metabolomics

In the study of the metabolome, a distinction can be made between the quantification of the exo-metabolome (metabolic footprinting) and the endo-metabolome (metabolic fingerprinting), the two being closely related [42]. Cellular metabolism is influenced mainly by extracellular conditions such as osmolality or nutrient availability. At the same time, the metabolic footprinting monitors the consumption from and secretion into the growth medium of metabolites and highly reflects the cell's metabolism [39], [42]. Analysing the endo-metabolome is more complex than the exo-metabolome since metabolic fingerprinting requires the arrest of metabolism (quenching), efficient separation of extracellular metabolites from the medium as well as unselective extraction of metabolites. In contrast, the study of the exo-metabolome only requires a separation of metabolites in the medium. Thus, the study of intracellular metabolomes is more technically challenging and more likely to be biased [39].

The technique of detecting the metabolites can serve as a further subdivision of metabolomics. In untargeted metabolomics, thousands of unknown features are profiled. However, this is a great challenge and is used chiefly in the discovery of novel metabolites associated with a specific phenomenon. The most used technique is semi-targeted metabolomics, where many molecules are identified and quantified. This experiment is considered semi-targeted since the list of metabolites is defined, but the hypothesis may not be. In semi-targeted metabolomics, the metabolites are only quantified in relative terms, unlike in targeted

metabolomics, where absolute quantification is possible by purified standards such as isotope-labelled standards [40], [44]. Relative quantification is more straightforward to accomplish than absolute quantification, explaining its wide use. However, an important aspect of relative metabolite quantification is that the absolute amounts of metabolites in the sample under study affect the interpretation of measured relative changes. Thus, metabolites present at low concentrations may show significant relative changes in an experiment, even though these changes occur in a concentration range that may be too low to have biological significance [40].

1.3.3 Technique analysis of metabolomics

The most widely used techniques for the investigation of molecular composition are nuclear-magnet resonance (NMR) and mass spectrometry (MS). NMR is mainly used for targeted, quantitative metabolomics and detects the intrinsic magnetic property of atomic nuclei (also called the "spin"), which contains and decodes information about the chemical environment and thereby about the molecular structure [36], [44].

In MS, molecules are first ionised (adding either a positive or negative charge) and then passed through an electronic field. By mass-to-charge ratio (m/z), data of intact ions are collected at each time point, and the intensities are measured. Each ion has its own retention time in the mass spectrum, depending on the instrumental setup [44]. Multiple reaction monitoring (MRM) is an approach in MS, usually performed by a triple-quadrupole mass spectrometer. The first quadrupole filters the parent ion with a defined molecular weight, the second quadrupole fragments the selected molecules, and the third quadrupole detects characteristic fragments. For these reasons, parent and fragment ions must be pre-defined, the necessary energy for fragmentation needs to be optimised, and the retention time has to be defined before data acquisition for each metabolite [44].

MS is used mainly for semi-targeted and untargeted metabolomics, as it has a higher sensitivity, higher throughput and can measure more molecules in a complex biological sample. A major advantage of NMR over MS is that the analysis is non-destructive. In addition, the metabolites are measured quantitatively since the number of molecules is equal to the number of nuclei [38], [44]. However, this disadvantage in MS can be overcome by using internal standards prior to extraction and quantification of metabolites [44], [45].

Both liquid chromatography (LC) and gas chromatography (GC) are used for the separation of metabolites [44]. Advantages of LC are that a smaller volume (10-100 µL) is required than with a GC (0.1-0.2 mL) and the sensitivity is much higher (limit of detection (LOD) is around 0.5 nM for LC and 0.5 µM for GC). GC also requires the derivatisation of the molecules into the gaseous state. However, GC is superior to LC in

terms of separation resolution, reproducibility and robustness and the quantification it also higher with GC than with LC. However, these disadvantages of LC can be overcome by using well established and robust commercial kits for example by Biocrates Life Sciences or using a "black-box" such as the one from AB SCIEX Lipidyzer [38].

Another possibility for chemical analysis is by flow injection analysis (FIA), which is usually coupled to spectrophotometry or MS. Here, the sample is injected with a defined volume into a flow carrier solution steam, where it meets the carrier solution and reacts with it. The reaction product is then measured by a detector (MS or spectrophotometer). The sample is quantified by the amount of reaction product formed [46], [47].

1.3.4 Multivariate data analysis

Multivariate data analysis is a set of techniques to characterise the complex data generated by modern instrumentation. Principal component analysis (PCA) is the pioneer in chemometric analysis and allows the extraction and visualisation of systemic variations. The assumption here is that, in the case of strongly correlated groups, there is a third variable which is not directly measurable but appears "in the background" and is largely responsible for the correlation between the groups. Through dimensionality reduction, unsupervised PCA greatly reduces the apparent variability within a group to make this third variable, also called the "principal component", visible. A more detailed evaluation of the data is possible using partial least-squares (PLS). The main difference with PCA is that PLS transformation is supervised. Therefore, groups are pre-defined and the variables between the groups are illustrated as a second data table. With both methods, it provides a visual overview and a summary of all samples in the data set, across multiple variables. In addition, clusters, trends, and outliers become visible [41], [48], [49].

Other data processing techniques that are not feasible without multivariate computational tools include hierarchy clustering, numerous statistical tests such as t-test, ANOVA, and correspondence analysis. In addition, data visualisation plots are used to identify the largest differences between characteristics and specific signatures in the data [44]. For analysis of the metabolic pathway altered by cancer, a metabolite set enrichment analysis (MSEA) can be performed by also drawing on the quantitative data of the features present [50].

1.4 Aim of thesis

Accumulation of ascitic fluid in ovarian cancer patients is often associated with an aggressive progression and poorer prognosis. In clinical practice, these ascitic fluids are collected, which naturally contain pro-tumour components that can provide valuable information about the progression of the tumour. At present, a definitive diagnosis of the disease can only be obtained by a biopsy of the tumor tissue. To find a non-invasive method for diagnosis and prognosis, extracellular vesicles (EVs) are being investigated as essential mediators in the metabolic crosstalk of the tumour microenvironment (TME), which is a critical component in the pathogenesis of metastases and chemoresistance. At present, more focus has been placed on studying the cargo of EVs on proteomes and transcriptomes. Metabolomics is one of the younger "omics" family members and has been sparsely explored in the context of EVs.

This thesis aimed to characterize the complex metabolic signature of patient-derived biofluids and isolated EVs of ovarian cancer patients, focusing on finding differences between the biofluids, which are ascitic fluids and peritoneal washes, as well as EVs isolated from them. For this goal, three main intermediary objectives were defined:

I. **Implementation of AbsoluteIDQ® p180 kit (Biocrates).** The ready-to-use metabolomic kit enables targeted metabolomics. Here, the metabolites are isolated by detailed predetermined steps and detected by liquid chromatography- mass spectrometry and flow injection analysis. With the use of internal standards, the quantification of the metabolites has been done. In-house implementation of the method was done in order to analyse biofluids and isolated EVs from ovarian cancer patients.

II. **Metabolite extraction from different biological samples.** The focus was on the metabolome of the ascitic fluids and peritoneal washes as well as the corresponding EVs from ovarian cancer patients. In addition, samples of culture media supernatants, bean extracts and algae extracts were also explored with the p180 metabolomic kit from Biocrates as a way to test performance on different matrices.

III. **Metabolomic profiling of biofluids and EVs.** Main differences and commonalities between the four groups (ascitic fluids, peritoneal washes, EVs from ascitic fluids, EVs from peritoneal washes) were uncovered using multivariate data analysis such as PCA, hierarchical clustering and metabolic enrichment analysis.

2. Materials and methods

2.1 Patient biofluid samples and EVs

Permission for the use of ascitic fluids and peritoneal washes was obtained from 20 ovarian cancer patients treated at the Instituto Português de Oncologia de Lisboa Francisco Gentil (IPOLFG) between the years 2006 and 2013. Peritoneal wash samples were obtained during the standard-of-care surgery in patients without ascites by injecting 50-200 mL of saline solution into the peritoneal cavity, rinsing the area and recollecting the liquid. For ascitic fluids, a puncture of the peritoneal cavity is undertaken using a drainage bag and collecting the fluid inside the cavity. Immediately after collecting the biofluids, samples were centrifuged at 250 × g for 2 minutes before the supernatant was stored at -80 °C. Those samples were then transported the lab facilities at iBET at -80 °C. All samples were anonymised.

2.1.1 EV isolation and characterisation

Samples were used to isolate EVs in 2021 (approximately ten years after collection). EV isolation of all samples was performed according to Thery et al. [51] with some minor modifications and was followed through by the previous master's student using the "gold-standard" differential centrifugation method [52]–[54].

Briefly, larger volumes of biofluids were centrifuged, the supernatant recollected, and then further centrifuged. First, the biofluids were centrifuged at 2.000 × g to remove dead cells and other cells. Next, the supernatant was collected and further centrifuged at 12.000 × g. This centrifugation removed larger EVs and cell debris. Subsequent centrifugations at 110.282 × g were used to recover and purify the small EVs [54]–[56]. The whole centrifugation procedure was additionally done with phosphate-buffered saline (PBS) but without any sample as a control. At the last step of the centrifugation from PBS, the pellet was resuspended in water, being the extraction blank. To characterize the isolation process, for one of the ascitic fluid samples, both the isolated and discarded fractions, were collected to determine step-by-step characterisation [54], [57].

Western blot, transmission electron microscopy (TEM) and nanoparticle tracking analysis (NTA) were applied to verify the enrichment in EVs during and at the end of the isolation procedure. Western blot allows the identification of marker proteins in the EV fractions, both those typical EV components such as CD63 and tumour susceptibility gene 101 (TSG101) and those of expected contaminants namely Apolipoprotein-I (ApoA-I). Using NTA, the particle concentration and size in the fractions can be determined to ensure that mainly the small EVs (50-150 nm) were isolated. Finally, TEM shows the morphology of cells, where cup-shaped like morphology indicates the presence of EVs [57].

Using these three techniques, the enrichment in EVs was demonstrated, according to the guidelines of the International Society for Extracellular Vesicles (ISEV). The isolation of EVs was successful, shown in Trindade, Mendes et al. [58]. 10 out of 20 ascitic fluids (AFs), and 3 out of 5 peritoneal washes (PWs), were used to isolate EVs. A total of 20 ascitic fluids (AF1-20), 5 peritoneal washes (PW1-5), 10 EVs isolated from ascitic fluids (AF1-EV – AF10-EV), and 3 EVs isolated from peritoneal washes (PW1-EV – PW3-EV) were analysed. All samples were measured by Nanodrop to determine the protein concentration.

2.2 Metabolite extraction, quantification, and analysis

For the analysis of the metabolites of the biofluids and EVs, the ready-to-use commercial kit by Biocrates AbsoluteIDQ® p180 was used. Internal and external standards, as well as quality controls provided by Biocrates were used to ensure quality, reproducibility, and stability. The kit allows fully automated measurement up to 188 metabolites. The lipids and hexose are measured by FIA-MS, and LC-MS measures the small molecules such as biogenic amines and amino acids. Kit preparation and data analysis were performed, according to manufacturer's instructions. With the AbsoluteIDQ® p180 kit, an Ultimate 3000 Rapid Separation Quaternary HPLC System (Thermo Scientific), connected to a QTRAP 6500+ with TurboV™ Ion Source mass spectrometer (SCIEX) and an AbsoluteIDQ p180 Kit UHPLC column (Biocrates Life Sciences) were used and controlled by Analyst 1.7.2 software.

2.2.1 Implementation of metabolomic kit: first experiment

The first experiment aimed to find the ideal volume for the metabolite extraction and detection of the biofluids to ensure the highest yield of metabolites with a high performance of the analytical instruments. In addition, it was determined whether the EV concentration tested was sufficient to analyze metabolites.

2.2.1.1 System suitability test (SST) of the first experiment

Before starting any analysis with the metabolomic kit by Biocrates, a system suitability test (SST) must be performed according to manufacturer's protocol to check the inter-day system performance and to warm-up the system.

First, the system was cleaned with the wash solvent containing 50% acetonitrile (Optima™ LC-MS Fisher), 20% methanol (Optima™ LC-MS Fisher), 15% isopropanol (Optima™ LC-MS Fisher) and 15% water (Optima™ LC-MS Fisher). Next, the SST for the LC-MS was performed. The analytical column was installed and flushed for 20 minutes with 95% acetonitrile and 5% water at a 0.5 mL/min flow rate. After that, the starting conditions of 100% water with a flow rate of 0.8 mL/min and column oven temperature of 50 °C were equilibrated. The electro spray ionisation (ESI) electrode (SCIEX) positions were adjusted. Depending on the analysis, different positions were used: for the LC analysis x-axis was 8 and y-axis 2; for FIA analysis the x- and y-axis were 5. After the system had been calibrated, the system performance was evaluated by analysing blanks (methanol) and testmixes (one for the LC-SST and one for the FIA-SST, provided by Biocrates). The testmixes contain external standards in defined concentrations. If the results of the testmixes met the SST criteria, the experiment could be continued.

2.2.1.2 Implementation of the metabolomic kit in lab

	1	2	3
A	**Blank**	Cal7	QC2
B	**Zero** PBS	QC1	HepG2-EV
C	Cal1	QC2	AF-QC
D	Cal2	QC3	QC2
E	Cal3	**AF2** 2 µL	**AF4** 2 µL
F	Cal4	**AF2** 5 µL	**AF4** 5 µL
G	Cal5	**AF2** 10 µL	**AF4** 10 µL
H	Cal6	**AF2** 30 µL	**AF4** 30 µL

*Figure 1 – **Plate layout of the first experiment.** AF2 and AF4 were tested in four volumes (2, 5, 10 and 30 µL) and HepG2 with a total particle number of 2.0 × 10^9/well. Cal1-7 – calibration standards in seven concentration levels, QC1-3 – quality controls in three concentration levels, AF-QC – pooled QC from AF2 and AF4.*

For the first experiment, 24 wells of a 96-well plate were used, provided by Biocrates (Figure 1). The wells contained some of the internal standards and a filter. One well, the only without any internal standards, was defined as the blank to detect the background noise of the system. One zero as PBS (Sigma #P4417-50TAB) was used for the limit of detection (LOD). To generate a calibration curve for the LC-MS part, seven wells were filled with calibration standards in seven concentration levels (Cal1-7). Five wells were taken for the quality controls (QCs): QCs were available in three concentration levels (QC1-3), whereby QC2 in three replicates were placed on the plate for normalisation and validation of the analytical performance. Those three QC2 were distributed throughout the plate. Biocrates provided the seven calibration standards and the three quality controls.

Two ascitic fluid samples (AF2 and AF4) and one EV from culture media of ES-2 ovarian cancer cell line, previously isolated and characterised, were analysed in the first experiment to implement the method. For the EV, a total number of 2.0 × 10^9 particles per well were loaded, whereas four volumes were tested for ascitic fluids: 2 µL, 5 µL, 10 µL and 30 µL. AF2 had a total protein concentration of 29.922 ug/µL whereas AF4 had 45.058 ug/µL, both measured by Nanodrop. In order to avoid systemic errors by pipetting small volumes of 2 µL and 5 µL, 10 µL of each sample, they were pipetted and diluted with water to get the same concentration as with 2 µL, respectively 5 µL. (10 µL sample + 50 µL water and 10 µL sample + 10 µL water). Since the QC, provided in the kit, are pooled human plasma, in-house QC pooled with the two ascitic fluids each 10 µL were made and named "AF-QC".

As described in the manufacturer's protocol for human plasma, first, the ascitic fluids and AF-QC were centrifuged for 5 minutes at 5000 × g and 4 °C (Eppendorf). The reconstituted QC1-3 were centrifuged for 5 minutes at 2750 × g and 4 °C. First centrifugation of the samples and quality controls helped to separate unnecessary proteins and cell components from the liquid. For the HepG2-EV, there was no need for centrifugation since the sample has undergone many centrifugations during the EV isolation process.

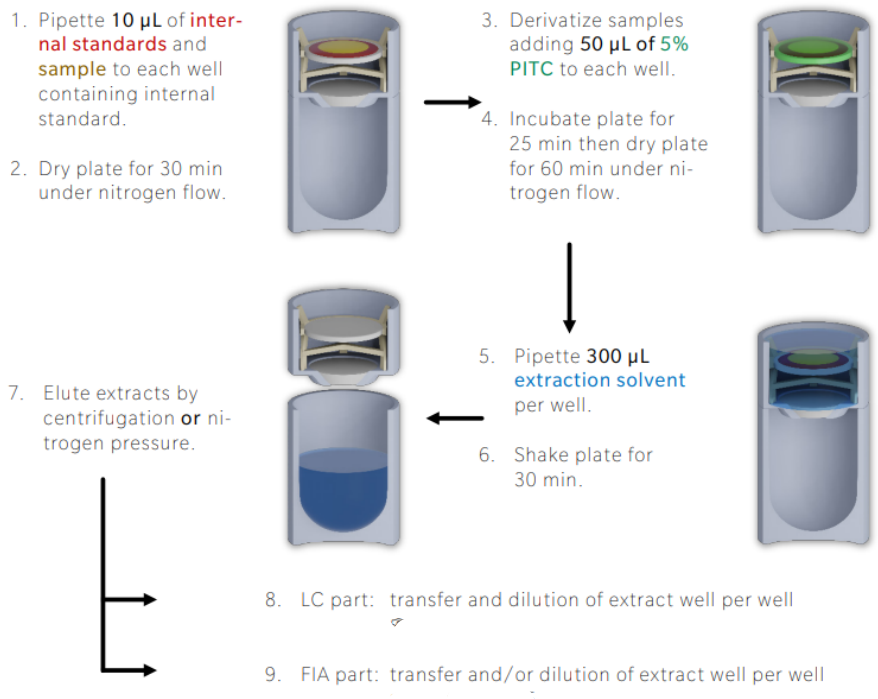

*Figure 2 – **Overview of lab work.** Between step 1. and step 2. an additional drying step was included due to filter capacity limitations of higher sample volume (30 µL). Source of figure: Biocrates* [59].

First, 10 µL of ISTD mix was added to each well except the blank (Figure 2). The ISTD mix was provided by Biocrates and contained additional internal standards. Due to filter capacity limitations, the 30 µL of the two ascitic fluids were loaded in two steps with a drying step in between. In detail, 15 µL of AF2 and AF4 were loaded onto the plate, followed by 30 minutes of drying under nitrogen**.** Next, 10 µL PBS as zero, 10 µL of the reconstituted Cal1-7 and 10 µL of QC1-3 were loaded onto the plate as well as the missing 15 µL of AF2 and AF4. Afterwards, all remaining samples and AF-QC were added to the plate, using 10 µL of each. A second drying step under nitrogen was performed., before adding 50 µL of derivatisation solution, which contained approximately 31% ethanol (Merck), 31% water, 31% pyridine (Carlo Erba), and 6% phenylisothiocyanate (PITC) (Sigma) to each well, including the blank. The plate was incubated for 25 minutes, followed by a 60 minute drying step under nitrogen. Next, 300 µL of extraction solvent containing 5 mM ammonium acetate (Carlo Erba) in methanol was added to each well, and the plate was shaken for 30 minutes at 450 rpm at room temperature. The plate was centrifuged for 2 minutes at 500 × g. As a last step the capture plate, which contained the sample extracts, were separated from the upper filter plate.

To transfer the sample extracts to the LC and FIA plate, first 150 µL from each well from the capture plate was taken and transferred to the LC plate. All wells were diluted with 150 µL of water. For the FIA analysis, 50 µL from the capture plate were transferred to the FIA plate and diluted with 450 µL FIA solvent

(Biocrates). Both LC and FIA plates were sealed and shaken for 5 minutes at 600 rpm (Eppendorf). The LC plate was run first, followed by the FIA plate, which was done the day after.

2.2.2 Analysis of samples: second experiment

The method implemented in the first experiment was used to examine the other samples of biofluids as well as the isolated EVs. In addition, samples from two other projects were included in the experiment to implement methods for further analysis.

2.2.2.1 SST of the second experiment

SST was performed as mentioned previously in section 2.2.1.1 to check the inter-day system performance and to warm-up the system.

2.2.2.2 Analysis of biofluids and EVs

	1	2	3	4	5	6	7	8	9	10	11	12
A	**Blank**	**Zero** extraction blank	Cal7	**AF2 - EV** category 2	**AF4 - EV** category 2	**AF5 - EV** category 3	**AF8** 10 µL	**AF19** 10 µL	**PW1** 10 µL	**PW3 - EV** category 0	Project 1	Project 2
B	**Zero** PBS	**Zero** extraction blank	QC1	**AF2 - EV** category 3	**AF4 - EV** category 3	**AF13** 10 µL	**AF8 - EV** category 0	QC2	**PW1** 30 µL	**PW4** 10 µL	Project 1	Project 2
C	**Zero** PBS	Cal1	QC2	**AF11** 10 µL	**AF5** 5 µL	**AF14** 10 µL	**AF15** 10 µL	**AF10** 10 µL	**PW1 - EV** category 1	**PW4** 30 µL	Project 1	Project 2
D	**Zero** PBS	Cal2	QC3	**AF3** 10 µL	**AF5** 10 µL	**AF6** 10 µL	**AF16** 10 µL	**AF10 -EV** category 1	**PW2** 10 µL	Project 1	Project 1	Project 2
E	**Zero** water	Cal3	**AF1** 10 µL	**AF3 - EV** category 0	**AF5** 15 µL	**AF6 - EV** category 1	**AF17** 10 µL	**AF10 -EV** category 2	**PW2** 30 µL	QC2	Project 1	Project 2
F	**Zero** water	Cal4	**AF1 - EV** category 0	**AF12** 10 µL	**AF5 - EV** category 1	**AF6 - EV** category 2	**AF9** 10 µL	**AF20** 10 µL	**PW2 - EV** category 1	Project 1	Project 1	Project 2
G	**Zero** water	Cal5	**AF2** 10 µL	**AF4** 10 µL	QC2	**AF7** 10 µL	**AF9 - EV** category 1	**PW5** 10 µL	**PW3** 10 µL	Project 1	Project 2	Project 2
H	**Zero** extraction blank	Cal6	**AF2 - EV** category 1	**AF4 - EV** category 1	**AF5 - EV** category 2	**AF7 - EV** category 0	**AF18** 10 µL	**PW5** 30 µL	**PW3** 30 µL	Project 1	Project 2	QC2

*Figure 3 – **Plate layout of the second experiment.** Twenty samples of ascitic fluids and five samples of peritoneal washes were tested, whereby peritoneal washes were analysed in two volumes (10 and 30 µL). Furthermore, ten EVs, isolated from ascitic fluids and three EVs, isolated from peritoneal washes, were analysed. Category 0 – lower than 5.0 × 10^9 particles/well: AF1-EV, AF3-EV, AF7-EV, AF8-EV and PW3-EV; category 1 – 5.0 × 10^9 particles/well: AF2-EV, AF4-EV, AF5-EV, AF6-EV, AF9-EV, AF10-EV, PW1-EV and PW2-EV; category 2 – 1.2 × 10^{10} particles/well: AF2-EV, AF4-EV, AF5-EV, AF6-EV and AF10-EV; category 3 – 4.0 × 10^{10} particles/well: AF2-EV, AF4-EV and AF5-EV.*

For the analysis of the biofluids and ÈVs, a 96 well plate with an integrated filter and some internal standards was used (Figure 3). One well was used for the blank without any internal standards. Three different zeros, each in replicates of three, were added to the plate and used for individual calculations of the LOD. PBS was considered as the zero of the ascitic fluids (AF1-20), Project 1 and Project 2. For AF1–10-EV and PW1–3-EV EVs, the extraction blank was used as the zero. Water was used as a back-up zero for the EVs, in case that the extraction blank does not give good results. QC2 were added in five replicates and distributed throughout the plate to validate the kit's performance and allow cross-plate normalisation.

As described in the implementation of the method, the ascitic fluids, peritoneal washes and quality controls were centrifuged. For ascitic fluid samples, 10 µL were added to the corresponding well except for AF5, which was additionally tested at 5 µL and 15 µL. To avoid systemic error by pipetting small volumes, 10 µL of AF5 were diluted with water to get the same concentration as 5 µL of AF5 (10 µL AF5 + 10 µL water). All PWs (PW1-5) were analysed at 10 µL and 30 µL. For all the EVs, no centrifugation was needed. Four categories were assembled for all EVs (AF1–10-EV and PW1–3-EV), depending on the total particle number: category 0 was below 5.0×10^9 particles per well. Category 1 contained all EVs with 5.0×10^9 particles per well. Category 2 with 1.2×10^{10} and category 3 with 4.0×10^{10} particles per well were generated from the more concentrated EVs. If more than 15 µL were needed to achieve the total particle number, sequential loading with additional drying was performed. A detailed plan of the drying steps can be found in the appendix (Table A. 1 & 2).

Since additional wells were available, samples from other projects were included in the kit preparation. Ten samples from Project 1, consisting of supernatants from culture media and nine samples from Project 2, consisting of animal plasma, algae and beans extracts, were analysed. 10 µL per sample from Project 1 and Project 2 were loaded onto the plate.

The derivatisation, incubation, extraction, centrifugation of the plate and the separation of the capture plate to the LC and FIA plates was performed as previously described in section 2.2.1.2. The LC plate was run first, and the FIA plate the day after.

2.3 Data transformation and normalisation

All sample concentrations were normalised on the observed concentration changes of the five replicates from QC2, using MetIDQ™ (Biocrates). Concentration data, produced by MetIDQ™, were normalised by MetaboAnalyst 5.0 Web Server [60]. Normalisation between samples were achieved dividing by the median metabolite concentration for each sample. Metabolite concentrations were log-transformed and normalised by auto-scaling, where the variables are mean-centred and divided by the standard deviation of each variable. Those normalisation methods obtained a Gaussian-like distribution of the metabolites. The symmetry of the boxplots of the metabolites was used to evaluate the normalisation choice. The five replicates of QC2 were also checked after normalisation to evaluate if the QC data points cluster together to validate the stability of the analytical performance [61], [62].

2.4 Statistical analysis

Multivariate data analysis was used to visualize the data generated by MetIDQ™. PCA was used to reduce the dimensions and to distinguish similarities and differences of the samples. Hierarchical clustering analysis (HCA) was used to show the top 25 metabolites selected by t-test/ANOVA. Metabolite set enrichment analysis (MSEA) of the quantitative data was performed to gain knowledge of affected metabolic pathways. For the presentation of the differences among the groups, MetaboAnalyst 5.0 was used [41], [49], [60]–[62].

3. Results and discussion

3.1 Characterization of samples

3.1.1 Patient cohort

Ascitic fluids and peritoneal washes were collected during surgical resection of the tumour tissue. Ascitic fluid samples were taken corresponding to 16 high-grade serous adenocarcinomas (HGSC), one low-grade serous adenocarcinoma (LGSC) and other tree samples without specific information. From the peritoneal washes, in total five samples were analysed: two HGSCs, one without specific information, one of endometrium carcinoma and one of non-gynecological adenocarcinoma. All samples, including the peritoneal washes were tested positive for neoplastic cells. Positive peritoneal cytology is a sign of peritoneal metastasis [63]. CA125, one of the biomarkers for ovarian cancer, is present in elevated levels in the blood, serum and ascitic fluid [64]. The cut-off value is 250 U/mL [65]. All patient samples exceed this threshold in this study. AF11–AF20, PW4 and PW5 were delivered at a later date, and some information regarding particle concentration, as well as patient-relevant information, are still missing. Nevertheless, all samples were analysed (Table 1).

*Table 1 – **Table of the patient cohort.** The IPOLFG provided ascitic fluids and peritoneal washes from ovarian cancer patients between 200-1000 µL, including patient characterization. EVs are available from ascitic fluids AF1–10 and peritoneal washes PW1–3 (AF1-EV – AF10-EV, PW1-EV – PW3-EV). Sample ID: AF – Ascitic fluid; PW – peritoneal wash; AF-EV – isolated extracellular vesicle from ascitic fluid; PW-EV – isolated EV from peritoneal wash. Histological classification: ADC – adenocarcinoma; EC – endometrium carcinoma; NG-ADC – non-gynecological adenocarcinoma. Status: DD – diseased from disease; DF – disease-free; DC – disease carrier. CA125 – Cancer Antigen. Nanodrop: measured µg/µL proteins. N.A. – not available.*

	Sample ID	Volume (µL)	Histological classification	Histological grade	Histological stage	Status	CA125 (U/mL)	Nanodrop (µg /µL protein)		Sample ID
Ascitic fluids	AF1	250	serous ADC	high grade	III C	DD	3776.4	39.634	Isolated EVs from ascitic fluids	AF1-EV
	AF2	200	serous ADC	high grade	IV B	DD	6872.9	29.933		AF2-EV
	AF3	1000	serous ADC	high grade	III C	DF	98836.0	55.903		AF3-EV
	AF4	200	serous ADC	low grade	I C	DF	724.3	45.058		AF4-EV
	AF5	1000	serous ADC	high grade	III C	DD	31423.0	31.256		AF5-EV
	AF6	200	serous ADC	high grade	III C	DD	83582.3	44.376		AF6-EV
	AF7	1000	serous ADC	high grade	III B	DC	88858.8	43.020		AF7-EV
	AF8	1000	serous ADC	high grade	III C	DC	877.0	57.710		AF8-EV
	AF9	1000	serous ADC	high grade	III C	DC	22755.2	42.836		AF9-EV
	AF10	1000	serous ADC	high grade	IV A	DF	561.4	35.853		AF10-EV
	AF11	N.A.	serous ADC	high grade	III C	DD	N.A.	N.A.		-
	AF12	N.A.	serous ADC	high grade	IV B	DD	N.A.	N.A.		-
	AF13	62	serous ADC	high grade	III A	DD	1751.7	N.A.		-
	AF14	N.A.	serous ADC	high grade	IV B	DD	N.A.	N.A.		-
	AF15	N.A.	serous ADC	high grade	III C	DD	N.A.	N.A.		-
	AF16	N.A.	serous ADC	high grade	III C	DD	N.A.	N.A.		-
	AF17	N.A.	serous ADC	high grade	IV B	DC	N.A.	N.A.		-
	AF18	N.A.	N.A.	N.A.	N.A.	DD	N.A.	N.A.		-
	AF19	N.A.	N.A.	N.A.	N.A.	DD	N.A.	N.A.		-
	AF20	N.A.	N.A.	N.A.	N.A.	DF	N.A.	N.A.		-
Peritoneal washes	PW1	1000	EC	-	I A	DD	7778.6	45.015	Isolated EVS from peritoneal washes	PW1-EV
	PW2	200	serous ADC	high grade	IV A	DF	9299.1	42.762		PW2-EV
	PW3	200	NG-ADC	-	IV B	DD	928.1	35.402		PW3-EV
	PW4	N.A.	serous ADC	N.A.	IV B	DC	N.A.	N.A.		-
	PW5	N.A.	serous ADC	high grade	III C	DC	3707.5	N.A.		-

3.1.2 Isolated EVs

EVs from ascitic fluids (AF1-EV – AF10-EV) and three EV samples from peritoneal washes (PW1-EV – PW3-EV) were available for metabolomics. The volume of the isolated EV samples was limited and ranged from 40 to 100 µL. Exact volumes of EV samples can be found in Table 2. 10 EV samples were isolated from patients with HGSC, nine from ascitic fluid and one from the peritoneal wash. The other EVs were different regarding tumour classification: one LGSC, one endometrium carcinoma and one from non-gynecological adenocarcinoma (Table 2).

*Table 2 – **Table of isolated EVs.** Sample ID: AF-EV – isolated extracellular vesicle from ascitic fluid; PW-EV – isolated extracellular vesicle from peritoneal wash. Histological classification: ADC – adenocarcinoma; EC – endometrium carcinoma; NG-ADC – non-gynecological adenocarcinoma. Status: DD – diseased from disease; DF – disease-free; DC – disease carrier. Nanodrop: measured µg/µL proteins. NTA – nanoparticle tracking analysis. N.A. – not available.*

	Sample ID	Histological classification	Histological grade	Histological stage	Status	Volume (µL)	Nanodrop (µg /µL protein)	NTA (particle/mL)
Ascitic fluid	AF1-EV	serous ADC	high grade	III C	DD	64	0.098	1.60E+10
	AF2-EV	serous ADC	high grade	IV B	DD	65	0.708	1.08E+12
	AF3-EV	serous ADC	high grade	III C	DF	55	0.357	1.00E+11
	AF4-EV	serous ADC	low grade	I C	DF	100	3.178	1.35E+13
	AF5-EV	serous ADC	high grade	III C	DD	62	2.103	1.50E+12
	AF6-EV	serous ADC	high grade	III C	DD	50	3.042	4.40E+11
	AF7-EV	serous ADC	high grade	III B	DC	40	0.914	N.A.
	AF8-EV	serous ADC	high grade	III C	DC	65	0.116	2.12E+10
	AF9-EV	serous ADC	high grade	III C	DC	60	0.151	1.22E+11
	AF10-EV	serous ADC	high grade	IV A	DF	55	0.641	4.40E+11
Peritoneal wash	PW1-EV	EC	-	I A	DD	60	0.531	2.40E+11
	PW2-EV	serous ADC	high grade	IV A	DF	80	0.193	8.25E+10
	PW3-EV	NG-ADC	-	IV B	DD	100	0.055	1.60E+10

For all EVs except for AF7-EV, because it was isolated to a later date, data from NTA and Nanodrop were available, indicating the EVs concentration. The hypothesis of the experimental workplan was that more concentrated EVs concerning the measured particles lead to higher extractions of metabolites. These values were thus taken to find suitable concentrations and loading volumes for further analysis.

3.2 Implementation of AbsoluteIDQ® p180 kit

3.2.1 Classes of metabolites

Using the AbsoluteIDQ® p180 kit 21 biogenic amines, 21 amino acids, one hexose, 40 acylcarnitines (Cx:y), 15 sphingolipids (SM Cx:y), and 90 glycerophospholipids (14 of which belong to lysoglycerophosphocholines (lysoPC Cx:y) and 76 to glycerophosphocholines (PC Cx:y)) can be measured and quantified. A detailed list of metabolites can be found in the appendix (Table A. 3–9). Cx:y identifies the chain of lipids, whereby x stands for the number of carbons in the side chain and y for the double bonds present in the chain. However, the technology is limited since both – the localisation of the double bonds and the configuration of the carbon atoms – cannot be differentiated. In the case of phospholipids, a distinction is made between an ester (a) and an ether (e) in the glycerol moiety, where the two letters determine the positions of the two glycerol (aa = diacyl, ae = acyl-alkyl), with a single letter representing a single fatty acid (a = acyl, e = alkyl). In the case of phospholipids, a further distinction is made between lysophosphatidylcholines (lysoPC), where only a single fatty acid can be present, and phosphatidylcholines (PC). In the case of sphingolipids, a distinction is made between sphingomyelins (SM) and hydroxysphingomyelins (SM(OH)) [66].

3.2.2 Selection of samples

Only 24 wells were available, with 12 wells already occupied for the standards. For ascitic fluid and peritoneal washes, PBS was chosen as zero because PBS most closely resembles the matrix of the biofluids. Replicates of three zeros is recommended, to calculate the LOD of the samples in high precision. However, since we have a limited number of wells, and the first experiment serves as implementation, no replicates of the zero were done. Cal1-Cal7 are used for the quantification of the LC-MS, which measures the biogenic amines and amino acids. Quality controls in three concentration levels validate the analytical performance, with QC2 in replicates. Therefore, it is recommended by Biocrates to use replicates of three to five to have a higher quality of data and for data normalisation. Since few wells are available in the implementation of the method, QC2 was used in three replicates. Finally, those QC2 were distributed to achieve quality control over the whole plate. The blank, which detects the background of the MS system, does not contain any internal standards but will be treated the same as all samples and standards.

Two ascitic fluids of different concentrations were used to implement the method. AF2, with a protein concentration of 29.992 µg/µL was lower concentrated than AF4 with 45.058 µg/µL. These two ascitic fluids were chosen because they represent the protein concentration range of all ascitic fluids, and as enough

volume was available. To find the best concentration for metabolite detection, both ascitic fluids were tested at 2, 5, 10, and 30 µL.

EVs from culture media of ES2-cells were pipetted onto the plate with a total number of 2.0×10^9 particles per well, resulting in a volume of 18 µL. The particle number was chosen so that approximately 80% of the EVs from the patient cohort with 10 µL would reach similar protein concentration. Nevertheless, by changing the loading volume, EV concentrations of some samples could potentially be increased when the methodology is implemented.

3.2.3 Validation of the analytical performance

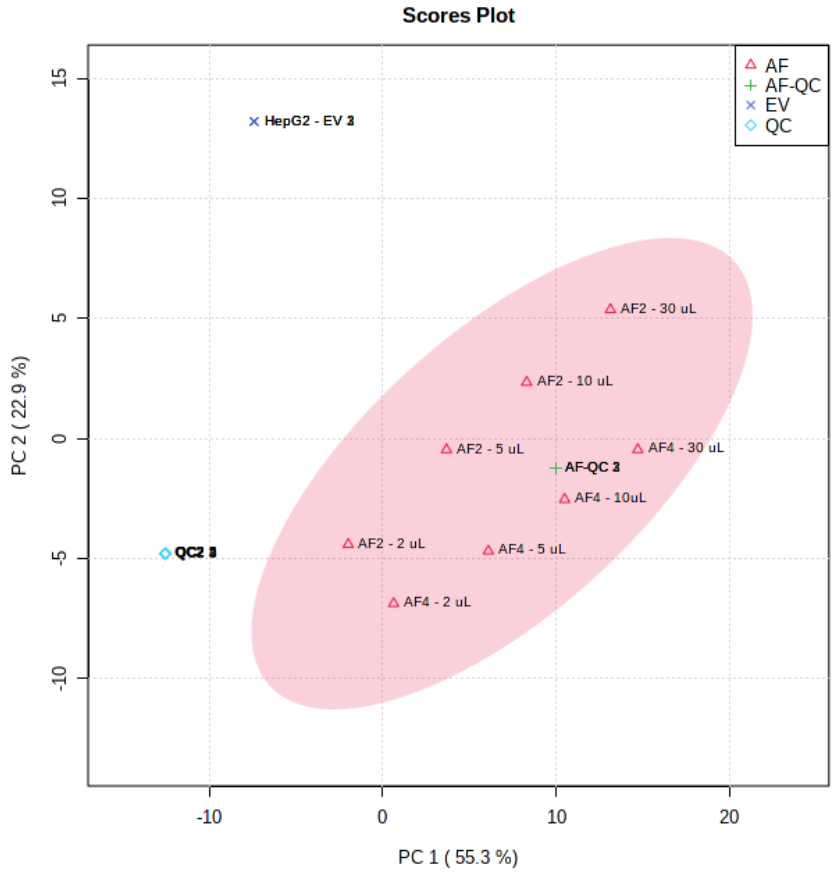

*Figure 4 – **PCA from the first experiment.** AF2 and AF4 in four volume levels (2, 5, 10 and 30 µL). QC2 and HepG2-EV are clearly separated from the ascitic fluids and from each other. QC2 in three replicates are clustered together, indicating good analytical performance. No further advantages of AF-QC could be seen.*

The analytical performance of the experiment was evaluated by PCA (Figure 4). It can be observed that the three QC2 from different wells of the plate cluster closely together, suggesting that the method reproducibility and robustness is given by showing the same results. Moreover, QC2s are separated from the ascitic fluids, which was expected as the QC2 is a spiked human plasma sample, therefore, different from ascitic

fluid samples. No further advantages of the in-house AF-QC could be seen and therefore it was excluded from further analysis.

3.2.4 Analysis of ascitic fluids

3.2.4.1 Selection of the best loading volume

For both AF2 and AF4, it was shown that higher volumes correspond to more detected and quantified metabolites (Figure 5). In detail, 116 metabolites were detected in 2 µL volume of AF4, from which 111 were quantified and five were only detected. At 5 µL, the number of identified metabolites increased to 123, whereby 117 were quantified. This number increased at higher loading volumes (140 detected metabolites, from which 132 were quantified at 10 µL), reaching its peak at 30 µL loading volume in which 143 metabolites were quantified from 155 detected metabolites. The same trend can be observed with AF2 and similar results were achieved (2 µL: 111 identified/102 quantified metabolites – 5 µL: 125/119 – 10 µL: 139/131 – 30 µL: 156/147).

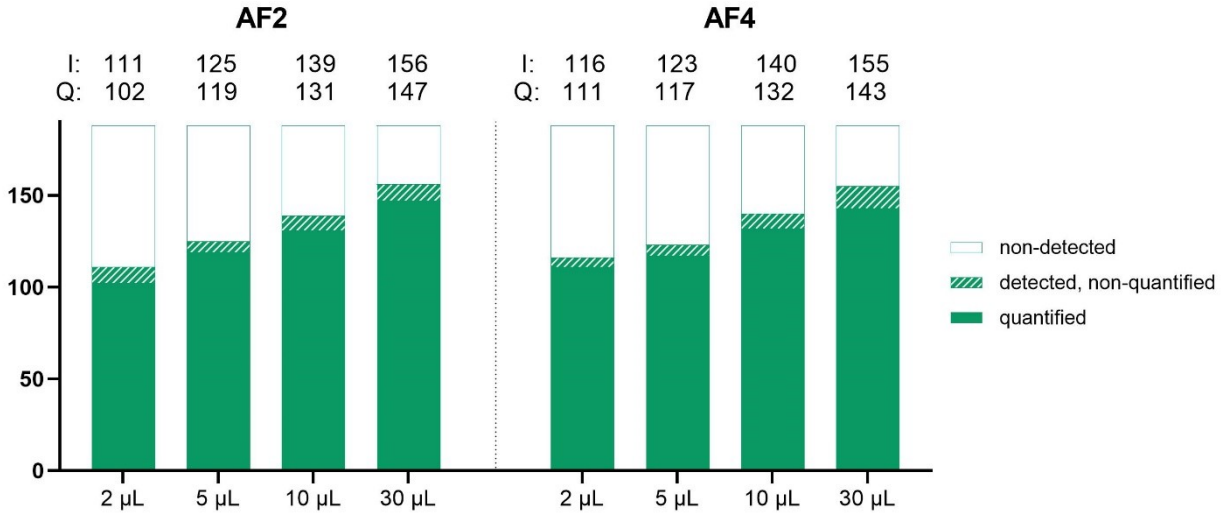

*Figure 5 – **Metabolites quantified and detected in AF2 and AF4 samples at four distinct volumes.** Most metabolites could be detected and quantified at 30 µL. Lower volume yield fewer metabolites. I – number of identified metabolites (detected, non-quantified + quantified metabolites), Q – number of quantified metabolites. X-axis: loading volume – y-axis: number of metabolites. In theory, a total of 188 metabolites can be detected with the kit.*

An additional important aspect to evaluate the results is the performance of the MS. The performance of the LC is shown by the fact that (i) peaks are well separated from each other, indicating good detectability of individual metabolites, and (ii) there is no sign of tailing or fronting of the individual peaks in the diagrams. In the FIA analysis, good performance can be observed when no signal occurs until about 0.7 minutes in retention time, followed by an intensity increase reaching a plateau until a drop of signal at around 1.7 minutes in retention time happens.

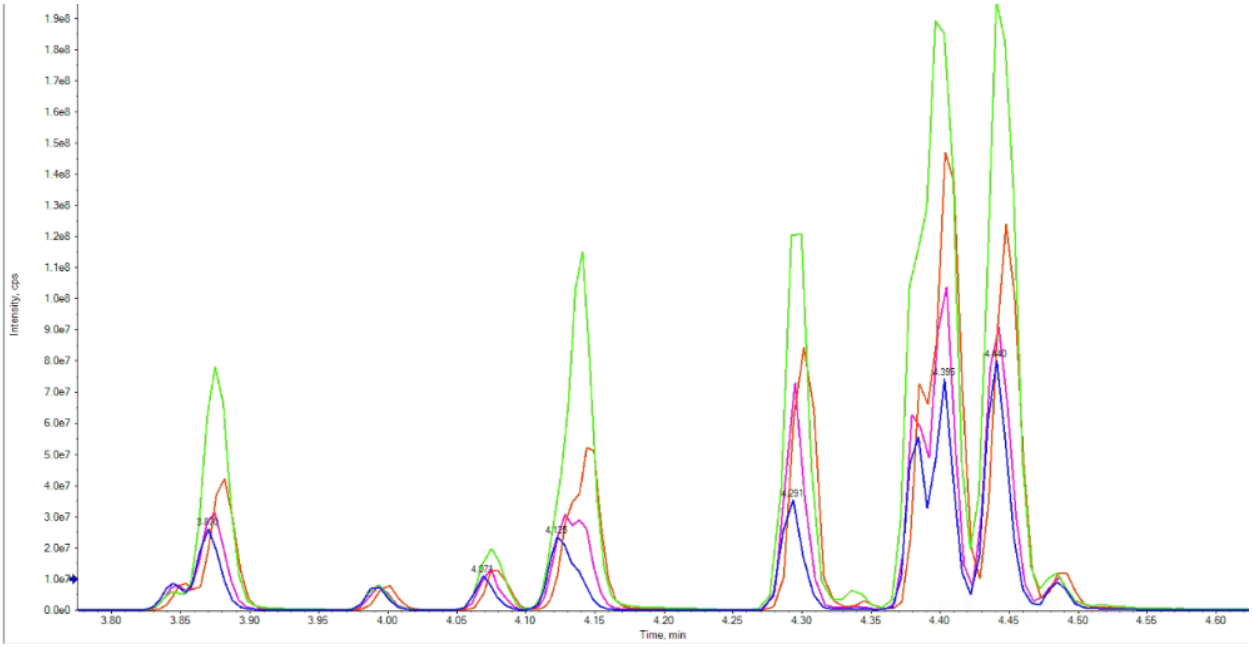

*Figure 6 – **LC diagram of AF2 in four loading volumes**. Between 4.35 and 4.45 minutes, no clear separation of the peak intensities can be seen at 30 µL. Blue – 2 µL; pink – 5 µL; red – 10 µL; green – 30 µL. X-axis – time (min); y-axis – intensity (cps).*

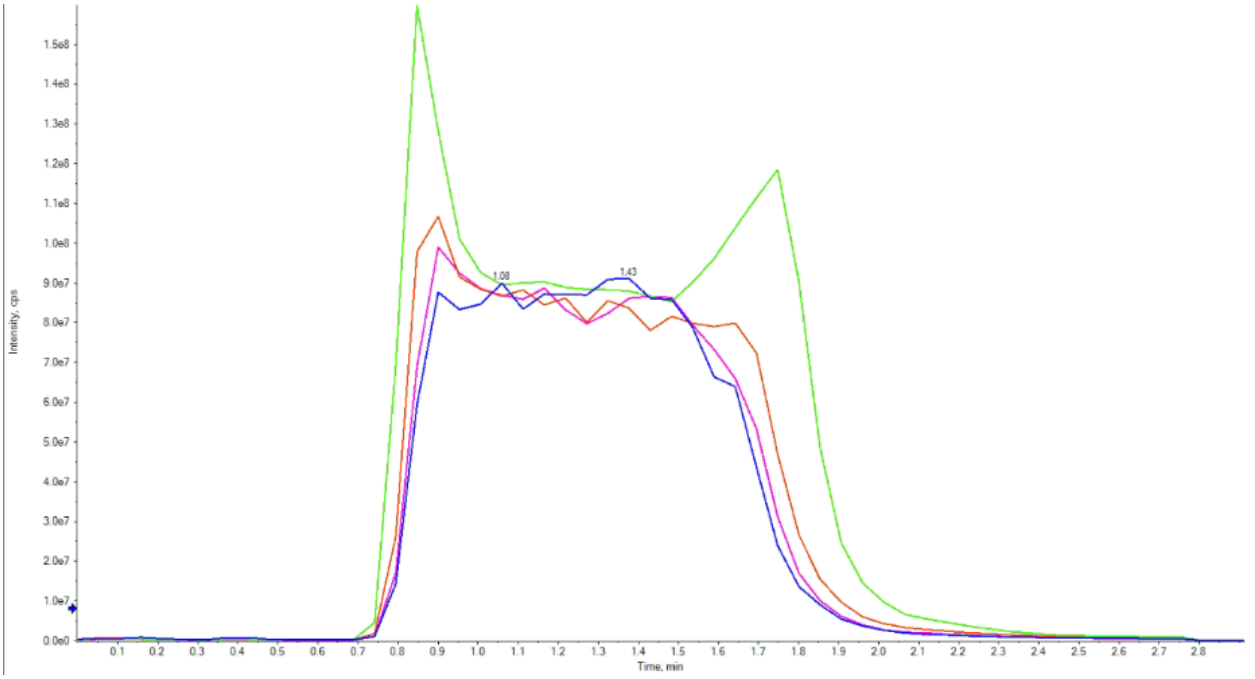

*Figure 7 – **FIA diagram of AF2 in four loading volumes.** Conspicuous peaks at the beginning and at the end of the signal at 30 µL, indicating saturation of the sample. Blue – 2 µL; pink – 5 µL; red – 10 µL; green – 30 µL. X-axis – time (min); y-axis – intensity (cps).*

Both AF2 and AF4 showed signs of metabolite saturation at 30 µL (Figure 6 and 7 of AF2, Figures A.1 and A.2 of AF4 in appendix). Although the peaks are well separated in the LC analysis, an overlap of two peaks were detected between 4.35 minutes and 4.45 minutes in retention time. Slight fronting could be detected, which indicated exceeding the analytical column capacity. In the FIA analysis, the saturation becomes even more evident, as unnatural peaks are present both at the beginning and the end of the signal.

These results suggest an overload of the analytical column at 30 µL sample loading, or oversaturation in the FIA analysis, suggesting that these results are not reliable. The second highest metabolite yield was obtained at 10 µL. No signs of overloading or saturation were detected in either FIA or LC diagram. As a result, 10 µL loading volume was considered for further analysis.

3.2.4.2 Metabolites detected and quantified in AF2 and AF4

*Table 3 – **Identified and quantified metabolites of AF2 and AF4 at 10 µL divided by the classes of metabolites**. Potential metabolites – number of metabolites, which can be measured by Biocrates p180 metabolomic kit in total. Q – quantified metabolites. NQ – D – non-quantified, detected metabolites, ND – non-detected metabolites.*

		AF2 – 10 µL			**AF4 – 10 µL**		
	Potential metabolites	*Q*	*NQ - D*	*ND*	*Q*	*NQ - D*	*ND*
Acylcarnitines	40	11	6	23	12	63	25
Amino acids	21	21	0	0	20	1	0
Biogenic amines	21	8	2	11	7	4	10
Lyso-phosphatidylcholines	14	7	0	7	8	0	6
Phosphatidylcholines	76	68	0	8	70	0	6
Sphingolipids	15	15	0	0	14	0	1
Sugars	1	1	0	0	1	0	0
Total	188	131	8	49	132	8	48

Investigating the metabolite classes of AF2 at 10 µL, 11/40 acylcarnitines, 21/21 amino acids, 8/21 biogenic amines, 7/14 lysophosphatidylcholines, 68/76 phosphatidylcholines, 15/15 sphingolipids, and 1/1 hexose were quantified (Table 3). Six acylcarnitines and two biogenic amines could be detected but not quantified. In total, 139 metabolites could be identified, of which 131 were quantified. A similar picture is seen in AF4 at 10 µL: 132 metabolites of 140 identified metabolites were quantified. Looking more closely at the metabolite classes in this sample, 12/40 acylcarnitines, 20/21 amino acids, 7/21 biogenic amines, 8/14 lysophosphatidylcholines, 14/15 sphingolipids, and 1/1 hexose could be quantified, whereas three acylcarnitines, one amino acid and four biogenic amines were only detected but not quantified (Table 3).

Interestingly, little difference in metabolite extraction was seen, although AF4 had higher total protein concentration (45.058 µg/µL) than AF2 (29.933 µg/µL). Similar metabolites can be detected in both ascitic

fluids while only the concentrations of those varied. Concluding, the concentrations of the metabolites need to be analysed in more detail later.

3.2.5 Analysis of HepG2-EV

3.2.5.1 Metabolites of HepG2-EV

In the HepG2-EV sample, isolated from culture media of ES2- cells, 86 metabolites were identified, 74 quantified and 12 non-quantified (Figure 8). Most of the detected metabolites were from the lipid family: 5 lysophosphatidylcholines, 50 phosphatidylcholines and 14 sphingolipids were quantified in the EVs. Five acylcarnitines could be detected, with only three being quantified. The results of the amino acids and biogenic amines are modest. Not a single metabolite could be quantified among the amino acids, but nine amino acids could be detected. In addition, two biogenic amines could be quantified, and another nine biogenic amines fell below the limit of quantification and could, therefore, only be detected. No hexose could be identified in the EVs. Due to the fact that EVs have a lipid membrane, it makes sense that primarily lipids could be detected [35].

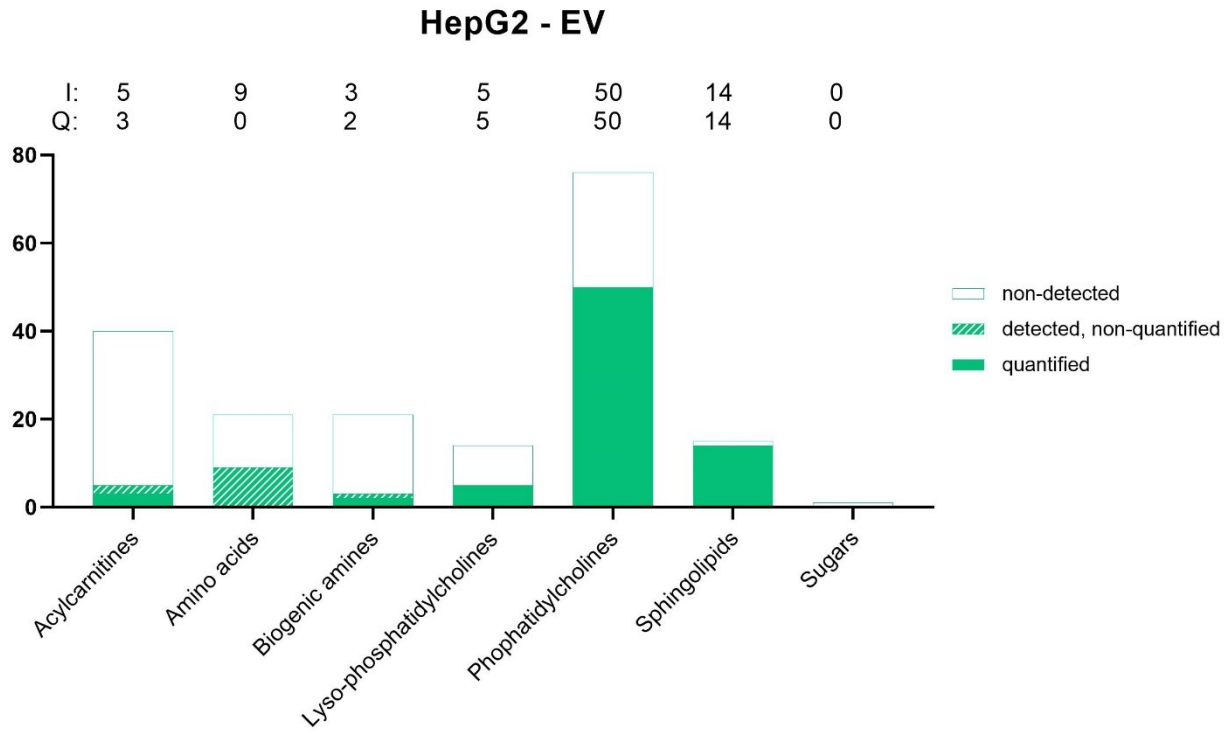

*Figure 8 – **Identified and quantified metabolites from HepG2-EV.** Mostly phospholipids and sphingolipids can be detected in the EVs. I – number of identified metabolites (detected, non-quantified + quantified metabolites), Q – number of quantified metabolites. X-axis: metabolite classes – y-axis: number of metabolites. In theory, 40 acylcarnitines, 21 amino acids, 21 biogenic amines, 14 lyso-phosphatidylcholines, 76 phosphatidylcholines, 15 sphingolipids and 1 hexose can be detected in total with the kit.*

3.2.5.2 Focus on biogenic amines and amino acids

The main goal of the investigation of the EVs was to detect not only lipids but also some other metabolites from other classes, such as biogenic amines and amino acids. With MetIDQ™, only the concentrations of metabolites over the lower limit of quantification (LLOQ) are valid and can be quantified. However, in the MS system, a concentration is measured even for the non-quantifiable metabolites. These values are unreliable and only indicate metabolites present in the sample, but the exact concentration is too low to measure accurately. Nonetheless, this value serves well as an indication of how much EV concentration is still missing to overcome the cut-off value of the LLOQ, which is indicated for each individual metabolite by MetIDQ™. The multiplier was calculated to exceed the threshold for all amino acids and biogenic amines that were detected but below the LLOQ. This calculation was also used for the metabolites from the biogenic amines and amino acids that were under the LOD. An estimated value of MetIDQ™ is also given here, which may be considered rough approximation (Table 4).

*Table 4 – **Calculation of x-fold of amino acids and biogenic amines for exceed LLOQ and LOD**. Light green – metabolites in 2,5-fold concentration; middle-light green – metabolites in 6-fold concentration; dark green – metabolites in 20-fold concentration; red – more than 20-fold concentration needed to catch those metabolites. LOD – limit of detection; LLOQ – lower limit of quantification, given by Biocrates; EV conc. – measured concentration of metabolite in µM; x-fold – the multiplicator to exceed the LLOQ of each metabolite.*

Metabolites >LOD, <LLOQ

Metabolite	LLOQ [µM]	EV conc. [µM]	x-fold
Alanine	20.00	**11.300**	1.8
Glutamine	20.00	**4.810**	4.2
Glutamic acid	10.00	**2.940**	3.4
Isoleucine	5.00	**1.670**	3.0
Phenylalanine	5.00	**0.289**	17.3
Serine	5.00	**1.010**	5.0
Threonine	5.00	**3.030**	1.7
Tyrosine	5.00	**0.739**	6.8
Valine	10.00	**0.600**	16.7
Spermidine	0.25	**0.135**	1.9

Metabolites, <LLOQ, <LOD

Metabolite	LLOQ [µM]	EV conc. [µM]	x-fold
Arginine	5.00	**0.122**	41.0
Asparagine	5.00	**1.230**	4.1
Aspartic acid	5.00	**0.460**	10.9
Citrulline	5.00	**0.639**	7.8
Leucin	50.00	**1.360**	36.8
Methionine	5.00	**0.032**	156.3
ADMA	0.25	**0.013**	19.2
Creatinine	10.00	**0.429**	23.3
DOPA	0.50	**0.018**	27.8
Dopamie	1.00	**0.013**	76.9
Sarcosine	1.00	**0.026**	38.5
Serotonin	0.10	**0.003**	33.3

Nine amino acids are over LOD: Alanine, glutamine, glutamic acid, isoleucine, phenylalanine, serine, threonine, tyrosine and valine. Spermidine is the only biogenic amine over LOD. Other biogenic amines such as ADMA, creatinine, DOPA, dopamine, sarcosine and serotonin could not be detected. The amino acids arginine, asparagine, aspartic acid, citrulline, leucine and methionine were non-detectable in the EV.

With the previously described calculation and the knowledge of the volume of each isolated EV from the ovarian cancer patients, four concentration levels for the EVs were successfully designed. In the first experiment, 2.0×10^9 particle per well of EVs was used. Theoretically, at 2.5-fold concentration, which corresponds to 5.0×10^9 particle per well, three metabolites of amino acids and biogenic amines could

potentially be quantified more: alanine, threonine, and spermidine. Five more metabolites can be captured at a 6-fold concentration of 1.2×10^{10} particle per well: glutamine, glutamic acids, isoleucine, serine, and asparagine. If the concentration is increased to 20-fold the initial concentration of EVs, in theory, six more metabolites can be detected: phenylalanine, tyrosine, valine, aspartic acid, citrulline, and ADMA. The 20-fold concentration amounts to 4.0×10^{10} particle per well. Other metabolites such as arginine, leucine, methionine, creatinine, DOPA, dopamine, sarcosine, and serotonin, will probably not be detected even with a 20-fold concentration.

3.3 Validation of analytical method for biofluid and EV samples

3.3.1 Selection of samples and standards

For the analysis of the biofluids and EVs, a 96 well plate with an integrated internal standard was used. Three different zeros were used, whereas PBS was taken for the calculation of the LOD for the biofluids and the two projects. Since the results of the EVs, either taking water or extraction blank as zero, was almost the same, the extraction blank was taken as the zero for the EVs for further analysis because the extraction blank is the closest to the matrix of the EVs. All three zeros were in three replicates to get more accurate data for the calculation of the LOD. Calculation standards in seven concentration levels (Cal1-7) and quality controls in three concentration levels (QC1-3) were used again, whereas QC2 was presented in five replicates and distributed on the plate for later normalisation and validation of the analytical performance of the MS system.

From the biofluids, 20 ascitic fluids (AF1–20) and five peritoneal washes (PW1–5) were analysed. There was a suggestion that the peritoneal washes were less concentrated than the ascitic fluids, so the peritoneal washes were tested in 10 and 30 µL. In addition, AF5 were tested in three different volumes (5, 10 and 15 µL) to confirm which volume is the best to get the most metabolites and have good analytical performance.

Three EVs were isolated from the peritoneal washes (PW1-EV – PW3-EV) and the other 10 EVs from ascitic fluids (AF1-EV – AF10-EV). Three EVs from ascitic fluids were highly concentrated and could be analysed at 4.0×10^{10} particle per well (category 3): AF2-EV, AF4-EV and AF5-EV. Enough volume and concentration for category 2 with 1.2×10^{10} particle per well had AF2-EV, AF4-EV–AF6-EV, and AF10-EV. For category 1 – which was a total particle number of 5.0×10^{9} per well – AF2-EV, AF4–AF6-EV, AF9-EV, AF10-EV, PW1-EV and PW2-EV were analysed. For all the EVs that could not reach the total particle number of 5.0×10^{9} due to volume limitations, all the available volumes were loaded on the plate and generalised as category 0. Those were the EVs from AF1, AF3, AF7, AF8, and PW3 (Table A. 2).

3.3.2 Validation of the analytical performance

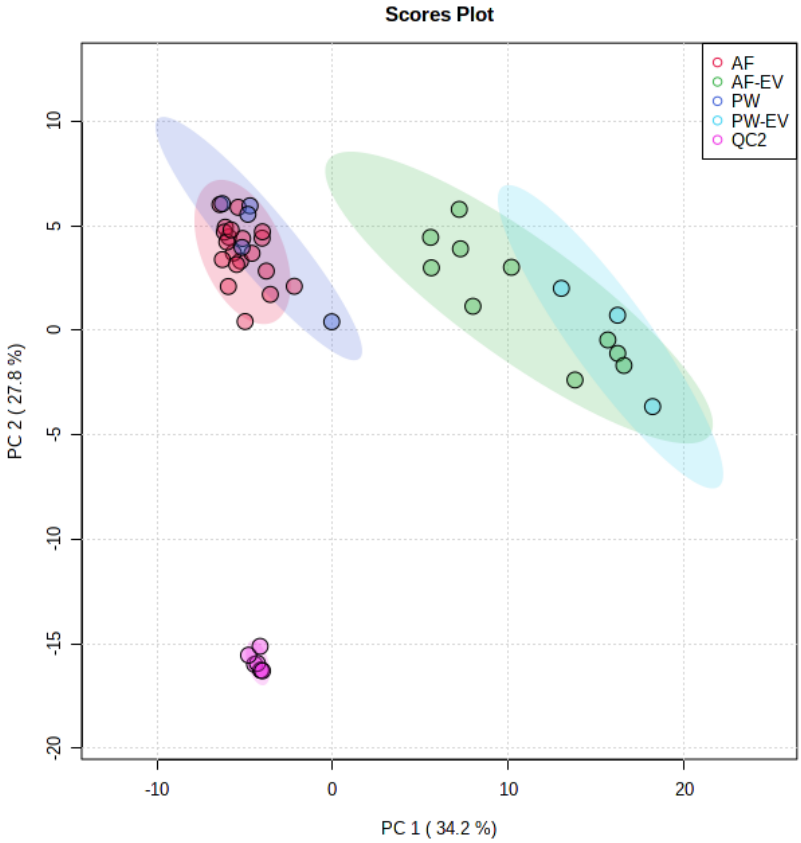

*Figure 9 – **PCA of the second experiment including QC2.** QC2 in five replicates are clustered together, indicating good analytical performance. AF – ascitic fluid; AF-EV – EV isolated from ascitic fluid; PW – peritoneal wash; PW-EV – EV isolated from peritoneal wash; QC2 – quality control concentration level 2 in five replicates.*

Normalization across samples and metabolites was performed to ensure a Gaussian-like distribution using MetaboAnalyst 5.0. The normalisation makes the metabolites more comparable, which were verified by the boxplots**,** where the metabolites are more symmetrical and in the same range. In addition, PCA score plot with all samples shows a clustering of the five QC2 data points, which were distributed on the plate. The clustered quality controls indicate a high performance of the analytical and data process platform. Therefore, the results can be seen as reproducible and reliable (Figure 9).

3.3.3 Selection of the volume for peritoneal washes

Similar to the results from section 3.2.4.1 from the ascitic fluids, there are signs of saturation of the metabolites at 30 µL of peritoneal washes. This is particularly evident in the FIA analysis (Figure 10), as unnatural peaks occurred at the beginning and the end of the intensity signal. In contrast, the FIA analyses of the

samples from 10 µL show good analytical performance, which is why only the data from the peritoneal washes of 10 µL are considered for further analyses.

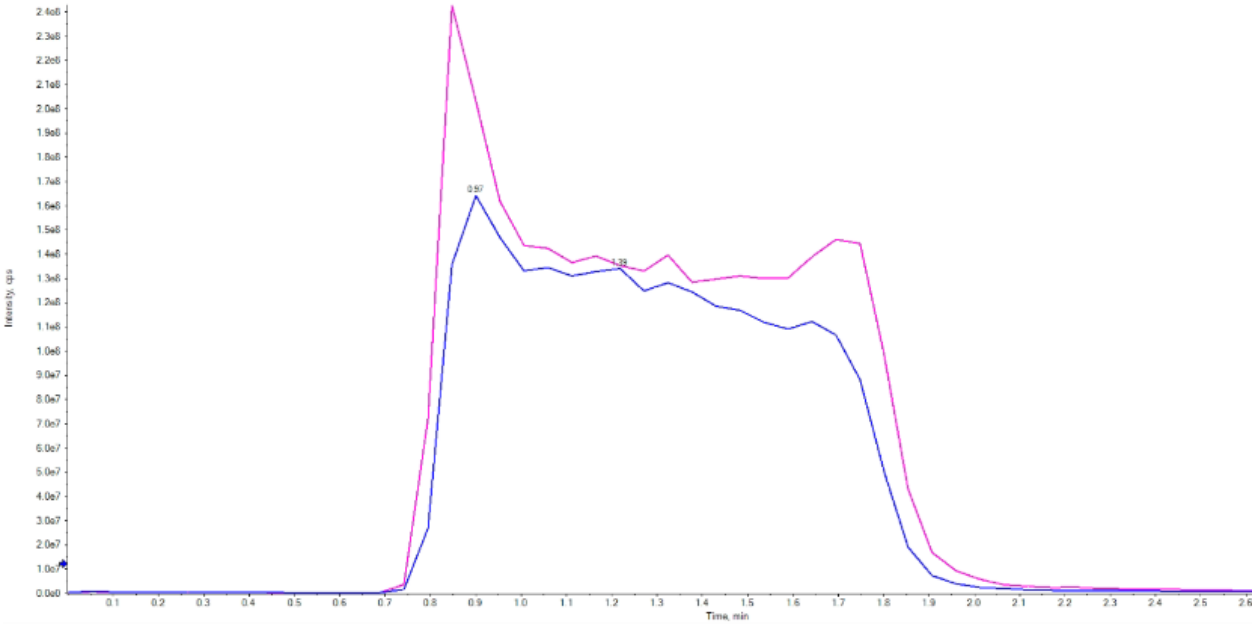

*Figure 10 – **FIA analysis of PW5 in 10 and 30 µL.** Clear sign of saturation due to unnatural peaks at the beginning and in the end of analysis. Blue – PW5 at 10 µL; pink – PW5 at 30 µL. X-axis – time (min); y-axis – intensity (cps).*

3.3.4 Selection of best EV loads

Three EVs were presented in all three concentration levels 1-3 (Figure 11). By comparing the yield of the metabolites at each concentration level, in AF2-EV and AF5-EV, the most metabolites at the concentration level 1 can be identified (AF2-EV: 97 metabolites, AF5-EV: 121 metabolites). In AF4-EV, most metabolites can be identified in the concentration level 2 (163 metabolites). However, considering the quantifiable metabolites, in all AF-EV, most can be quantified in concentration level 1 (AF2-EV:85 – AF4-EV: 151 – AF5-EV: 99 metabolites). Some metabolites are detectable at the lowest concentration and no longer found at higher concentrations due to matrix effects, probably caused by lipids such as lysophosphatidylcholines, which can interfere with the LC/MS analytical performances [67].

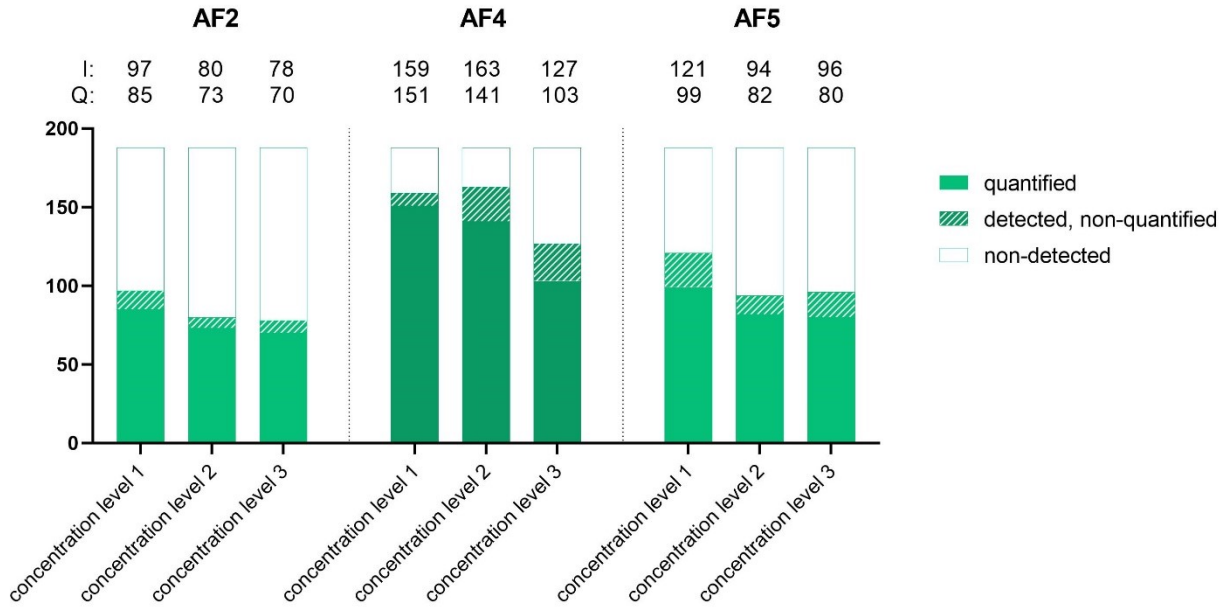

Figure 11 – ***Identified and quantified metabolites from AF2, AF4 and AF5 in three concentration levels.*** *In all samples, most metabolites can be quantified in the concentration level 1. Similar to that, most metabolites can be identified in concentration level 1 except for AF4, where most metabolites are identified in concentration level 2. Concentration level 1 – 5.0 × 10^9 particles/well; concentration level 2 – 1.2 × 10^{10} particles/well; concentration level 3 – 4.0 × 10^{10} particles/well. I – number of identified metabolites (detected, non-quantified + quantified metabolites), Q – number of quantified metabolites. X-axis: concentration levels – y-axis: number of metabolites. In theory, a total of 188 metabolites can be detected and quantified with the kit.*

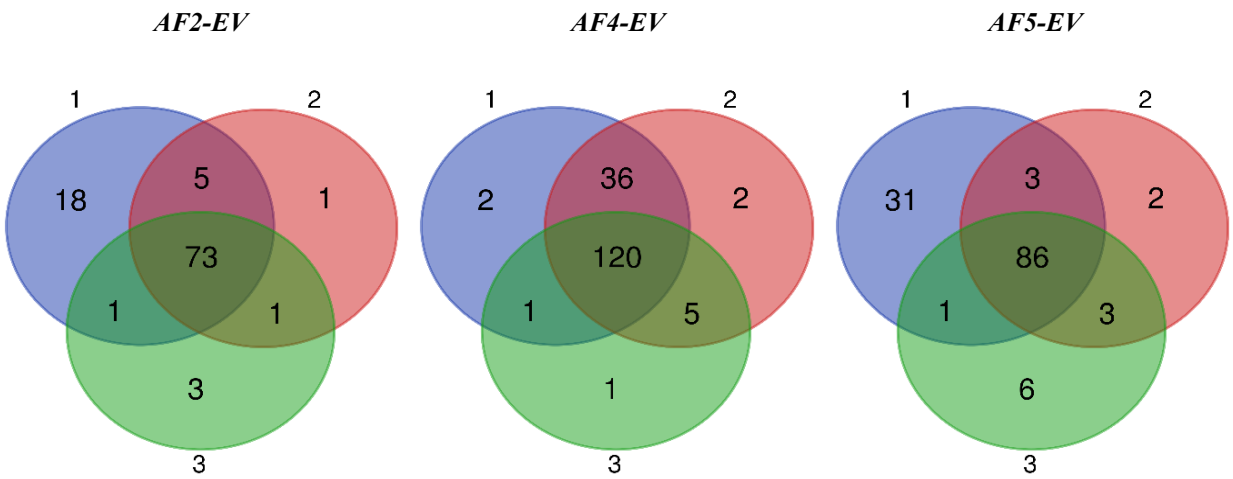

Figure 12 – ***Venn diagram showing the identified metabolites of AF2, AF4 and AF5 in three concentration levels****. Blue – concentration level 1 (5.0 × 10^9 particles/well); red – concentration level 2 (1.2 × 10^{10} particles/well); green – concentration level 3 (4.0 × 10^{10} particles/well).*

A closer look reveals that in AF2-EV 18 metabolites, in AF4-EV 2 and in AF5-EV 31 metabolites can only be found in concentration level 1 (Figure 12). Nevertheless, some metabolites are also uniquely present in concentration levels 2 and 3, proofing that some metabolites can only be detected in higher concentrations. Table 5 shows the metabolites that cannot be detected in the concentration level 1, however in higher concentrations, for instance some acylcarnitines and amino acids, they can be identified.

*Table 5 – **Metabolites, that can only be found in higher concentration levels than concentration level 1.** Mostly acylcarnitines, amino acids and biogenic amines can be detected in higher concentration levels than in concentration level 1. Concentration level 1 – 5.0 × 10^9 particles/well; concentration level 2 – 1.2 × 10^{10} particles/well; concentration level 3 – 4.0 × 10^{10} particles/well.*

Sample ID	Concentration level		
	2	**2+3**	**3**
AF2	Citrulline	PC ae C38:2	Alanine
			PC aa C30:2
			Arginine
AF4	Carnosine	T4-OH-Proline	Citrulline
	Met-SO	C16	
		C0	
		C2	
AF5	SM C22:3	Kynurenine	Phenylalanine
	Citrulline	PC aa C38:1	Alanine
		LysoPC a C18:2	Glycine
		Arginine	Methionin
			Valine
			Tyrosine

In addition to the yield of metabolites, only three EVs (AF2-EV, AF4-EV, AF5-EV) were available in the concentration level 3, five EVs (AF2-EV, AF4-EV – AF6-EV, AF10-EV) in the concentration level 2 and nine EVs (AF2-EV – AF6-EV, AF9-EV, AF10-EV, PW1-EV, PW2-EV) in the concentration level 1. The more samples are available from one concentration level, the more reliable are the results. Moreover, only in concentration levels 1 and 0, EVs of the peritoneal washes are available (PW1-EV in concentration level 0, PW2-EV and PW3-EV in concentration level 1).

By knowing that some metabolites are lost in the analysis of concentration level 1, the further analysis are continued with the samples from concentration levels 0 and 1 since those concentration levels detect most metabolites and by having a representing number of samples.

3.3.5 Metabolites of biofluids and EVs

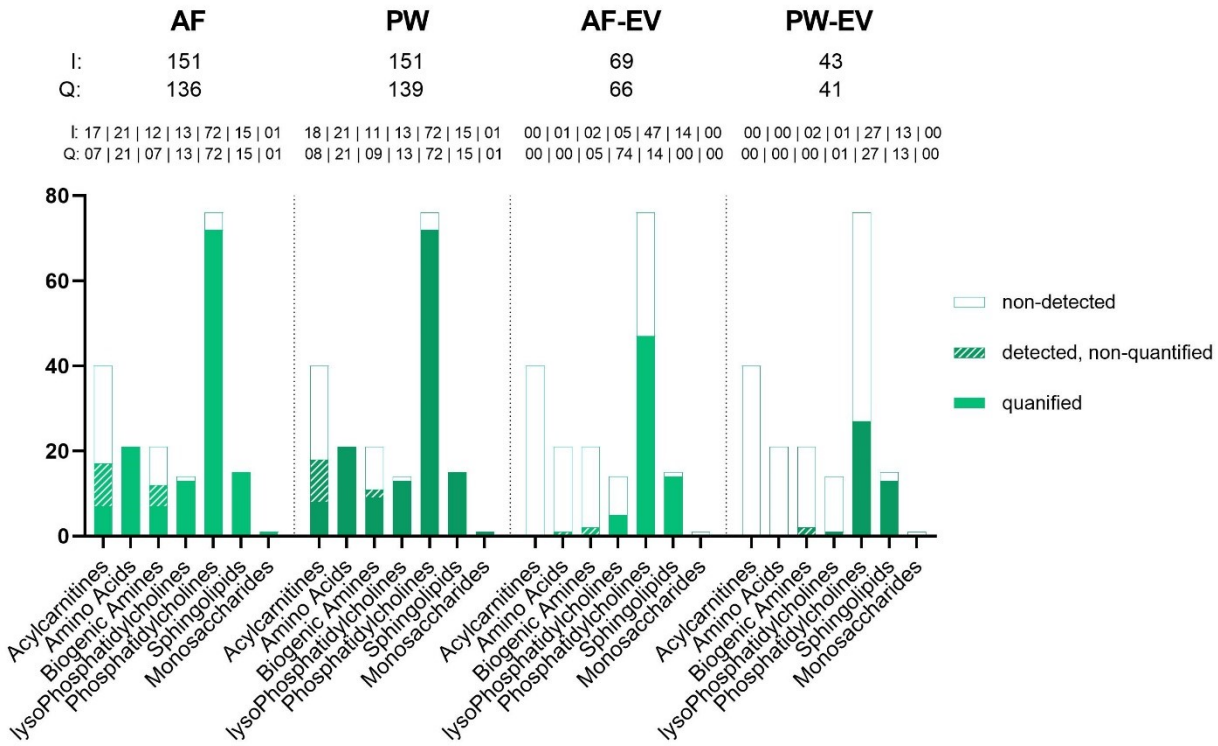

Figure 13 – ***Identified and quantified metabolites in at least 60% of samples within each group.*** *AF – ascitic fluid, PW – peritoneal wash, AF-EV – EV isolated from ascitic fluid, PW-EV – EV isolated from peritoneal wash; I – number of identified metabolites (detected, non-quantified + quantified metabolites), Q – number of quantified metabolites; first line of identified and quantified metabolites shows metabolites in total, second line shows identified and quantified metabolites per metabolite classes.*

Only metabolites that could be detected in at least 60% per sample per group are considered (Figure 13). In the AF, 151 metabolites could be detected, of which 136 were quantifiable: 17/40 acylcarnitines, 21/21 amino acids, 12/21 biogenic amines, 13/14 lysophosphatidylcholines, 72/76 phosphatidylcholines, 15/15 sphingomyelins and 1/1 monosaccharide could be detected. There are small differences in quantifiable metabolites compared to the identified metabolites (acylcarnitines - 7/40; amino acids: 21/21; biogenic amines - 9/21; lysophosphatidylcholines - 12/14; phosphatidylcholines - 72/76; sphingomyelins - 15/15; monosaccharide - 1/1).

Similar to AF, metabolite yields from PW showed that 139 of 151 identified metabolites were quantified with comparable distribution of metabolites, identifying 18/40 acylcarnitines, 21/21 amino acids, 11/21 biogenic amines, 13/14 lysophosphatidylcholines, 72/76 phosphatidylcholines, 15/15 sphingomyelins, and 1/1 monosaccharide. Of these, 8/40 acylcarnitines, 21/21 amino acids, 9/21 biogenic amines, 13/14 lysophosphatidylcholines, 72/76 phosphatidylcholines, 15/15 sphingomyelins and 1/1 monosaccharide were quantified.

While showing similarity within the group, EV results indicated a different behaviour compared to the before mentioned groups. In detail, 69 metabolites were found in AF-EVs, of which 66 were quantified, corresponding to the quantification of 5/14 lysophosphatidylcholines, 47/76 phosphatidylcholines, and 14/15 sphingomyelins within the AF-EVs. No acylcarnitines, amino acids, biogenic amines, nor monosaccharides could be quantified in the AF-EVs. Additionally, three additional metabolites could be detected but not quantified: One amino acid (threonine) and two biogenic amines (spermidine, spermine).

In PW-EVs, 43 metabolites could be identified, of which 41 were quantified, corresponding to 1/14 lysophosphatidylcholines, 27/76 phosphatidylcholines, and 13/15 sphingomyelins. Similar to AF-EVs, no acylcarnitines, amino acids, biogenic amines, or monosaccharides could be quantified in the PW-EVs. Two additional biogenic amines (spermine, spermidine) could only be identified but not quantified.

Biofluids have similar metabolite yields. However, they differ significantly from their respective EVs (Figure 14). Additionally, by looking more closely at the metabolite classes, one can see that the number of quantified/identified metabolites from different classes is comparable between biofluids and between the EVs, respectively. While all 21 amino acids can be detected and quantified in biofluids, none can be quantified in EVs, and only a single amino acid (threonine) can be detected in AF-EV. This trend can also be seen with the biogenic amines: While 12/21 (AF) and 11/21 (PW) biogenic amines can be detected in the biofluids, only two can be detected in EVs. Likewise, 7/21 (AF) and 9/21 (PW) biogenic amines can be quantified. By having a look at the sphingomyelins, not a big different among all groups can be found (15/15 sphingomyelins can be detected in both biofluids, 14/15 in AF-EV and 13/15 in the PW-EV). However, they vary a lot considering the metabolite concentration, which will be discussed in the next chapter. In both EVs, sphingomyelin C22:3 cannot be detected, and in PW-EV, sphingomyelin C20:2 cannot be identified. Moreover, a clear difference between biofluids and EVs can be seen regarding the acylcarnitines. In ascitic fluids, 17/40 can be detected, of which seven were quantified, and in peritoneal washes, there were 18/40, of which eight were quantified. In the respective EVs, not a single acylcarnitine were detected. By looking at the lysophosphatidylcholines, the same number of metabolites could be detected and quantified in the biofluids (13/14) whereas in the EVs, five (AF-EV) and one (PW-EV) lysophosphatidylcholine (lysoPC) were quantified. In both EV samples, lysophosphatidylcholine acyl C16:0 could be found, and another four (lysoPC a C17:0, lysoPC a C18:0, lysoPC a C18:1, lysoPC a C20:4) could be quantified in the AF-EVs. The situation is similar for phosphatidylcholines (PC): 72/76 PCs were quantified in each biofluid sample, only differing in PC aa C30:2, which was only detected and quantified in ascitic fluids and PC aa 42:2, which were only identified in peritoneal washes. However, looking at the 60% cut off results, both

metabolites are on the borderline, whether counted or excluded from the final analysis. Finally, hexose could be quantified in the biofluids, however it could not be found in the two EVs.

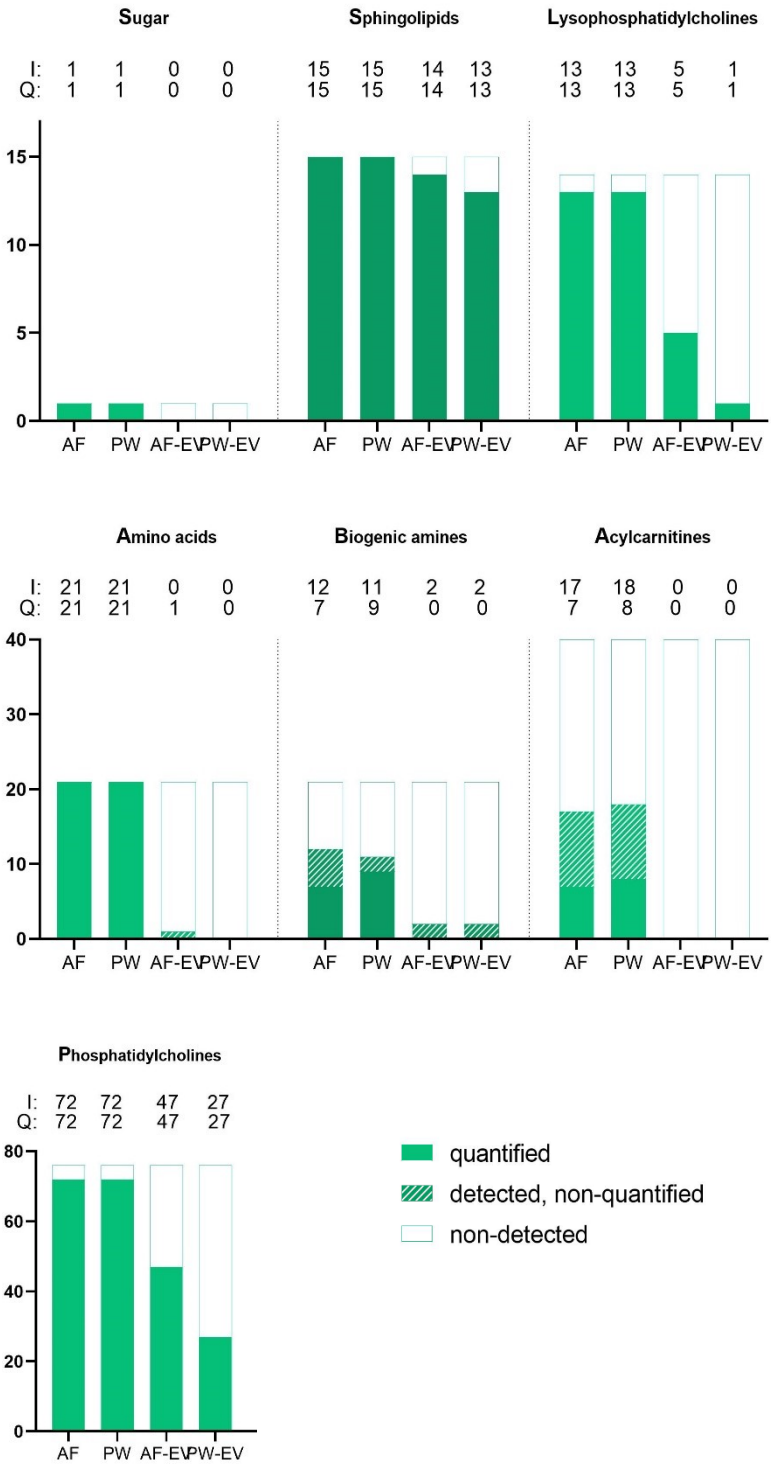

Figure 14 – ***Identified and quantified metabolites in at least 60% of samples within each group, divided by classes.*** *AF – ascitic fluid, PW – peritoneal wash, AF-EV – EV isolated from ascitic fluid, PW-EV – EV isolated from peritoneal wash; I – number of identified metabolites (detected, non-quantified + quantified metabolites), Q – number of quantified metabolites. X-axis: sample groups – y-axis: number of metabolites.*

3.4 *Multivariate analysis of biofluids and EVs*

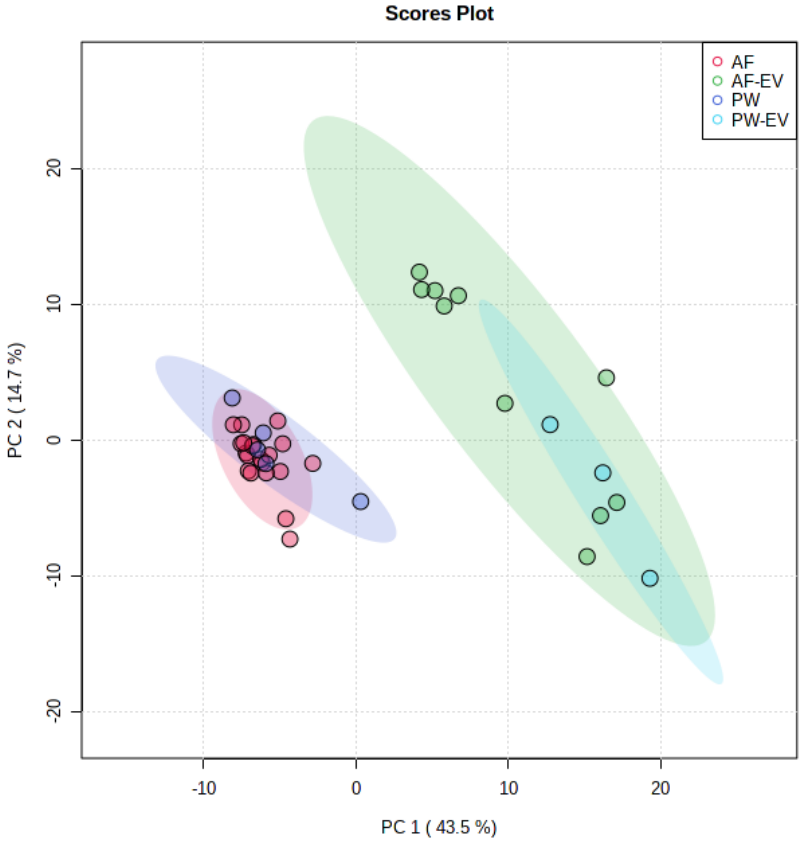

*Figure 15 – **PCA of the biofluids and EVs.** Biofluids and EVs, respectively, are clustered together whereas biofluids to EVs are far away from each other. AF – ascitic fluid; AF-EV – EV isolated from ascitic fluid; PW – peritoneal wash; PW-EV – EV isolated from peritoneal wash.*

As mentioned previously, the quality controls provided by the manufacturer were excluded from further analysis, as they are human plasma samples and would therefore distort data visualisation. The peak intensities of the metabolites found in the ascitic fluids, peritoneal washes, and respective EVs are shown in the PCA (Figure 15). A clear differentiation between the EVs and the biofluids can be observed. Unfortunately, no differentiation can be seen between the two biofluids or the EVs.

3.4.1 Differences and commonalities of the metabolites within the groups

Comparing identified metabolites between groups as shown in Figure 16 suggests, that among the 155 unique metabolites that could were found, 42 metabolites were present in all four groups (AF, PW, AF-EV, PW-EV). Interestingly, 148 metabolites can be detected in at least two groups, whereas only three metabolites (C16:1, PC aa C42:2, C14:2) in PW and 4 metabolites (DOPA, PC aa C30:2, alpha-AAA, C10:1) in AF were unique. 26 metabolites can be found in AF, PW and AF-EV, while one metabolite (spermine) can be found in PW, PW-EV and AF-EV, even though, as previously mentioned, spermine is in the 60% cut off very close to the limit of being included in AF. Another 79 metabolites have been detected only in the biofluids. No single metabolite was specific for AF/AF-EV nor PW/PW-EV, which is a sign that there are no metabolite differences in the sample and control groups. The complete list of metabolites can be found in Figure A. 3.

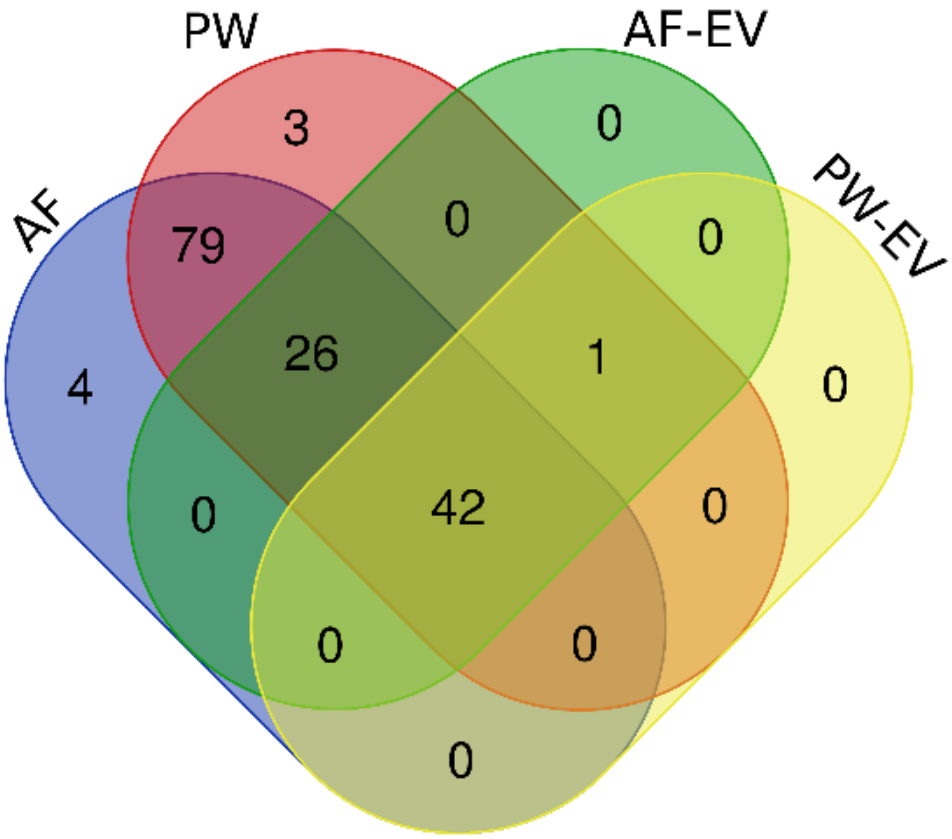

*Figure 16 – **Venn diagram showing the distribution of identified metabolites in at least 60% of samples within each group.** Of 155 metabolites, that can be detected in total, 148 metabolites can be found in at least two groups. AF – ascitic fluid; AF-EV – EV isolated from ascitic fluid; PW – peritoneal wash; PW-EV – EV isolated from peritoneal wash.*

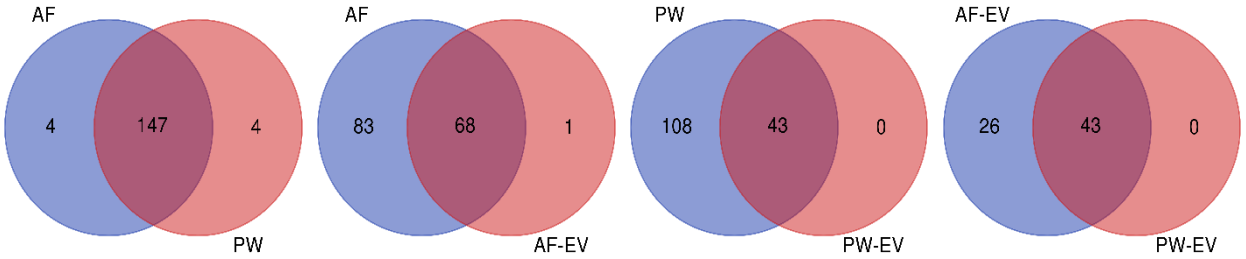

*Figure 17 – **Venn diagram comparing two groups with each other.** AF – ascitic fluid; AF-EV – EV isolated from ascitic fluid; PW – peritoneal wash; PW-EV – EV isolated from peritoneal wash.*

Comparing the individual groups (Figure 17), most differences can be seen between biofluids and the associated EVs. For example, 68 metabolites are common to AF and AF-EV. However, 83 metabolites cannot be detected in AF-EV. Conversely, one metabolite (spermine) cannot be detected in AF, whereby, spermine is close to the limit of the 60% cut-off and could potentially be false positive. The situation is similar for PW and PW-EV. Here, 43 can be detected in both groups, and 108 metabolites can only be found in PW. No metabolite is specific for PW-EV. By comparing the two biofluids, 147 metabolites were detected in both, and four metabolites were found specific in each group (AF: DOPA, PC aa C30:2, alpha-AAA. C10:1 - PW: C16:1, PC aa C42:2, spermine, C14:2). Comparing the two respective EVs, 43 metabolites could be detected in AF-EV and PW-EV. Another 26 metabolites could only be detected in the AF-EVs. A list of all metabolites can be found in Figure A. 4.

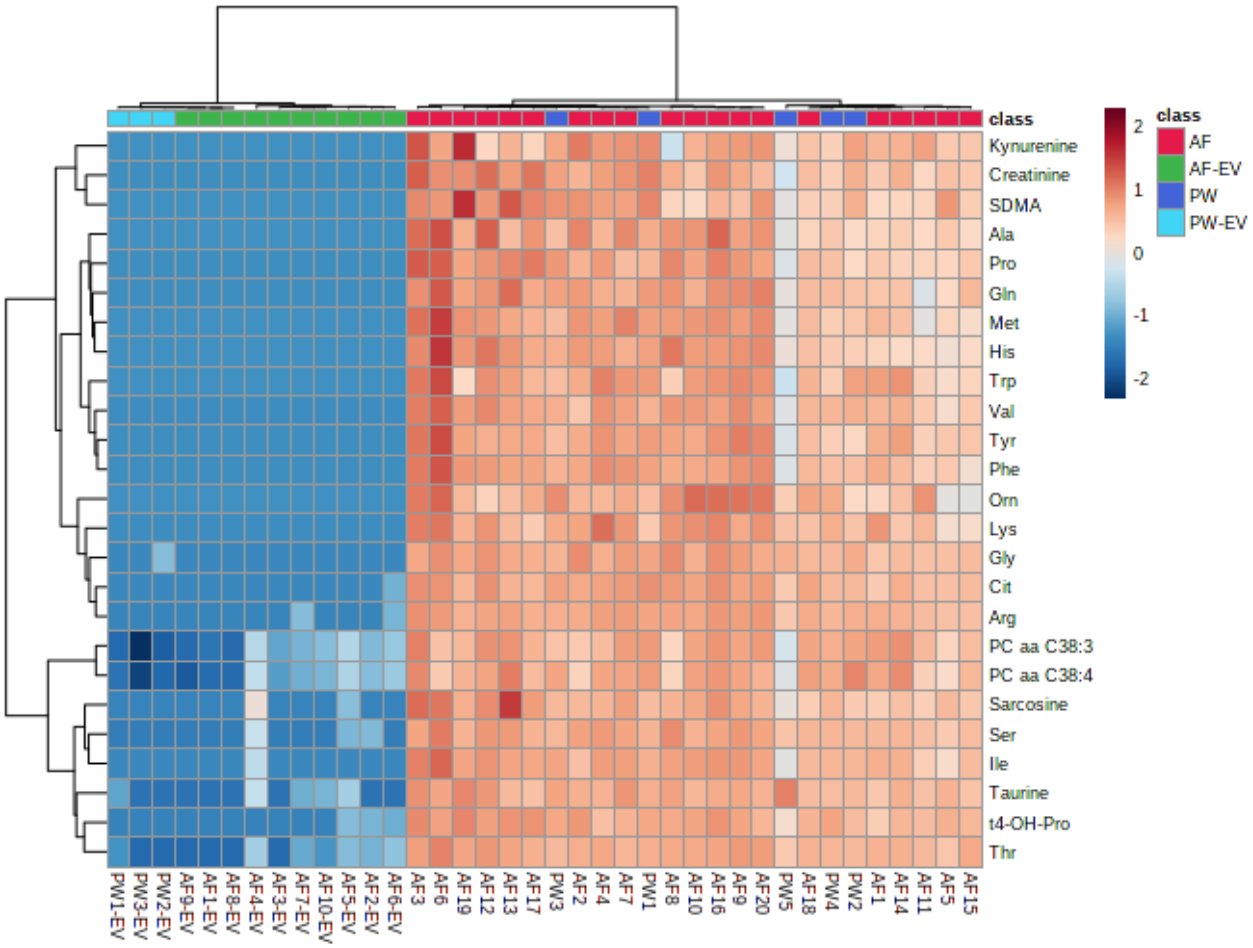

*Figure 18 – **Hierarchical clustering analysis of all samples based on the top 25 metabolites, selected by ANOVA.** Blue – under-expressed, red – over-expressed; Class: SDMA – symmetric dimethylarginine, Ala – alanine, Pro – proline, Gln – glutamine, Met – methionine, His – histidine, Trp – tryptophan, Val – valine, Tyr – tyrosine, Phe – phenylalanine, Orn – ornithine, Lys – lysine, Gly – glycine, Cit – citrulline, Arg – arginine, PC aa C38:3 – phosphatidylcholine diacyl C38:3, PC aa C38:4 – phosphatidylcholine diacyl C38:4, Ser – serine, Ile – isoleucine, t4-OH-Pro – trans-4-hydroxyproline, Thr – threonine; Samples: . AF – ascitic fluid; AF-EV – EV isolated from ascitic fluid; PW – peritoneal wash; PW-EV – EV isolated from peritoneal wash.*

Hierarchical clustering analysis (Figure 18) of the top 25 metabolites of the four groups (AF, PW, AF-EV, PW-EV) indicate a clear separation of biofluids from their EVs. It can be said that six biogenic amines (kyreurenine, creatinine, SDMA, sarcosine, t4-OH-proline and taurine), 17 amino acids (alanine, proline, glutamine, methionine, histidine, tryptophan, valine, tyrosine, phenylalanine, ornithine, lysine, glycine, citrulline, arginine, serine, isoleucine and threonine) and two phosphatidylcholines (PC aa C38:3, PC aa C38:4) are highly overexpressed in the biofluids compared to EVs. While the PW-EVs are separated from the AF-EVs, no clear separation between the two biofluids can be seen. Due to the fact that many metabolites can only be found in the biofluids and not in the EVs (mostly amino acids, biogenic amines and acylcarnitines), only the 42 metabolites that could be detected in all the groups were compared in the following data analysis.

3.4.2 Data analysis of the common 42 metabolites

Considering only the 42 metabolites that appear in all four groups, two outliers can be found in the PCA (Figure 19): AF8 and AF8-EV. A possible explanation could be that during sample preparation, two phases were observed during centrifugation of the samples for AF8, which did not occur for any other sample. Only the lower phase, which were more liquid than the upper one, was pipetted to the plate. Since this sample is clearly different from the others and differentiated in the results, AF8 and AF8-EV were excluded from further data analysis.

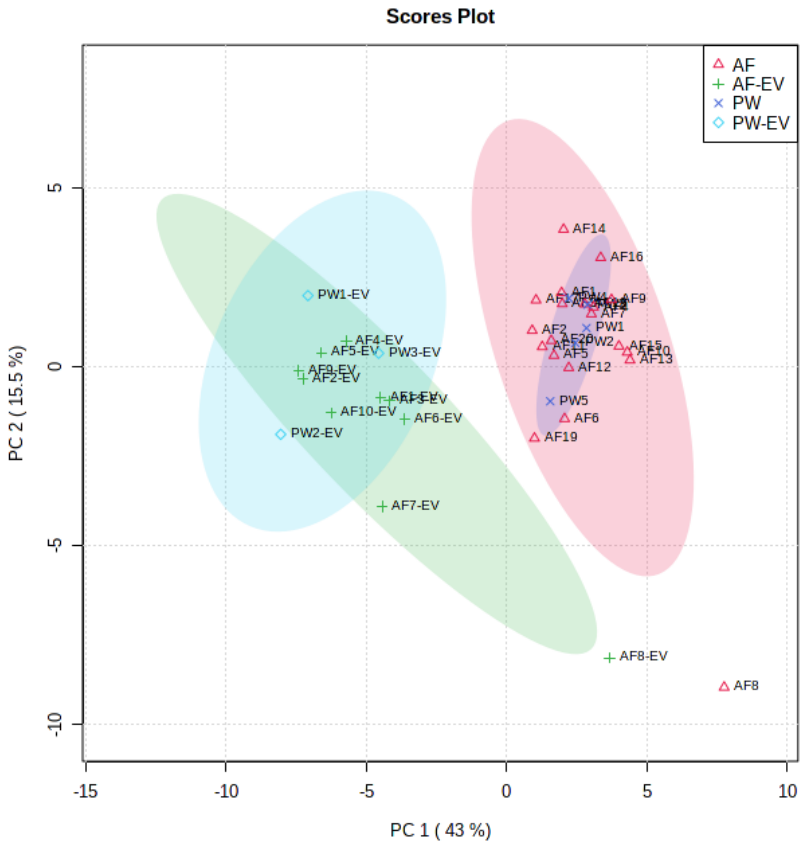

*Figure 19 – **PCA of the common 42 metabolites from all samples.** Two outliers become clear and are excluded from further analysis: AF8 and AF8-EV. Samples: AF – ascitic fluid; AF-EV – EV isolated from ascitic fluid; PW – peritoneal wash; PW-EV – EV isolated from peritoneal wash.*

Looking at the heat map (Figure 20), one can see that the biofluids clearly separate from EVs when observing the top 25 metabolites from the common pool identified in all samples. However, no demarcations can be detected between the two biofluids or the respective EVs. By comparing the expression of the metabolites, mainly phosphatidylcholines and sphingomyelins are distinguished that are either over (red) or under (blue) expressed. Especially sphingomyelins and phospholipids with a shorter side chain as 34 carbon atoms were enriched in the EVs, whereas phospholipids longer than 34 carbon atoms were overexpressed in biofluids. In addition, spermidine was detected in higher concentrations in EVs compared to biofluids.

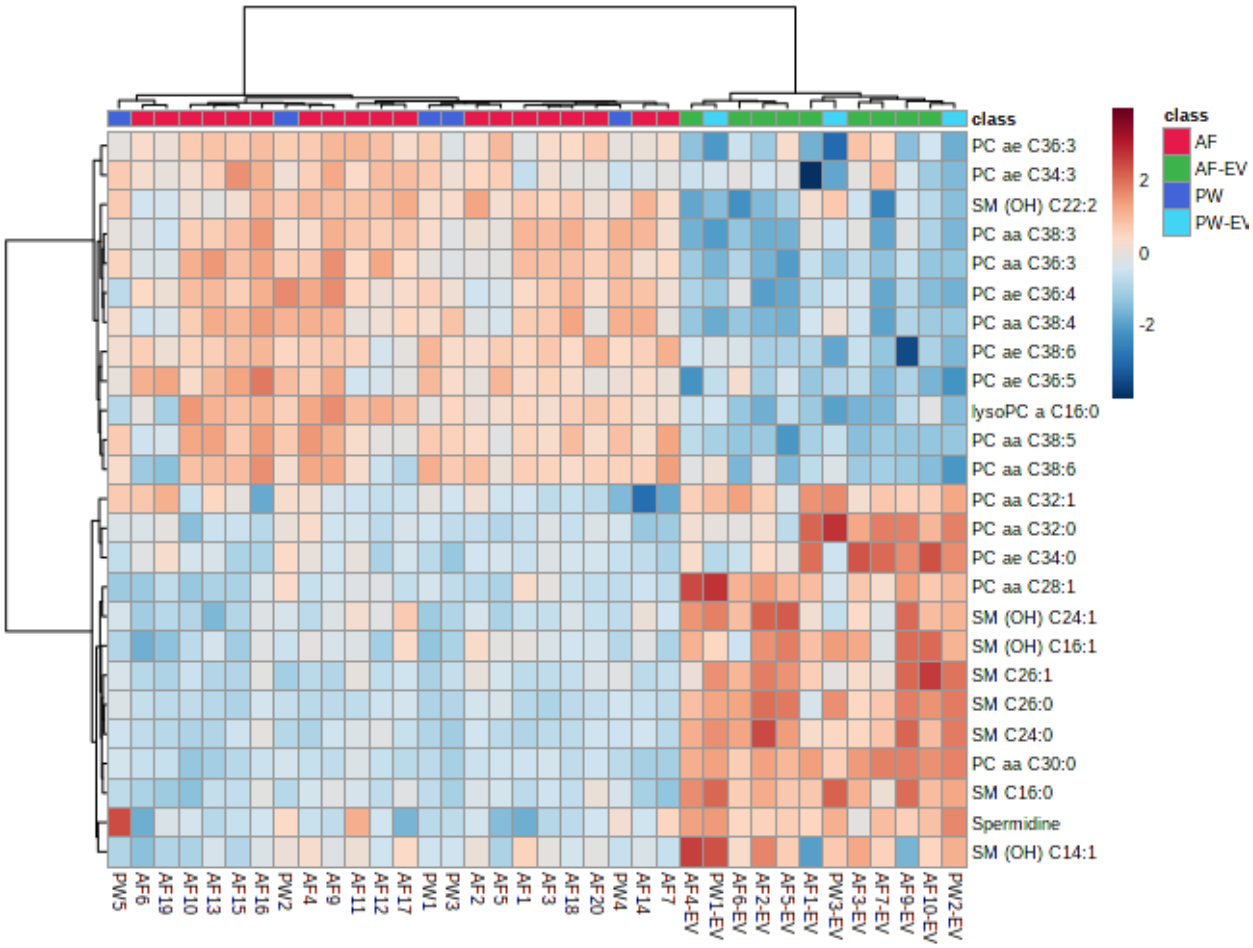

Figure 20 – ***Hierarchical clustering analysis of the common 42 metabolites from all samples, showing the top 25 metabolites.*** *Blue – under-expressed, red – over-expressed; Class: PC ae Cx:y – phosphatidylcholine acyl-alkyl, PC aa Cx:y – phosphatidylcholine diacyl, lysoPC a Cx:y – lysophosphatidylcholine acyl, SM (OH) Cx:y – hydroxysphingomyeline, SM Cx:y – sphingomyeline; Samples: AF – ascitic fluid; AF-EV – EV isolated from ascitic fluid; PW – peritoneal wash; PW-EV – EV isolated from peritoneal wash.*

These results are confirmed by the fact that sphingomyelins and phosphatidylcholines play a role in the rigidity as well as in the recognition and internalisation of EVs. In addition, sphingomyelins play a significant role in the formation and release of EVs and the regulation of cell survival and inflammation of the cell [68]. In comparison to the high concentration in these EVs, a high concentration of spermidine was also found in EVs of prostate cancer, which may be caused by the high activity of the enzyme ornithine decarboxylase, the rate-limiting enzyme in the polyamine synthase pathway [32]. Many other studies show that the biosynthesis of polyamines such as spermidine is upregulated in growing cells, therefore also likely in cancer cells. Additionally, a higher concentration of polyamines in the TME of cancer cells plays a role in cell migration, leading to metastasis. Furthermore, it helps cancer cells escape from the immune system [68].

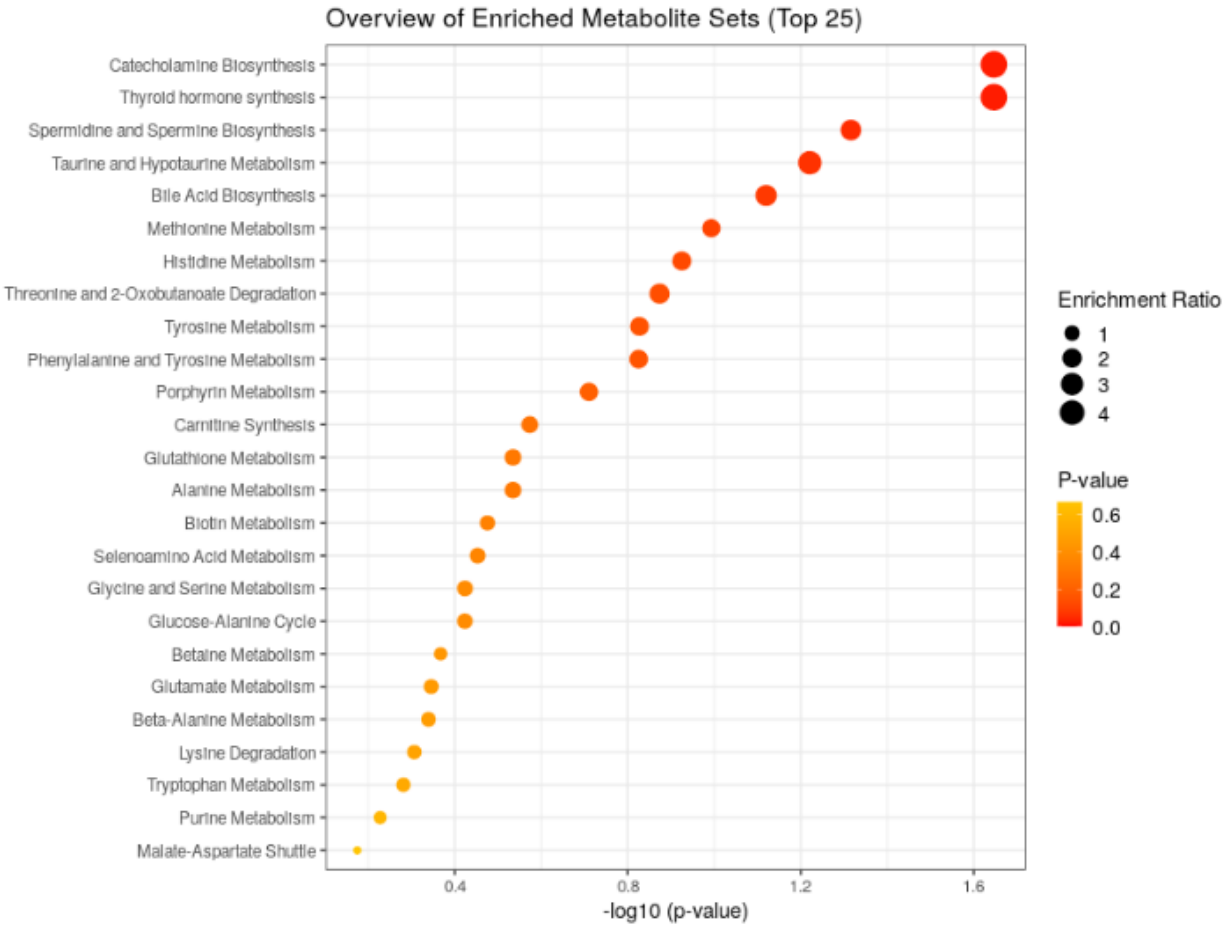

*Figure 21 – **Overview of enriched metabolite sets based on top 25 metabolism pathways**. Catecholamine biosynthesis and thyroid hormone synthesis are the most enriched activated metabolism pathways, followed by spermidine and spermine biosynthesis, taurine and hypotaurine metabolism and bile acid biosynthesis.*

Next, a metabolomic enrichment analysis was performed on biofluids, considering only amino acids and biogenic amines (Figure 21). Two metabolic pathways stand out. Highest enriched is the catecholamine pathway. Recently, norephedrine, a catecholamine, was shown to have a positive effect on angiogenesis in ovarian cancer by activating the b-adrenoreceptor, leading to increased expression of MMP-2 (matrix metalloprotease) and MMP-9 on the one hand, and increased synthesis at VPF/VEGF on the other. Both are proangiogenic factors [69]. The second highest pathway found enriched is the thyroid hormone metabolism. This is confirmed by the fact that in HGSC, the expression of DIO3 is increased to metabolise the tumour suppressor hormone T3 faster, leading to cancer proliferation and anaerobic glycolysis [70].

Moreover, spermine/spermidine metabolism, taurine/hydroxytaurine metabolism and bile acid metabolism are among the top 5 enrichment metabolism pathways. Spermine and spermidine are polyamines metabolised by Spermidine/spermine-N1-acetyltransferase (SSAT) through N-acetylation. A relationship between chemoresistance and SSAT is suspected, as the level of SSAT is induced lower in chemoresistant

ovarian cancer cell lines than in chemosensitive cell lines. It is strongly suspected that SSAT removes DNA-bound polyamines, allowing cisplatin to interact more extensively with the DNA [71], [72]. Additionally, taurine/hydroxytaurine metabolism is increased. This could be because taurine displays a strong growth-inhibitory effect on multiple cancer types, including ovarian cancer. It is also reported that the effect of taurine can overcome chemoresistance to cisplatin and paclitaxel, potentially explaining why the metabolism of taurine is increased here [72]. Finally, bile acid metabolism is among the top 5 metabolic pathways found enriched. Bile acids have a cytotoxic effect on ovarian cancer cells, such as chenodeoxycholic acid and deoxycholic acid, as they induce apoptosis of the cells. Low bile acid level can therefore most likely be considered a predictor of ovarian cancer [73].

4. Conclusion

Ovarian cancer is still considered a challenging cancer to treat. With a 5-year survival of less than 45% in higher stages, the urgency of finding diagnostic procedures that detect the disease earlier and non-invasive is more important than ever, in hope to find a better prognosis and targeted treatments without high relapse rates [10]. Ascitic fluid in the peritoneal cavity is one of the symptoms of ovarian cancer that mainly occurs in later stages and is associated with a poorer prognosis [8], [12]. In addition, ascitic fluid creates a conducive tumour microenvironment, which is beneficial for metastatic cancer [12].

EVs are produced and secreted by donor cells and contain much of the information of their origin in the cargo [29], [30]. EVs also play an important role in cell-cell communication, and there is evidence that cancer cells release more EVs into the TME than healthy cells [30], [32]. All these suggests that the study of the cargos of EVs is becoming increasingly important for finding a non-invasive method of biomarkers [11], [28], [68]. For a long time, the focus has been mainly on transcriptome and proteome data. However, to date, the study of the metabolome of EVs has not been advanced, which, considering that metabolic alteration is one of the hallmarks of cancer, seems significant [32], [74].

In this work the study and analysis of the complex metabolic profile of biofluids such as ascitic fluids and peritoneal washes, as well as their associated EVs is presented. For this purpose, the method of targeted metabolomics of biofluids and EVs was implemented using AbsoluteIDQ® p180 kit from Biocrates.

In summary, 155 metabolites could be found among all samples. While 151 metabolites could be detected in the biofluids, fewer metabolites could be found in the EVs (69 in AF-EV, 43 in PW-EV). The analysis of the EVs were focused only on lipids since no amino acids, acylcarnitines nor biogenic amines could be detected. Similar results were found by Smorlaz, M et al. [75], where most amino acids and biogenic amines could not reach the LOD and were excluded from further analysis. Nevertheless, it was observed that higher concentration of EVs increase the chances of detecting amino acids and biogenic amines, even though many other metabolites from the lipid section are non-detectable due to matrix effects [67].

Most importantly, a significant difference between biofluids and EVs were shown by PCA. The hierarchical component analysis made it clear that sphingolipids in general and phospholipids shorter than 34 carbon atoms in the main chain are enriched in the EVs and are probably part of the membrane. In contrast, long-chain phospholipids over 34 carbon atoms are present in higher concentrations in the biofluids. In addition to that, spermidine was quantified and enriched in the EVs.

Unfortunately, no differences were found between the biofluids or between the two EVs groups. However, since both ascitic fluids and peritoneal washes were tested positive for cancer cells, it can be assumed that there are hardly any differences in the metabolomic profile.

Nevertheless, further data analysis can be performed, for example, a detailed investigation of the quantification of metabolites and comparison of metabolites that are increased or decreased in different groups. Also, a comparison with the biofluids and the associated EVs can be made, mainly which metabolites come from the donor cell, and which are the same in all EVs. Furthermore, new data can be generated with biofluids and EVs from healthy patients and patients in an early stage of ovarian cancer and be compared with the previous data to investigate a non-invasive diagnostic method for ovarian cancer by finding a biomarker in the metabolome of the EV cargos. Here, enough volume for the isolation of the EVs should be considered since amino acids and biogenic amines can only be detected in higher concentrations. For the isolation, a considerable volume of biofluids is necessary.

Bibliography

[1] Y. Ahmed-Salim *et al.*, "The application of metabolomics in ovarian cancer management: a systematic review," *International Journal of Gynecologic Cancer*, p. ijgc-2020-001862, Oct. 2020, doi: 10.1136/ijgc-2020-001862.

[2] M. E. McDonald *et al.*, "Molecular Characterization of Non-responders to Chemotherapy in Serous Ovarian Cancer," *Int J Mol Sci*, vol. 20, no. 5, p. 1175, Mar. 2019, doi: 10.3390/ijms20051175.

[3] F. Bray, J. Ferlay, I. Soerjomataram, R. L. Siegel, L. A. Torre, and A. Jemal, "Global cancer statistics 2018: GLOBOCAN estimates of incidence and mortality worldwide for 36 cancers in 185 countries," *CA: A Cancer Journal for Clinicians*, vol. 68, no. 6, pp. 394–424, Nov. 2018, doi: https://doi.org/10.3322/caac.21492.

[4] P. A. Konstantinopoulos *et al.*, "Germline and somatic tumor testing in epithelial ovarian cancer: ASCO guideline," *Journal of Clinical Oncology*, vol. 38, no. 11, pp. 1222–1245, Apr. 2020, doi: 10.1200/JCO.19.02960.

[5] A. Burges and B. Schmalfeldt, "Ovarian cancer: diagnosis and treatment," *Deutsches Arzteblatt international*, vol. 108, no. 38, pp. 635–641, Sep. 2011, doi: 10.3238/arztebl.2011.0635.

[6] M. R. Radu *et al.*, "Ovarian Cancer: Biomarkers and Targeted Therapy," *Biomedicines*, vol. 9, no. 6, p. 693, Jun. 2021, doi: 10.3390/biomedicines9060693.

[7] A. Chandra *et al.*, "Ovarian cancer: Current status and strategies for improving therapeutic outcomes," *Cancer Med*, vol. 8, no. 16, pp. 7018–7031, Nov. 2019, doi: 10.1002/cam4.2560.

[8] B. P. Rickard *et al.*, "Malignant Ascites in Ovarian Cancer: Cellular, Acellular, and Biophysical Determinants of Molecular Characteristics and Therapy Response," *Cancers (Basel)*, vol. 13, no. 17, 2021, doi: 10.3390/cancers13174318.

[9] J. Prat, A. Ribé, and A. Gallardo, "Hereditary ovarian cancer," *Human Pathology*, vol. 36, no. 8, pp. 861–870, 2005, doi: https://doi.org/10.1016/j.humpath.2005.06.006.

[10] F. Plotti *et al.*, "Role of BRCA Mutation and HE4 in Predicting Chemotherapy Response in Ovarian Cancer: A Retrospective Pilot Study," *Biomedicines*, vol. 9, no. 1, p. 55, Jan. 2021, doi: 10.3390/biomedicines9010055.

[11] U. A. Matulonis, A. K. Sood, L. Fallowfield, B. E. Howitt, J. Sehouli, and B. Y. Karlan, "Ovarian cancer," *Nat Rev Dis Primers*, vol. 2, p. 16061, Aug. 2016, doi: 10.1038/nrdp.2016.61.

[12] M. Wróblewski, K. Szewczyk-Golec, I. Hołyńska-Iwan, J. Wróblewska, and A. Woźniak, "Characteristics of Selected Adipokines in Ascites and Blood of Ovarian Cancer Patients," *Cancers (Basel)*, vol. 13, p. 4702, Sep. 2021, doi: 10.3390/cancers13184702.

[13] N. Ahmed and K. L. Stenvers, "Getting to know ovarian cancer ascites: opportunities for targeted therapy-based translational research," *Front Oncol*, vol. 3, p. 256, Sep. 2013, doi: 10.3389/fonc.2013.00256.

[14] M. Cohen and P. Petignat, "The bright side of ascites in ovarian cancer," *Cell Cycle*, vol. 13, no. 15, p. 2319, 2014, doi: 10.4161/cc.29951.

[15] T. Singh, A. S. Neal, N. A. Moatamed, and S. Memarzadeh, "Exploring the Potential of Drug Response Assays for Precision Medicine in Ovarian Cancer," *Int J Mol Sci*, vol. 22, no. 1, p. 305, Dec. 2020, doi: 10.3390/ijms22010305.

[16] L. Puchades-Carrasco and A. Pineda-Lucena, "Metabolomics Applications in Precision Medicine: An Oncological Perspective," *Curr Top Med Chem*, vol. 17, no. 24, pp. 2740–2751, 2017, doi: 10.2174/1568026617666170707120034.

[17] K. O. Alfarouk, "Tumor metabolism, cancer cell transporters, and microenvironmental resistance," *Journal of Enzyme Inhibition and Medicinal Chemistry*, vol. 31, no. 6, pp. 859–866, Nov. 2016, doi: 10.3109/14756366.2016.1140753.

[18] A. N. Lau and M. G. vander Heiden, "Metabolism in the Tumor Microenvironment," *Annual Review of Cancer Biology*, vol. 4, no. 1, pp. 17–40, Mar. 2020, doi: 10.1146/annurev-cancerbio-030419-033333.

[19] D. Lucchetti, C. Ricciardi Tenore, F. Colella, and A. Sgambato, "Extracellular Vesicles and Cancer: A Focus on Metabolism, Cytokines, and Immunity," *Cancers (Basel)*, vol. 12, no. 1, p. 171, Jan. 2020, doi: 10.3390/cancers12010171.

[20] A. S. Dias, C. R. Almeida, L. A. Helguero, and I. F. Duarte, "Metabolic crosstalk in the breast cancer microenvironment," *European Journal of Cancer*, vol. 121, pp. 154–171, 2019, doi: https://doi.org/10.1016/j.ejca.2019.09.002.

[21] N. Ahmed, R. Escalona, D. Leung, E. Chan, and G. Kannourakis, "Tumour microenvironment and metabolic plasticity in cancer and cancer stem cells: Perspectives on metabolic and immune regulatory signatures in chemoresistant ovarian cancer stem cells," *Seminars in Cancer Biology*, vol. 53, pp. 265–281, 2018, doi: https://doi.org/10.1016/j.semcancer.2018.10.002.

[22] A. Mitra *et al.*, "Extracellular vesicles derived from ascitic fluid enhance growth and migration of ovarian cancer cells," *Scientific Reports*, vol. 11, no. 1, p. 9149, 2021, doi: 10.1038/s41598-021-88163-1.
[23] M. Nazemi and E. Rainero, "Cross-Talk Between the Tumor Microenvironment, Extracellular Matrix, and Cell Metabolism in Cancer," *Frontiers in Oncology*, vol. 10, p. 239, 2020, [Online]. Available: https://www.frontiersin.org/article/10.3389/fonc.2020.00239
[24] A. Morandi, E. Giannoni, and P. Chiarugi, "Nutrient Exploitation within the Tumor–Stroma Metabolic Crosstalk," *Trends in Cancer*, vol. 2, no. 12, pp. 736–746, Dec. 2016, doi: 10.1016/j.trecan.2016.11.001.
[25] A. Schulze and M. Yuneva, "The big picture: exploring the metabolic cross-talk in cancer," *Disease Models & Mechanisms*, vol. 11, no. 8, Aug. 2018, doi: 10.1242/dmm.036673.
[26] K. S. Reiners, J. Dassler-Plenker, C. Coch, and G. Hartmann, "Funktion von extrazellulären Vesikeln und Bedeutung für die labormedizinische Diagnostik," *LaboratoriumsMedizin*, vol. 41, no. 6, pp. 299–308, 2017, doi: doi:10.1515/labmed-2017-0078.
[27] M. Khawar, M. Abbasi, Z. Siddique, A. Arif, and N. Sheikh, "An Update on Novel Therapeutic Warfronts of Extracellular Vesicles (EVs) in Cancer Treatment: Where We Are Standing Right Now and Where to Go in the Future," *Oxidative Medicine and Cellular Longevity*, vol. 2019, pp. 1–21, Jul. 2019, doi: 10.1155/2019/9702562.
[28] A. Zebrowska, A. Skowronek, A. Wojakowska, P. Widlak, and M. Pietrowska, "Metabolome of Exosomes: Focus on Vesicles Released by Cancer Cells and Present in Human Body Fluids," *Int J Mol Sci*, vol. 20, no. 14, p. 3461, Jul. 2019, doi: 10.3390/ijms20143461.
[29] R. Isaac, F. C. G. Reis, W. Ying, and J. M. Olefsky, "Exosomes as mediators of intercellular crosstalk in metabolism," *cell metabolism*, vol. 33, no. 9, pp. 1744–1762, 2021, doi: 10.1016/J.CMET.2021.08.006.
[30] T. Altadill *et al.*, "Enabling Metabolomics Based Biomarker Discovery Studies Using Molecular Phenotyping of Exosome-Like Vesicles," *PLOS ONE*, vol. 11, p. e0151339, Mar. 2016, doi: 10.1371/journal.pone.0151339.
[31] R. Isaac, F. C. G. Reis, W. Ying, and J. M. Olefsky, "Exosomes as mediators of intercellular crosstalk in metabolism," *Cell Metabolism*, vol. 33, no. 9, pp. 1744–1762, 2021, doi: https://doi.org/10.1016/j.cmet.2021.08.006.
[32] M. Puhka *et al.*, "Metabolomic Profiling of Extracellular Vesicles and Alternative Normalization Methods Reveal Enriched Metabolites and Strategies to Study Prostate Cancer-Related Changes," *Theranostics*, vol. 7, no. 16, pp. 3824–3841, Aug. 2017, doi: 10.7150/thno.19890.
[33] M. Alharbi *et al.*, "Extracellular Vesicle Transmission of Chemoresistance to Ovarian Cancer Cells Is Associated with Hypoxia-Induced Expression of Glycolytic Pathway Proteins, and Prediction of Epithelial Ovarian Cancer Disease Recurrence," *Cancers (Basel)*, vol. 13, no. 14, p. 3388, Jul. 2021, doi: 10.3390/cancers13143388.
[34] Y. Sun, "Tumor microenvironment and cancer therapy resistance," *Cancer Letters*, vol. 380, no. 1, pp. 205–215, 2016, doi: https://doi.org/10.1016/j.canlet.2015.07.044.
[35] L. Cheng, R. A. Sharples, B. J. Scicluna, and A. F. Hill, "Exosomes provide a protective and enriched source of miRNA for biomarker profiling compared to intracellular and cell-free blood," *J Extracell Vesicles*, vol. 3, p. 10.3402/jev.v3.23743, Mar. 2014, doi: 10.3402/jev.v3.23743.
[36] M. Monteiro, M. Carvalho, M. Bastos, and P. Guedes de Pinho, "Metabolomics Analysis for Biomarker Discovery: Advances and Challenges," *Curr Med Chem*, vol. 20, Nov. 2012, doi: 10.2174/092986713804806621.
[37] O. Turkoglu *et al.*, "Metabolomics of biomarker discovery in ovarian cancer: a systematic review of the current literature," *Metabolomics*, vol. 12, no. 4, p. 60, Apr. 2016, doi: 10.1007/s11306-016-0990-0.
[38] D. S. Wishart, "Emerging applications of metabolomics in drug discovery and precision medicine," *Nature Reviews Drug Discovery*, vol. 15, no. 7, pp. 473–484, 2016, doi: 10.1038/nrd.2016.32.
[39] D. B. Kell, M. Brown, H. M. Davey, W. B. Dunn, I. Spasic, and S. G. Oliver, "Metabolic footprinting and systems biology: the medium is the message," *Nature Reviews Microbiology*, vol. 3, no. 7, pp. 557–565, 2005, doi: 10.1038/nrmicro1177.
[40] A. Muir, L. v Danai, and M. G. vander Heiden, "Microenvironmental regulation of cancer cell metabolism: implications for experimental design and translational studies," *Disease Models & Mechanisms*, vol. 11, no. 8, Aug. 2018, doi: 10.1242/dmm.035758.
[41] J. Trygg, E. Holmes, and T. Lundstedt, "Chemometrics in Metabonomics," *Journal of Proteome Research*, vol. 6, no. 2, pp. 469–479, Feb. 2007, doi: 10.1021/pr060594q.
[42] V. Behrends, H. D. Williams, and J. G. Bundy, "Metabolic Footprinting: Extracellular Metabolomic Analysis," in *Pseudomonas Methods and Protocols*, A. Filloux and J.-L. Ramos, Eds. New York, NY: Springer New York, 2014, pp. 281–292. doi: 10.1007/978-1-4939-0473-0_23.
[43] O. Fiehn and T. Kind, "Metabolite Profiling in Blood Plasma," in *Metabolomics: Methods and Protocols*, W. Weckwerth, Ed. Totowa, NJ: Humana Press, 2007, pp. 3–17. doi: 10.1007/978-1-59745-244-1_1.

[44] X. Liu and J. W. Locasale, “Metabolomics: A Primer,” *Trends Biochem Sci*, vol. 42, no. 4, pp. 274–284, Apr. 2017, doi: 10.1016/j.tibs.2017.01.004.
[45] T. D. Veenstra, “Metabolomics: the final frontier?,” *Genome Med*, vol. 4, no. 4, p. 40, Apr. 2012, doi: 10.1186/gm339.
[46] R. Pereiro and A. Sanz-Medel, “Flow Injection Analysis Techniques in Atomic Spectroscopy,” 2011. doi: 10.1002/9780470027318.a5106.pub2.
[47] W. Xu, R. C. Sandford, P. J. Worsfold, A. Carlton, and G. Hanrahan, “Flow Injection Techniques in Aquatic Environmental Analysis: Recent Applications and Technological Advances,” *Critical Reviews in Analytical Chemistry*, vol. 35, no. 3, pp. 237–246, Jul. 2005, doi: 10.1080/10408340500323362.
[48] B. Worley, S. Halouska, and R. Powers, “Utilities for quantifying separation in PCA/PLS-DA scores plots,” *Analytical Biochemistry*, vol. 433, no. 2, pp. 102–104, 2013, doi: https://doi.org/10.1016/j.ab.2012.10.011.
[49] K. H. Liland, “Multivariate methods in metabolomics – from pre-processing to dimension reduction and statistical analysis,” *TrAC Trends in Analytical Chemistry*, vol. 30, no. 6, pp. 827–841, 2011, doi: https://doi.org/10.1016/j.trac.2011.02.007.
[50] J. Xia and D. S. Wishart, “MSEA: a web-based tool to identify biologically meaningful patterns in quantitative metabolomic data,” *Nucleic Acids Res*, vol. 38, no. Web Server issue, pp. W71–W77, Jul. 2010, doi: 10.1093/nar/gkq329.
[51] C. Théry, S. Amigorena, G. Raposo, and A. Clayton, “Isolation and Characterization of Exosomes from Cell Culture Supernatants and Biological Fluids,” *Current Protocols in Cell Biology*, vol. 30, no. 1, pp. 3.22.1-3.22.29, Mar. 2006, doi: https://doi.org/10.1002/0471143030.cb0322s30.
[52] D. Yang *et al.*, “Progress, opportunity, and perspective on exosome isolation-efforts for efficient exosome-based theranostics,” *Theranostics*, vol. 10, no. 8, p. 3684, 2020.
[53] F. Royo, C. Théry, J. M. Falcón-Pérez, R. Nieuwland, and K. W. Witwer, “Methods for separation and characterization of extracellular vesicles: results of a worldwide survey performed by the ISEV rigor and standardization subcommittee,” *Cells*, vol. 9, no. 9, p. 1955, 2020.
[54] C. Théry *et al.*, “Minimal information for studies of extracellular vesicles 2018 (MISEV2018): a position statement of the International Society for Extracellular Vesicles and update of the MISEV2014 guidelines,” *Journal of Extracellular Vesicles*, vol. 7, no. 1, p. 1535750, Dec. 2018, doi: https://doi.org/10.1080/20013078.2018.1535750.
[55] A. Yekula *et al.*, “Large and small extracellular vesicles released by glioma cells in vitro and in vivo,” *Journal of Extracellular Vesicles*, vol. 9, no. 1, p. 1689784, Jan. 2020, doi: 10.1080/20013078.2019.1689784.
[56] H. T. Hu, T. Nishimura, and S. Suetsugu, “Ultracentrifugal separation, characterization, and functional study of extracellular vesicles derived from serum-free cell culture,” *STAR Protocols*, vol. 2, no. 3, p. 100625, Sep. 2021, doi: 10.1016/J.XPRO.2021.100625.
[57] S. Tiwari, V. Kumar, S. Randhawa, and S. K. Verma, “Preparation and characterization of extracellular vesicles,” *American Journal of Reproductive Immunology*, vol. 85, no. 2, p. e13367, Feb. 2021, doi: https://doi.org/10.1111/aji.13367.
[58] G. Trindade *et al.*, “Metabolic Profiling of Extracellular Vesicles from Ascitic Fluids of Ovarian Cancer Patients,” Oeiras, 2022.
[59] Biocrates, “User manual AbsoluteIDQ® p180 kit – SCIEX edition.” pp. 57–57, 2021.
[60] Z. Pang *et al.*, “MetaboAnalyst 5.0: narrowing the gap between raw spectra and functional insights,” *Nucleic Acids Research*, vol. 49, no. W1, pp. W388–W396, Jul. 2021, doi: 10.1093/nar/gkab382.
[61] R. Goodacre *et al.*, “Proposed minimum reporting standards for data analysis in metabolomics,” *Metabolomics*, vol. 3, no. 3, pp. 231–241, 2007, doi: 10.1007/s11306-007-0081-3.
[62] I. Karaman, “Preprocessing and Pretreatment of Metabolomics Data for Statistical Analysis,” in *Metabolomics: From Fundamentals to Clinical Applications*, A. Sussulini, Ed. Cham: Springer International Publishing, 2017, pp. 145–161. doi: 10.1007/978-3-319-47656-8_6.
[63] S. Naz *et al.*, “Role of peritoneal washing cytology in ovarian malignancies: correlation with histopathological parameters,” *World Journal of Surgical Oncology*, vol. 13, no. 1, p. 315, 2015, doi: 10.1186/s12957-015-0732-1.
[64] K. K. Gupta, V. K. Gupta, and R. W. Naumann, “Ovarian cancer: screening and future directions,” *International Journal of Gynecologic Cancer*, vol. 29, no. 1, p. 195, Jan. 2019, doi: 10.1136/ijgc-2018-000016.
[65] I. B. Vergote, M. Onsrud, O. P. Børmer, B. M. Sert, and M. Moen, “CA125 in peritoneal fluid of ovarian cancer patients,” *Gynecologic Oncology*, vol. 44, no. 2, pp. 161–165, 1992, doi: https://doi.org/10.1016/0090-8258(92)90032-E.
[66] C. Gieger *et al.*, “Genetics Meets Metabolomics: A Genome-Wide Association Study of Metabolite Profiles in Human Serum,” *PLOS Genetics*, vol. 4, no. 11, pp. e1000282-, Nov. 2008, [Online]. Available: https://doi.org/10.1371/journal.pgen.1000282

[67] P. Panuwet *et al.*, "Biological Matrix Effects in Quantitative Tandem Mass Spectrometry-Based Analytical Methods: Advancing Biomonitoring," *Crit Rev Anal Chem*, vol. 46, no. 2, pp. 93–105, 2016, doi: 10.1080/10408347.2014.980775.

[68] M. Harmati, M. Bukva, T. Böröczky, K. Buzás, and E. Gyukity-Sebestyén, "The role of the metabolite cargo of extracellular vesicles in tumor progression," *Cancer Metastasis Rev*, vol. 40, no. 4, pp. 1203–1221, Dec. 2021, doi: 10.1007/s10555-021-10014-2.

[69] D. Chakroborty, C. Sarkar, B. Basu, P. S. Dasgupta, and S. Basu, "Catecholamines Regulate Tumor Angiogenesis," *Cancer Research*, vol. 69, no. 9, pp. 3727–3730, Apr. 2009, doi: 10.1158/0008-5472.CAN-08-4289.

[70] D. Moskovich *et al.*, "DIO3, the thyroid hormone inactivating enzyme, promotes tumorigenesis and metabolic reprogramming in high grade serous ovarian cancer," *Cancer Letters*, vol. 501, pp. 224–233, 2021, doi: https://doi.org/10.1016/j.canlet.2020.11.011.

[71] A. E. Pegg, "Spermidine/spermine-N1-acetyltransferase: a key metabolic regulator," *American Journal of Physiology-Endocrinology and Metabolism*, vol. 294, no. 6, pp. E995–E1010, Jun. 2008, doi: 10.1152/ajpendo.90217.2008.

[72] S. Baliou, A. M. Kyriakopoulos, D. A. Spandidos, and V. Zoumpourlis, "Role of taurine, its haloamines and its lncRNA TUG1 in both inflammation and cancer progression. On the road to therapeutics? (Review)," *Int J Oncol*, vol. 57, no. 3, pp. 631–664, Sep. 2020, doi: 10.3892/ijo.2020.5100.

[73] W. Yang *et al.*, "Identification of Potential Biomarkers and Metabolic Profiling of Serum in Ovarian Cancer Patients Using UPLC/Q-TOF MS," *Cellular Physiology and Biochemistry*, vol. 51, no. 3, pp. 1134–1148, 2018, doi: 10.1159/000495492.

[74] A. Morandi and S. Indraccolo, "Linking metabolic reprogramming to therapy resistance in cancer," *Biochimica et Biophysica Acta (BBA) - Reviews on Cancer*, vol. 1868, no. 1, pp. 1–6, 2017, doi: https://doi.org/10.1016/j.bbcan.2016.12.004.

[75] M. Smolarz *et al.*, "The Lipid Composition of Serum-Derived Small Extracellular Vesicles in Participants of a Lung Cancer Screening Study," *Cancers (Basel)*, vol. 13, no. 14, 2021, doi: 10.3390/cancers13143414.

List of figures

List of tables

Appendix

*Table A. 1 – **Drying schedule of the application of biofluids to the kit**.*

Sample ID	Drying steps (µL)				total volume (µL)	Nanodrop (µg/µL)	total particle (µg)
	1st	2nd	3rd	4th			
AF1	-	-	-	10	10	39.634	396340
AF2	-	-	-	10	10	29.933	299330
AF3	-	-	-	10	10	55.903	559030
AF4	-	-	-	10	10	45.058	450580
AF5 - 5 µL	-	-	-	5	5	31.256	156280
AF5 - 10 µL	-	-	-	10	10	31.256	312560
AF5 - 15 µL	-	-	-	15	15	31.256	468840
AF6	-	-	-	10	10	44.376	443760
AF7	-	-	-	10	10	43.020	430,2
AF8	-	-	-	10	10	57.710	577,1
AF9	-	-	-	10	10	42.836	428360
AF10	-	-	-	10	10	35.853	358530
AF11	-	-	-	10	10	N.A.	N.A.
AF12	-	-	-	10	10	N.A.	N.A.
AF13	-	-	-	10	10	N.A.	N.A.
AF14	-	-	-	10	10	N.A.	N.A.
AF15	-	-	-	10	10	N.A.	N.A.
AF16	-	-	-	10	10	N.A.	N.A.
AF17	-	-	-	10	10	N.A.	N.A.
AF18	-	-	-	10	10	N.A.	N.A.
AF19	-	-	-	10	10	N.A.	N.A.
AF20	-	-	-	10	10	N.A.	N.A.
PW1 - 10 µL	-	-	-	10	10	45.015	450150
PW1- 30 µL	-	-	15	15	30	45.016	1350480
PW2 - 10 µL	-	-	-	10	10	42.762	427620
PW2 - 30 µL	-	-	15	15	30	42.763	1282890
PW3 - 10 µL	-	-	-	10	10	35.402	354020
PW3 - 30 µL	-	-	15	15	30	35.403	1062090
PW4 - 10 µL	-	-	-	10	10	N.A.	N.A.
PW4 - 30 µL	-	-	15	15	30	N.A.	N.A.
PW5 - 10 µL	-	-	-	10	10	N.A.	N.A.
PW5 - 30 µL	-	-	15	15	30	N.A.	N.A.

Table A. 2 – ***Drying schedule of the application of EVs to the kit.***

Sample ID	Drying steps (µL)				total volume (µL)	NTA (particle/mL)	total particle	concentration level
	1st	2nd	3rd	4th				
AF1-EV-0	15	15	15	15.00	60.00	1,60E+10	9,60E+08	0
*AF2-EV-1**	-	-	-	10.00	10.00	1,08E+12	5,00E+09	1
AF2-EV-2	-	-	-	11.11	11.11	1,08E+12	1,20E+10	2
AF2-EV-3	-	15	15	7.04	37.04	1,08E+12	4,00E+10	3
AF3-EV-1	15	15	15	0,10	45.10	1,00E+11	4,51E+09	0
*AF4-EV-1**	-	-	-	10.00	10.00	1,35E+13	5,00E+09	1
*AF4-EV-2**	-	-	-	10.00	10.00	1,35E+13	1,20E+10	2
*AF4-EV-3**	-	-	-	10.00	10.00	1,35E+13	4,00E+10	3
*AF5-EV-1**	-	-	-	10.00	10.00	1,50E+12	5,00E+09	1
*AF5-EV-2**	-	-	-	10.00	10.00	1,50E+12	1,20E+10	2
AF5-EV-3	-	-	15	11.67	26.67	1,50E+12	4,00E+10	3
AF6-EV-1	-	-	-	11.36	11.36	4,40E+11	5,00E+09	1
AF6-EV-2	-	-	15	12.27	27.27	4,40E+11	1,20E+10	2
AF7-EV-0	-	11	11	10.00	32.00	1,54E+10	4,93E+08	0
AF8-EV-0	15	15	15	15.00	60.00	2,12E+10	1,27E+09	0
AF9-EV-1	-	15	15	10.98	40.98	1,22E+11	5,00E+09	1
AF10-EV-1	-	-	-	11.36	11.36	4,40E+11	5,00E+09	1
AF10-EV-2	-	-	15	12.27	27.27	4,40E+11	1,20E+10	2
PW1-EV-1	-	-	10	10.83	20.83	2,40E+11	5,00E+09	1
PW2-EV-1	15	15	15	15.61	60.61	8,25E+10	5,00E+09	1
PW3-EV-0	15	15	15	15.00	60.00	1,60E+10	9,60E+08	0

Table A. 3 – ***Biochemical names of acylcarnitines****.*

	Acylcarnitines		
1	CO	Carnitine	*1*
2	C2	Acetylcarnitine	*2*
3	C3	Propionylcarnitine	*3*
4	C3:1	Propenoylcarnitine	*4*
5	C3-OH	Hydroxypropionylcarnitine	*5*
6	C4	Butyrylcarnitine	*6*
7	C4:1	Butenylcarnitine	*7*
8	C4-OH (C3-DC)	Hydroxybutyrylcarnitine	*8*
9	C5	Valerylcarnitine	*9*
10	C5:1	Tiglylcarnitine	*10*
11	C5:1-DC	Glutaconylcarnitine	*11*
12	C5-DC (C6-OH)	Glutarylcarnitine (Hydroxyhexanoylcarnitine)	*12*
13	C5-M-DC	Methylglutarylcarnitine	*13*
14	C5-OH (C3-DC-M)	Hydroxyvalerylcarnitine (Methylmalonylcarnitine)	*14*
15	C6 (C4:1-DC)	Hexanoylcarnitine (Fumarylcarnitine)	*15*
16	C6:1	Hexenoylcarnitine	*16*
17	C7-DC	Pimelylcarnitine	*17*
18	C8	Octanoylcarnitine	*18*
19	C9	Nonaylcarnitine	*19*
20	C10	Decanoylcarnitine	*20*
21	C10:1	Decenoylcarnitine	*21*
22	C10:2	Decadienylcarnitine	*22*
23	C12	Dodecanoylcarnitine	*23*
24	C12:1	Dodecenoylcarnitine	*24*
25	C12-DC	Dodecanedioylcarnitine	*25*
26	C14	Tetradecanoylcarnitine	*26*
27	C14:1	Tetradecenoylcarnitine	*27*
28	C14:1-OH	Hydroxytetrade-cenoylcarnitine	*28*
29	C14:2	Tetradecadienylcarnitine	*29*
30	C14:2-OH	Hydroxytetradecadienyl-carnitine	*30*
31	C16	Hexadecanoylcarnitine	*31*
32	C16:1	Hexadecenoylcarnitine	*32*
33	C16:1-OH	Hydroxyhexadecenoylcarnitine	*33*
34	C16:2	Hexadecadienylcarnitine	*34*
35	C16:2-OH	Hydroxyhexadecadienyl-carnitine	*35*
36	C16-OH	Hydroxyhexadecanoylcarnitine	*36*
37	C18	Octadecanoylcarnitine	*37*
38	C18:1	Octadecenoylcarnitine	*38*
39	C18:1-OH	Hydroxyoctadecenoylcarnitine	*39*
40	C18:2	Octadecadienylcarnitine	*40*

Table A. 4 – ***Biochemical names of amino acids.***

	Amino acids		
1	Ala	Alanine	*41*
2	Arg	Arginine	*42*
3	Asn	Asparagine	*43*
4	Asp	Aspartate	*44*
5	Cit	Citrulline	*45*
6	Gin	Glutamine	*46*
7	Glu	Glutamate	*47*
8	Gly	Glycine	*48*
9	His	Histidine	*49*
10	Ile	Isoleucine	*50*
11	Leu	Leucine	*51*
12	Lys	Lysine	*52*
13	Met	Methionine	*53*
14	Orn	Ornithine	*54*
15	Phe	Phenylalanine	*55*
16	Pro	Proline	*56*
17	Ser	Serine	*57*
18	Thr	Threonine	*58*
19	Trp	Tryptophan	*59*
20	Tyr	Tyrosine	*60*
21	Val	Valine	*61*

Table A. 5 – ***Biochemical names of biogenic amines.***

	Biogenic amines		
1	Ac-Orn	Acetylornithine	*62*
2	ADMA	Asymmetric dimethylarginine	*63*
3	SDMA	Symmetric dimethylarginine	*64*
4	alpha-AAA	alpha-Aminoadipic acid	*65*
5	Carnosine	Carnosine	*66*
6	Creatinine	Creatinine	*67*
7	DOPA	Dihydroxyphenylalanine	*68*
8	Dopamine	Dopamine	*69*
9	Histamine	Histamine	*70*
10	Kynurenine	Kynurenine	*71*
11	Met-SO	Methionine sulfoxide	*72*
12	Nitro-Tyr	Nitrotyrosine	*73*
13	c4-OH-Pro	cis-4-Hydroxyproline	*74*
14	t4-OH-Pro	trans-4-Hydroxyproline	*75*
15	PEA	Phenylethylamine	*76*
16	Putrescine	Putrescine	*77*
17	Sarcosine	Sarcosine	*78*
18	Serotonin	Serotonin	*79*
19	Spermidine	Spermidine	*80*
20	Spermine	Spermine	*81*
21	Taurine	Taurine	*82*

Table A. 6 – ***Biochemical names of lysophosphatidylcholines.***

	Lysophosphatidylcholines		
1	lysoPC a C14:0	lysoPhosphatidylcholine acyl C14:0	*83*
2	lysoPC a C16:0	lysoPhosphatidylcholine acyl C16:0	*84*
3	lysoPC a C16:1	lysoPhosphatidylcholine acyl C16:1	*85*
4	lysoPC a C17:0	lysoPhosphatidylcholine acyl C17:0	*86*
5	lysoPC a 018:0	lysoPhosphatidylcholine acyl C18:0	*87*
6	lysoPC a C18:1	lysoPhosphatidylcholine acyl C18:1	*88*
7	lysoPC a C18:2	lysoPhosphatidylcholine acyl C18:2	*89*
8	lysoPC a C20:3	lysoPhosphatidylcholine acyl C20:3	*90*
9	lysoPC a C20:4	lysoPhosphatidylcholine acyl C20:4	*91*
10	lysoPC a 024:0	lysoPhosphatidylcholine acyl C24:0	*92*
11	lysoPC a 026:0	lysoPhosphatidylcholine acyl 026:0	*93*
12	lysoPC a C26:1	lysoPhosphatidylcholine acyl C26:1	*94*
13	lysoPC a C28:0	lysoPhosphatidylcholine acyl C28:0	*95*
14	lysoPC a C28:1	lysoPhosphatidylcholine acyl C28:1	*96*

Table A. 7 – ***Biochemical names of phosphatidylcholines 1/2.***

	Phosphatidylcholines		
1	PC aa C24:0	Phosphatidylcholine diacyl C24:0	*97*
2	PC aa C26:0	Phosphatidylcholine diacyl C26:0	*98*
3	PC aa C28:1	Phosphatidylcholine diacyl C28:1	*99*
4	PC aa 030:0	Phosphatidylcholine diacyl C30:0	*100*
5	PC aa C30:2	Phosphatidylcholine diacyl C30:2	*101*
6	PC aa 032:0	Phosphatidylcholine diacyl C32:0	*102*
7	PC aa 032:1	Phosphatidylcholine diacyl C32:1	*103*
8	PC aa C32:2	Phosphatidylcholine diacyl C32:2	*104*
9	PC aa C32:3	Phosphatidylcholine diacyl C32:3	*105*
10	PC aa C34:1	Phosphatidylcholine diacyl C34:1	*106*
11	PC aa C34:2	Phosphatidylcholine diacyl C34:2	*107*
12	PC aa C34:3	Phosphatidylcholine diacyl C34:3	*108*
13	PC aa C34:4	Phosphatidylcholine diacyl C34:4	*109*
14	PC aa C36:0	Phosphatidylcholine diacyl C36:0	*110*
15	PC aa C36:1	Phosphatidylcholine diacyl C36:1	*111*
16	PC aa C36:2	Phosphatidylcholine diacyl C36:2	*112*
17	PC aa C36:3	Phosphatidylcholine diacyl C36:3	*113*
18	PC aa C36:4	Phosphatidylcholine diacyl C36:4	*114*
19	PC aa C36:5	Phosphatidylcholine diacyl C36:5	*115*
20	PC aa C36:6	Phosphatidylcholine diacyl C36:6	*116*
21	PC aa C38:0	Phosphatidylcholine diacyl C38:0	*117*
22	PC aa C38:1	Phosphatidylcholine diacyl C38:1	*118*
23	PC aa C38:3	Phosphatidylcholine diacyl C38:3	*119*
24	PC aa C38:4	Phosphatidylcholine diacyl C38:4	*120*
25	PC aa C38:5	Phosphatidylcholine diacyl C38:5	*121*
26	PC aa C38:6	Phosphatidylcholine diacyl C38:6	*122*
27	PC aa C40:1	Phosphatidylcholine diacyl C40:1	*123*
28	PC aa C40:2	Phosphatidylcholine diacyl C40:2	*124*
29	PC aa C40:3	Phosphatidylcholine diacyl C40:3	*125*
30	PC aa C40:4	Phosphatidylcholine diacyl C40:4	*126*
31	PC aa C40:5	Phosphatidylcholine diacyl C40:5	*127*
32	PC aa C40:6	Phosphatidylcholine diacyl C40:6	*128*
33	PC aa 042:0	Phosphatidylcholine diacyl C42:0	*129*
34	PC aa C42:1	Phosphatidylcholine diacyl C42:1	*130*
35	PC aa C42:2	Phosphatidylcholine diacyl C42:2	*131*
36	PC aa C42:4	Phosphatidylcholine diacyl C42:4	*132*
37	PC aa C42:5	Phosphatidylcholine diacyl C42:5	*133*
38	PC aa C42:6	Phosphatidylcholine diacyl 042:6	*134*

Table A. 8 – ***Biochemical names of phosphatidylcholines 2/2.***

	Phosphatidylcholines		
39	PC ae 030:0	Phosphatidylcholine acyl-alkyl C30:0	*135*
40	PC ae 030:1	Phosphatidylcholine acyl-alkyl C30:1	*136*
41	PC ae 030:2	Phosphatidylcholine acyl-alkyl C30:2	*137*
42	PC ae 032:1	Phosphatidylcholine acyl-alkyl 032:1	*138*
43	PC ae 032:2	Phosphatidylcholine acyl-alkyl 032:2	*139*
44	PC ae 034:0	Phosphatidylcholine acyl-alkyl C34:0	*140*
45	PC ae 034:1	Phosphatidylcholine acyl-alkyl 034:1	*141*
46	PC ae C34:2	Phosphatidylcholine acyl-alkyl 034:2	*142*
47	PC ae 034:3	Phosphatidylcholine acyl-alkyl 034:3	*143*
48	PC ae C36:0	Phosphatidylcholine acyl-alkyl C36:0	*144*
49	PC ae 036:1	Phosphatidylcholine acyl-alkyl 036:1	*145*
50	PC ae C36:2	Phosphatidylcholine acyl-alkyl 036:2	*146*
51	PC ae 036:3	Phosphatidylcholine acyl-alkyl 036:3	*147*
52	PC ae 036:4	Phosphatidylcholine acyl-alkyl C36:4	*148*
53	PC ae 036:5	Phosphatidylcholine acyl-alkyl 036:5	*149*
54	PC ae 038:0	Phosphatidylcholine acyl-alkyl C38:0	*150*
55	PC ae C38:1	Phosphatidylcholine acyl-alkyl C38:1	*151*
56	PC ae C38:2	Phosphatidylcholine acyl-alkyl C38:2	*152*
57	PC ae C38:3	Phosphatidylcholine acyl-alkyl C38:3	*153*
58	PC ae C38:4	Phosphatidylcholine acyl-alkyl C38:4	*154*
59	PC ae C38:5	Phosphatidylcholine acyl-alkyl C38:5	*155*
60	PC ae C38:6	Phosphatidylcholine acyl-alkyl C38:6	*156*
61	PC ae C40:1	Phosphatidylcholine acyl-alkyl C40:1	*157*
62	PC ae C40:2	Phosphatidylcholine acyl-alkyl C40:2	*158*
63	PC ae C40:3	Phosphatidylcholine acyl-alkyl C40:3	*159*
64	PC ae C40:4	Phosphatidylcholine acyl-alkyl C40:4	*160*
65	PC ae C40:5	Phosphatidylcholine acyl-alkyl C40:5	*161*
66	PC ae C40:6	Phosphatidylcholine acyl-alkyl C40:6	*162*
67	PC ae C42:0	Phosphatidylcholine acyl-alkyl C42:0	*163*
68	PC ae C42:1	Phosphatidylcholine acyl-alkyl C42:1	*164*
69	PC ae C42:2	Phosphatidylcholine acyl-alkyl C42:2	*165*
70	PC ae C42:3	Phosphatidylcholine acyl-alkyl C42:3	*166*
71	PC ae C42:4	Phosphatidylcholine acyl-alkyl C42:4	*167*
72	PC ae C42:5	Phosphatidylcholine acyl-alkyl C42:5	*168*
73	PC ae C44:3	Phosphatidylcholine acyl-alkyl C44:3	*169*
74	PC ae C44:4	Phosphatidylcholine acyl-alkyl C44:4	*170*
75	PC ae C44:5	Phosphatidylcholine acyl-alkyl C44:5	*171*
76	PC ae C44:6	Phosphatidylcholine acyl-alkyl C44:6	*172*

Table A. 9 – ***Biochemical names of sphingolipids and sugars.***

	Shingolipids		
1	SM (OH) C14:1	Hydroxysphingomyeline C14:1	*173*
2	SM C16:0	Sphingomyeline C16:0	*174*
3	SM C16:1	Sphingomyeline C16:1	*175*
4	SM (OH) C16:1	Hydroxysphingomyeline C16:1	*176*
5	SM C18:0	Sphingomyeline 018:0	*177*
6	SM C18:1	Sphingomyeline C18:1	*178*
7	SM C20:2	Sphingomyeline 020:2	*179*
8	SM C22:3	Sphingomyeline C22:3	*180*
9	SM (OH) 022:1	Hydroxysphingomyeline 022:1	*181*
10	SM (OH) 022:2	Hydroxysphingomyeline C22:2	*182*
11	SM C24:0	Sphingomyeline 024:0	*183*
12	SM C24:1	Sphingomyeline C24:1	*184*
13	SM (OH) C24:1	Hydroxysphingomyeline 024:1	*185*
14	SM C26:0	Sphingomyeline C26:0	*186*
15	SM C26:1	Sphingomyeline C26:1	*187*

	Sugars		
1	H1	Hexose	*188*

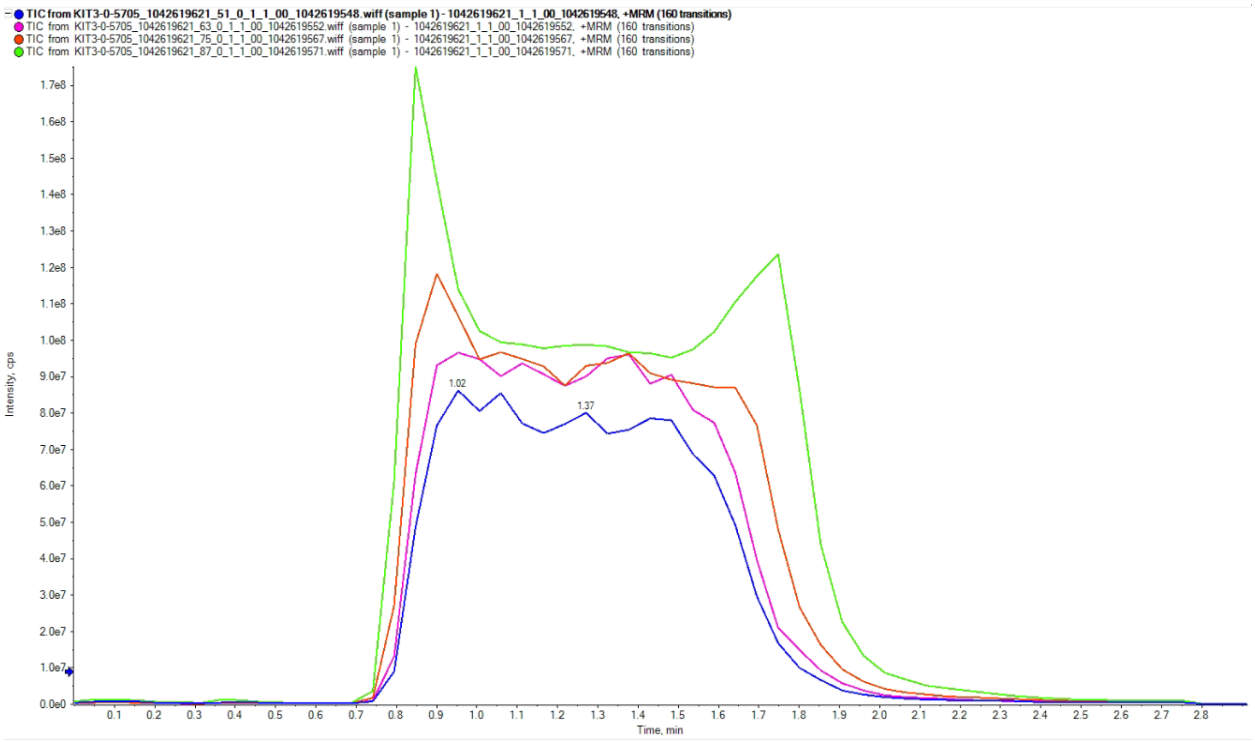

Figure A. 1 – ***FIA diagram of AF2 in four loading volumes.*** *Conspicuous peaks at the beginning and at the end of the signal at 30 µL, indicating saturation of the sample. Blue – 2 µL; pink – 5 µL; red – 10 µL; green – 30 µL. X-axis – time (min); y-axis – intensity (cps).*

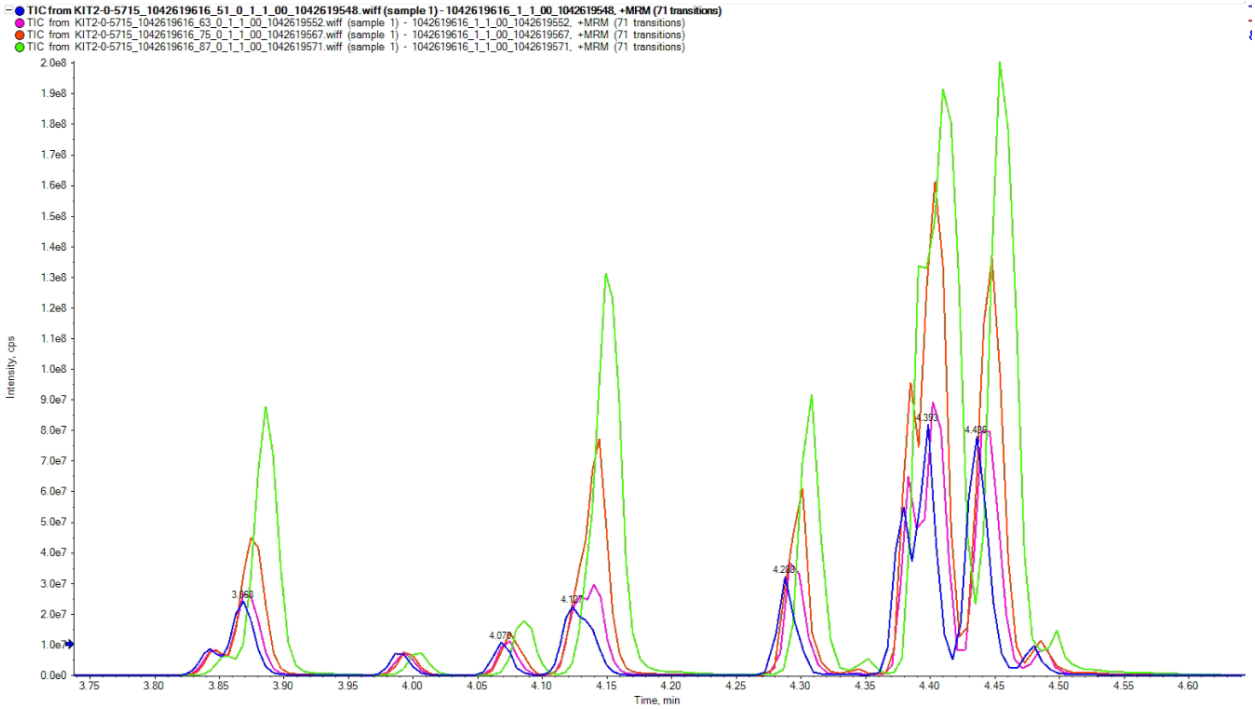

Figure A. 2 – ***LC diagram of AF4 in four loading volumes****. Between 4.35 and 4.45 minutes, no clear separation of the peak intensities can be seen at 30 µL. Blue – 2 µL; pink – 5 µL; red – 10 µL; green – 30 µL. X-axis – time (min); y-axis – intensity (cps).*

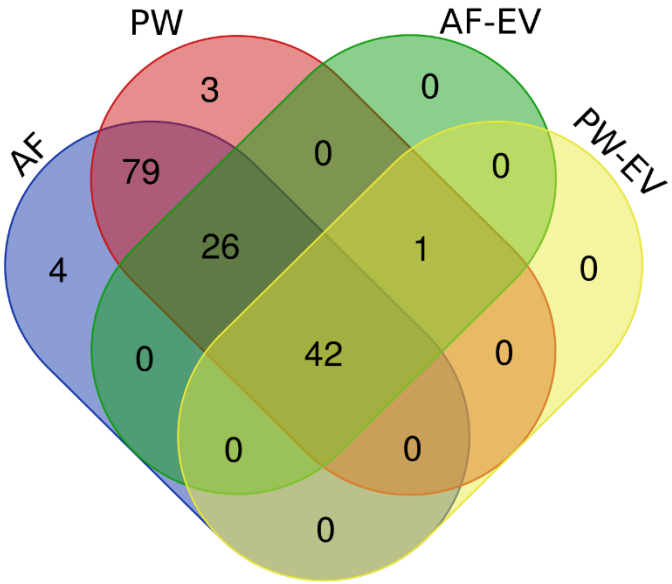

all groups		AF + PW			(not PW-EV)	AF	PW	(not AF)
42		**79**			**26**	**4**	**3**	**1**
PC aa C38:6	SM C18:0	PC ae C42:2	Gly	Glu	PC aa C32:3	DOPA	C16:1	Spermine
PC aa C36:5	SM (OH) C14:1	C18	C16	PC aa C40:2	lysoPC a C20:4	PC aa C30:2	PC aa C42_2	
SM C16:0	PC aa C36:3	PC ae C42:5	H1	PC aa C42:0	SM C20:2	alpha-AAA	C14:2	
PC aa C32:1	PC aa C38:0	Creatinine	C5	Ser	PC aa C40:3	C10:1		
SM (OH) C16:1	PC aa C34:1	C8	Met	lysoPC a C18:2	PC aa C24:0			
PC aa C38:1	PC ae C34:1	Phe	PC ae C44:5	C18:2	PC ae C38:5			
PC aa C34:3	SM C26:1	t4-OH-Pro	C0	lysoPC a C24:0	PC ae C38:4			
PC aa C28:1	SM C16:1	PC aa C42:4	Orn	Leu	PC ae C36:0			
SM C26:0	PC ae C34:3	SM C22:3	C6 (C4:1-DC)	PC ae C38:0	PC ae C40:3			
SM (OH) C24:1	PC aa C38:3	PC ae C30:0	PC aa C42:6	Kynurenine	lysoPC a C17:0			
PC ae C36:3	PC aa C30:0	ADMA	PC ae C38:1	lysoPC a C28:0	PC aa C40:4			
Spermidine	SM (OH) C22:2	PC ae C44:3	SDMA	Cit	lysoPC a C18:1			
PC ae C38:6	PC aa C36:2	C12	Met-SO	Val	PC ae C38:2			
PC ae C36:4	PC aa C38:5	lysoPC a C16:	PC ae C30:1	C4	PC aa C42:5			
PC ae C34:0	SM C24:1	C3-DC (C4-OH	PC ae C44:4	C10	PC ae C40:5			
PC ae C34:2		Ala	PC ae C40:1	Pro	PC aa C40:6			
SM C24:0		PC ae C44:6	PC ae C42:3	PC ae C40:4	PC ae C36:2			
lysoPC a C16:0		C18:1	PC aa C34:4	PC ae C32:2	PC aa C36:0			
PC aa C36:1		lysoPC a C20:	His	C14	PC aa C32:2			
SM C18:1		Taurine	PC aa C36:6	Arg	PC aa C40:5			
PC aa C38:4		Lys	Trp	PC ae C42:1	PC ae C40:6			
PC aa C32:0		lysoPC a C26:	C2	lysoPC a C26:0	lysoPC a C18:0			
PC ae C36:5		Carnosine	Asp	Tyr	PC ae C38:3			
SM (OH) C22:1		Sarcosine	C14:1	PC ae C36:1	Thr			
PC aa C36:4		Gln	PC ae C30:2	lysoPC a C28:1	PC ae C40:2			
PC ae C32:1		Asn	PC ae C42:4		PC aa C42:1			
PC aa C34:2		Ile	C3					

Figure A. 3 – ***List of metabolites, compared in all four groups.***

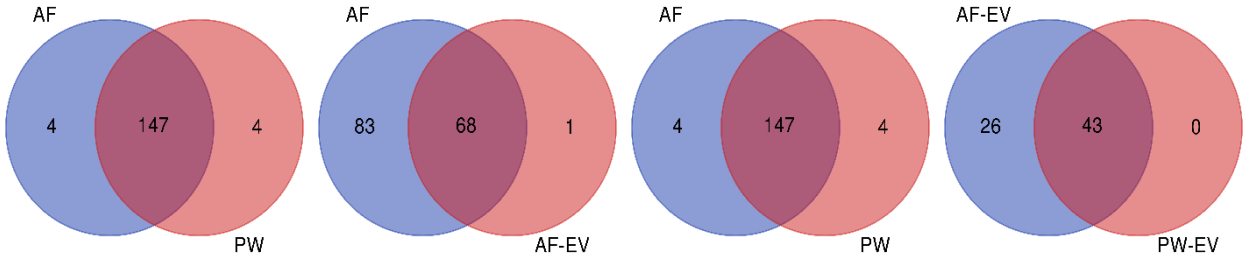

AF	AF + PW						PW
4	147						4
DOPA	PC ae C42:2	Ala	PC ae C36:4	PC aa C40:6	PC ae C34:1	Arg	C16:1
PC aa C30:2	PC aa C32:3	PC aa C28:1	PC ae C34:0	His	lysoPC a C24:(	PC ae C42:1	PC aa C42:2
alpha-AAA	lysoPC a C20:4	PC ae C44:6	PC ae C34:2	PC ae C36:2	Leu	lysoPC a C26:(	Spermine
C10:1	C18	C18:1	PC ae C44:5	PC ae C36:5	PC aa C40:5	PC aa C42:1	C14:2
	PC ae C42:5	SM C26:0	PC aa C40:4	SM (OH) C22:1	SM C26:1	PC aa C38:5	
	PC aa C38:6	SM (OH) C24:1	lysoPC a C18:(	PC aa C36:6	SM C16:1	Tyr	
	SM C20:2	PC ae C36:3	SM C24:0	Trp	PC ae C34:3	PC ae C36:1	
	PC aa C36:5	PC ae C38:5	PC ae C38:2	C2	PC ae C38:0	SM C24:1	
	Creatinine	lysoPC a C20:4	C0	Asp	PC ae C40:6	lysoPC a C28:1	
	C8	Taurine	PC aa C42:5	C14:1	Kynurenine	C3	
	Phe	Lys	Orn	PC aa C36:4	lysoPC a C18:(	PC aa C34:2	
	SM C16:0	lysoPC a C26:(	lysoPC a C16:(	PC ae C30:2	lysoPC a C28:(	Ile	
	t4-OH-Pro	Carnosine	C6 (C4:1-DC)	PC ae C42:4	Cit		
	PC aa C42:4	Sarcosine	PC aa C42:6	PC aa C36:0	PC aa C38:3		
	SM C22:3	Spermidine	PC ae C38:1	PC ae C32:1	PC aa C30:0		
	PC ae C30:0	Gln	SDMA	SM C18:0	PC ae C38:3		
	PC aa C32:1	PC ae C38:4	PC aa C36:1	Glu	Val		
	SM (OH) C16:1	PC ae C36:0	Met-SO	PC aa C40:2	Thr		
	PC aa C40:3	Asn	SM C18:1	PC aa C42:0	C4		
	ADMA	PC ae C40:3	PC ae C40:5	SM (OH) C14:1	C10		
	PC ae C44:3	Gly	PC ae C30:1	PC aa C36:3	Pro		
	C12	C16	PC aa C38:4	Ser	SM (OH) C22:2		
	PC aa C38:1	H1	PC aa C32:0	PC aa C32:2	PC ae C40:4		
	PC aa C24:0	C5	PC ae C44:4	lysoPC a C18:(	PC aa C36:2		
	lysoPC a C16:1	Met	PC ae C40:1	PC aa C38:0	PC ae C32:2		
	C3-DC (C4-OH)	lysoPC a C17:(	PC ae C42:3	C18:2	PC ae C40:2		
	PC aa C34:3	PC ae C38:6	PC aa C34:4	PC aa C34:1	C14		

AF		AF + AF-EV			AF-EV
83		68			1
PC ae C42:2	Gly	PC aa C32:3	lysoPC a C18:1	PC ae C34:3	Spermine
C18	C16	lysoPC a C20:4	SM C24:0	PC ae C40:6	
PC ae C42:5	H1	PC aa C38:6	PC ae C38:2	lysoPC a C18:0	
DOPA	C5	SM C20:2	PC aa C42:5	PC aa C38:3	
Creatinine	Met	PC aa C36:5	lysoPC a C16:0	PC aa C30:0	
C8	PC ae C44:5	SM C16:0	PC aa C36:1	PC ae C38:3	
Phe	PC aa C30:2	PC aa C32:1	SM C18:1	Thr	
t4-OH-Pro	C0	SM (OH) C16:1	PC ae C40:5	SM (OH) C22:2	
PC aa C42:4	Orn	PC aa C40:3	PC aa C38:4	PC aa C36:2	
SM C22:3	alpha-AAA	PC aa C38:1	PC aa C32:0	PC ae C40:2	
PC ae C30:0	C6 (C4:1-DC)	PC aa C24:0	PC aa C40:6	PC aa C42:1	
ADMA	PC aa C42:6	PC aa C34:3	PC ae C36:2	PC aa C38:5	
PC ae C44:3	PC ae C38:1	PC aa C28:1	PC ae C36:5	SM C24:1	
C12	SDMA	SM C26:0	SM (OH) C22:1	PC aa C34:2	
lysoPC a C16:1	Met-SO	SM (OH) C24:1	PC aa C36:4		
C3-DC (C4-OH)	PC ae C30:1	PC ae C36:3	PC aa C36:0		
Ala	PC ae C44:4	PC ae C38:5	PC ae C32:1		
PC ae C44:6	PC ae C40:1	Spermidine	SM C18:0		
C18:1	PC ae C42:3	PC ae C38:4	SM (OH) C14:1		
lysoPC a C20:3	PC aa C34:4	PC ae C36:0	PC aa C36:3		
Taurine	His	PC ae C40:3	PC aa C32:2		
Lys	PC aa C36:6	lysoPC a C17:0	PC aa C38:0		
lysoPC a C26:1	Trp	PC ae C38:6	PC aa C34:1		
Carnosine	C2	PC ae C36:4	PC ae C34:1		
Sarcosine	Asp	PC ae C34:0	PC aa C40:5		
Gln	C14:1	PC ae C34:2	SM C26:1		
Asn	PC ae C30:2	PC aa C40:4	SM C16:1		

PW				PW + PW-EV		PW-EV
108				43		0
PC ae C42:2	lysoPC a C26:(	Met-SO	PC aa C40:5	PC aa C38:6	SM (OH) C14:1	
PC aa C32:3	Lys	PC ae C40:5	PC ae C40:6	PC aa C36:5	PC aa C36:3	
lysoPC a C20:4	Sarcosine	PC ae C30:1	PC ae C38:0	SM C16:0	PC aa C38:0	
C18	Carnosine	PC ae C44:4	Kynurenine	PC aa C32:1	PC aa C34:1	
PC ae C42:5	Gln	PC ae C42:3	lysoPC a C18:(	SM (OH) C16:1	PC ae C34:1	
SM C20:2	PC ae C38:4	PC ae C40:1	lysoPC a C28:1	PC aa C38:1	SM C26:1	
Creatinine	PC ae C36:0	PC aa C34:4	Cit	PC aa C34:3	SM C16:1	
C8	Asn	PC ae C40:6	PC ae C38:3	PC aa C28:1	PC ae C34:3	
Phe	PC ae C40:3	His	Val	SM C26:0	PC aa C38:3	
t4-OH-Pro	Gly	PC ae C36:2	Thr	SM (OH) C24:1	Spermine	
C16:1	C16	PC aa C36:6	C4	PC ae C36:3	PC aa C30:0	
PC aa C42:4	H1	Trp	C10	Spermidine	SM (OH) C22:2	
SM C22:3	lysoPC a C17:(	C2	Pro	PC ae C36:4	PC aa C36:2	
PC ae C30:0	Met	Asp	PC ae C40:4	PC ae C38:6	PC aa C38:5	
PC aa C40:3	C5	C14:1	PC ae C32:2	PC ae C34:0	SM C24:1	
ADMA	PC ae C44:5	PC ae C30:2	PC ae C40:2	PC ae C34:2	PC aa C34:2	
PC ae C44:3	PC aa C40:4	PC ae C42:4	C14	SM C24:0		
C12	lysoPC a C18:1	PC aa C36:0	Arg	lysoPC a C16:0		
PC aa C24:0	PC ae C38:2	Glu	PC ae C42:1	PC aa C36:1		
lysoPC a C16:1	C0	PC aa C40:2	lysoPC a C26:(	SM C18:1		
C3-DC (C4-OH)	PC aa C42:5	PC aa C42:0	PC aa C42:1	PC aa C38:4		
Ala	Orn	Ser	Tyr	PC aa C32:0		
PC ae C44:6	C6 (C4:1-DC)	PC aa C32:2	PC ae C36:1	PC ae C36:5		
C18:1	PC aa C42:6	lysoPC a C18:1	lysoPC a C28:1	SM (OH) C22:1		
PC ae C38:5	PC ae C38:1	C18:2	C3	PC aa C36:4		
lysoPC a C20:4	PC aa C42:2	lysoPC a C24:(	Ile	PC ae C32:1		
Taurine	SDMA	Leu	C14:2	SM C18:0		

AF-EV	PW-EV + AF-EV		PW-EV
26	43		0
PC aa C40:6	PC aa C38:6	PC aa C30:0	
PC aa C32:3	PC ae C36:5	PC ae C36:4	
lysoPC a C20:4	SM (OH) C22:1	PC ae C38:6	
PC ae C36:2	PC aa C36:5	PC ae C34:0	
SM C20:2	PC aa C36:4	PC ae C34:2	
PC aa C40:3	SM C16:0	SM C24:0	
PC aa C36:0	PC aa C32:1	SM (OH) C22:2	
PC aa C24:0	SM (OH) C16:1	PC aa C36:2	
PC aa C32:2	PC ae C32:1	lysoPC a C16:0	
PC ae C38:5	SM C18:0	PC aa C38:5	
PC aa C40:5	PC aa C38:1	SM C24:1	
PC ae C38:4	SM (OH) C14:1	PC aa C36:1	
PC ae C40:6	PC aa C34:3	SM C18:1	
PC ae C36:0	PC aa C36:3	PC aa C34:2	
lysoPC a C18:(	PC aa C28:1	PC aa C38:4	
PC ae C40:3	SM C26:0	PC aa C32:0	
lysoPC a C17:(	PC aa C38:0	Spermine	
PC ae C38:3	SM (OH) C24:1		
Thr	PC ae C36:3		
PC aa C40:4	PC aa C34:1		
lysoPC a C18:1	PC ae C34:1		
PC ae C38:2	Spermidine		
PC aa C42:5	SM C26:1		
PC ae C40:2	SM C16:1		
PC aa C42:1	PC ae C34:3		
PC ae C40:5	PC aa C38:3		

Figure A. 4 – ***List of metabolites within two groups compared.***